# Discovery of novel MKL1 target genes important for cancer progression and metastasis:

# A focus on WNT1 inducible signaling pathway protein 1 (WISP1/CCN4)

**INAUGURALDISSERTATION**

zur

Erlangung der Würde eines Doktors der Philosophie

vorgelegt der

Philosophisch-Naturwissenschaftlichen Fakultät

der Universität Basel

von

**Irem Gürbüz**

aus der Türkei

Basel, 2015

Genehmigt von der Philosophisch-Naturwissenschaftlichen Fakultät auf Antrag von

Prof. Dr. Ruth Chiquet-Ehrismann
Prof. Dr. Gerhard M. Christofori

Basel, 09.12.2014

Prof. Dr. Jörg Schibler
Dekan

***To my parents,***

***Handan and Erdal Gürbüz***

## ACKNOWLEDGMENTS

First of all, I would like to thank my thesis advisor Prof. Ruth Chiquet-Ehrismann for giving me the opportunity to work in her lab. She was always available for discussions and ready to help with every problem I faced throughout my project. She was not only a great guide but also encouraged me to pursue my own ideas.

I would like to thank my thesis committee members, Prof. Gerhard M. Christofori and Prof. Nancy E. Hynes for the valuable advices and scientific input in the project. Additionally, I want to thank Prof. Hynes for all the cell lines she provided.

I am thankful to Dr. Maria B Asparuhova for her supervision and friendship. She shared her expertise with me and gave me great advices. Furthermore, I would like to thank Jacqueline Ferralli for her priceless experimental support and being my “German teacher”.

I would like to thank all present and past members of the Chiquet lab for the really nice and cooperative working atmosphere. I am especially thankful to my twin PhD sister, Francesca for her great friendship. It was very nice to have her around during all these years, right from the start till the end.

I would like to thank FMI facilities, especially to Tim Roloff, Hubertus Kohler, Ragna Sack, Daniel Hess and Jeremy Keusch for helping me with various experiments.

Likewise, I would like to thank the very nice people I met at the FMI. It was a great pleasure to work here. In particular, I want to thank my friends, Serap, Cristina, Atılgan, Baran, Keith and Biter for being “my family in Basel”.

Last but not the least, I am grateful to my parents, Handan and Erdal Gürbüz for supporting me throughout my life and being always there for me even if we are physically apart from each other.

## TABLE OF CONTENTS

**SUMMARY**

Tenascin-C (TNC) is involved in tumor initiation and metastasis, and high TNC expression has been associated with poor prognosis in cancers such as glioma, breast, colon and lung carcinoma (Orend and Chiquet-Ehrismann, 2006; Oskarsson, 2013). Previous studies have shown that the transcriptional regulator megakaryoblastic leukemia-1 (MKL1) induces TNC expression in both normal and transformed mammary epithelial cells, and that this induction requires the potential DNA-binding SAP domain of MKL1 (Asparuhova et al., 2011). Therefore, we postulated that SAP-dependent MKL1 action might be responsible for the tumor-specific induction of TNC. By transcript profiling analyses, we identified genes that are co-regulated with TNC in HC11 mouse mammary epithelial cells. We found that the expression of this gene set is associated with high-proliferative poor-outcome classes in human breast cancer and with reduced survival rate for breast cancer patients independent of tumor grade. Many of the newly discovered SAP-dependent/SRF-independent MKL1 target genes are strongly implicated in cell proliferation, cell motility and cancer. Indeed, downregulation of these transcripts by overexpression of MKL1 lacking the SAP domain inhibited cell growth as well as cell migration. Interestingly, many of the SAP-dependent MKL1 target genes, including WNT1 inducible signaling pathway protein 1 (WISP1/CCN4) that we studied further, were mechanoresponsive (Gurbuz et al., 2014).

WISP1 is a secreted, matricellular protein assigned to the CCN family, and aberrant WISP1 expression is observed in various pathologies including fibrosis and cancer (Berschneider et al., 2011). However, relatively little is known about the mechanistic details of its function. In our studies, we found that endogenous WISP1 expression correlates with the metastatic potential of isogenic mouse breast cancer cell lines. Furthermore, we observed that WISP1 mRNA levels within the mouse mammary gland tissue significantly increased upon irradiation, a treatment known to induce modifications in the tumor microenvironment leading to increased metastasis (Ruegg et al., 2011). Finally, we produced recombinant WISP1 protein and confirmed that WISP1 is N-glycosylated and that the secreted form of the protein undergoes

additional post-translational modifications that increase its size and possibly add functional diversity to the protein. Using our purified recombinant protein we generated specific anti-WISP1 antibodies. In the future, these antibodies can be used to detect WISP1 in various tumor tissues.

# CHAPTER 1: INTRODUCTION

## 1.1 Signaling in Cancer: From Extracellular Space to Nucleus

### 1.1.1 The Extracellular Matrix

The extracellular matrix (ECM) is a non-cellular structure and is present in all tissues and organs. It not only passively provides physical support for tissues, organs and individual cells, but also actively modulates cellular responses, such as cell migration, proliferation, differentiation and survival through biochemical and biomechanical cues (Frantz et al., 2010; Mouw et al., 2014). ECM binds to soluble growth factors to control their localization, function and presentation to cells, and provides binding sites for cell-surface receptors, such as integrins and syndecans (Harburger and Calderwood 2009; Hynes, 2009; Rozario and DeSimone 2010). Through cell surface receptors, ECM is involved in the transmission of extracellular signals and in the regulation of gene transcription.

ECM is composed of proteoglycans (e.g., perlecan and decorin) and glycoproteins (e.g., collagens and non-collagenous proteins, including tenascins, laminins and fibronectin) (Frantz et al. 2010; Rozario and DeSimone 2010; Mouw et al., 2014). ECM proteins share common structural motifs, such as the Arg-Gly-Asp (RGD) sequence that is involved in the recognition and binding to cell surface receptors of the integrin family (Hynes, 2009; Rozario and DeSimone 2010). Collagen is the most abundant protein within the ECM and makes up 30% of the total protein mass of a multicellular animal (Frantz et al. 2010; Rozario and DeSimone 2010; Mouw et al., 2014). Another fibrous glycoprotein within the ECM is fibronectin (FN). FN is secreted as a soluble dimer and then assembled into insoluble elastic fibrils by cells. The fibrillar fibronectin is biologically active and is involved in cellular processes such as adhesion, migration, proliferation, and differentiation, as well as in development, wound healing and metastasis of tumor cells (Baneyx et al., 2002). Likewise, a structurally related ECM glycoprotein family, the tenascins can modulate cellular behavior such as cell migration during wound healing and tissue development (Tucker and Chiquet-Ehrismann, 2009).

The composition of the ECM varies among tissues or physiological states, such as normal versus cancer (Frantz et al., 2010; Mouw et al., 2014). Similar to soluble growth factors, the molecular composition and the physical properties of the matrix (e.g., stiffness, elasticity) can influence cell behavior and cell fate (Rozario and DeSimone 2010). The rigidity or compliance of the ECM plays an important role in the differentiation and organization of various tissues and organs. When mesenchymal stem cells were plated on collagen-coated acrylamide gels that possess the elasticity of brain, muscle or bone tissues they gave rise to neurogenic, myogenic and osteogenic cell fates, respectively (Engler et al., 2006). In the case of normal mammary epithelial cells, when cultured on a flexible ECM, such as a floating 3D collagen gel, they differentiate into tubules (Wozniak et al., 2003). On the other hand, when encountering a stiff ECM with high collagen concentration mammary epithelial cells obtain an undifferentiated, proliferative, and malignant phenotype (Wozniak et al., 2003; Paszek et al., 2005).

In addition, ECM is dynamically remodeled, and its molecular components are subjected to post-translational modifications that influence its tensile strength and elasticity (Butcher et al., 2009; Frantz et al., 2010). To maintain tissue homeostasis, ECM composition and remodeling are tightly controlled by secretion of various ECM proteins, enzymes and growth factors. FN, tenascins, collagens, proteoglycans, metalloproteinases (MMPs), tissue inhibitors of MMPs, lysyl oxidase (LOX) that crosslinks and stiffens the ECM, and transforming growth factor-β (TGF-β) which induces ECM gene transcription are crucial players in this regulatory process (Butcher et al., 2009; Hynes, 2009; Frantz et al., 2010; Mouw et al., 2014). Deregulation of the matrix remodeling circuit may alter ECM composition and organization, and promote diseases including solid tumors (Figure 1), the hardening of arterial walls, atherosclerosis, and fibrosis (Lessey et al., 2012). For instance, as a result of increased collagen production as well as crosslinking in the stroma, tumors are stiffer than the surrounding healthy tissue and cancers are often diagnosed by a change of tissue rigidity sensed by palpation (Huang and Ingber, 2005; Butcher et al., 2009; Levental et al., 2009). Furthermore, women with mammographically dense breast tissue (high relative ratio of

ECM collagen to adipose cell volume ratio) have a four- to six-fold increased risk of developing breast cancer, and stiff crosslinked collagen was shown to be a poor prognosis factor in breast cancer (Boyd et al., 1998; Boyd et al., 2011; Conklin et al., 2011).

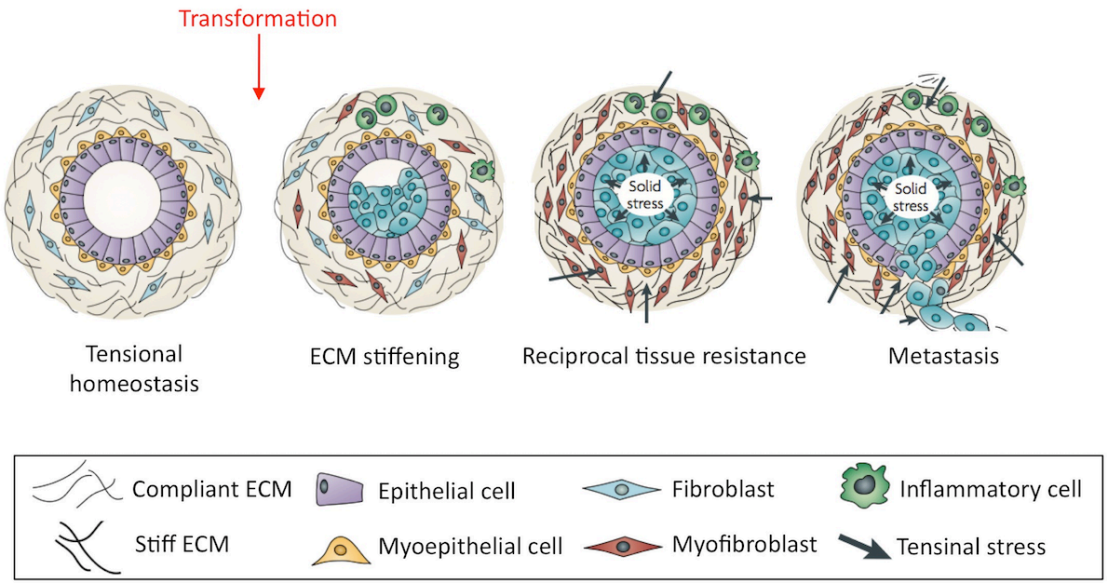


**Figure 1:** Increased extracellular matrix (ECM) stiffness compromises mechanoreciprocity and contributes to tumor progression in mammary tissue. Transformed epithelial cells secrete soluble factors that activate stromal cells and stimulate ECM remodeling and tissue stiffening. The activated stroma leads to increased survival and proliferation of tumor cells, and stimulate immune cell infiltration. The expanding tumor mass exerts outward projecting compression forces on the basement membrane. ECM balances these forces by an inward projecting resistance force. The modified tensional homeostasis facilitates tumor migration and invasion. (Adapted from Butcher et al., 2009).

### 1.1.2 Mechanotransduction through Rho GTPase signaling and its role in tumor progression

Rho family small GTPases, such as Rho, Rac, and Cdc42, are involved in multiple cellular events, including cell contraction and actin cytoskeleton organization, microtubule dynamics, cell polarity, cell migration, neurite outgrowth and cytokinesis (Amano et al., 2010). All members of the family have distinct roles in cytoskeletal organization. Rho regulates stress fiber formation and cell contraction; Rac and Cdc42 regulate the formation of lamellipodia and filopodia, respectively, and promote the formation of cell protrusions (Hall, 2005).

Under normal physiological conditions all cells are exposed to different types of mechanical forces and adapt to these forces by changing their cytoskeletal organization and by remodeling the microenvironment to re-establish the force equilibrium (Butcher et al., 2009; Lessey et al., 2012). The forces acting on cells can be cyclic, such as the blood flow, heartbeat or breathing, whereas others are sustained for varying periods of time (Butcher et al., 2009; Lessey et al., 2012). Endothelial cells and vascular smooth muscle cells lining blood vessels experience parallel forces, pulsatile stretching and shear forces during blood flow (Lessey et al., 2012; Burridge and Wittchen, 2013). Cells in the skeletal system (e.g. bones, joints, cartilage, ligaments) are exposed to perpendicular compression force (Lessey et al., 2012). Cells are able to sense these physical cues and translate them into biochemical signals, a phenomenon called cellular mechanotransduction. Mechanical signals are perceived and transmitted to the actin cytoskeleton through cell surface receptors of the integrin family that act as mechanoreceptors (Ridley and Hall, 1992; Wang et al., 1993; Chrzanowska-Wodnicka and Burridge, 1996). Mechanotransduction provides a finely regulated feedback circuit and enables a reciprocal interaction between the cells and their microenvironment.

To balance internal and external forces and to maintain tissue homeostasis, cells evaluate the exogenous mechanical signals within the tissue microenvironment and generate an endogenous tension. Multiple signaling pathways are involved in the integration of mechanical signals and generation of the reciprocal force response, and many of them converge in the activation of the small GTPase Rho (Lessey et al., 2012). Rho is responsible for the tension that is generated within the cells (Chrzanowska-Wodnicka and Burridge, 1996). Activation of Rho stimulates myosin contractility and results in actin stress fiber assembly (Ridley and Hall, 1992). Stress fibers consist of actin filaments, myosin II, and many other proteins, and are force-generating and tension-bearing structures (Burridge and Wittchen, 2013). Several downstream effector molecules of Rho, including the Rho-associated kinase (Rho-kinase/ROCK/ROK) and mDia are involved in these responses (Amano et al., 2010). ROCK and mDia act concurrently to facilitate actin stress fiber formation (Watanabe et al., 1999). The ratio of these two effector proteins is

reflected in the pattern of stress fibers; ROCK activity is associated with large condensed stress fibers, whereas mDia activity induces the assembly of filamentous F-actin (Watanabe et al., 1999). Once Rho is activated, it interacts with ROCK and activates it (Amano et al., 1996). The activated ROCK regulates myosin light chain (MLC) activity either directly by phosphorylation of the protein (Amano et al., 1996) or indirectly by phosphorylation and consequent inhibition of the MLC phosphatase (Kimura et al., 1996). The activation of MLC promotes assembly of myosin II, and generates a contractile force on actin filaments, which consequently results in the formation of stress fibers and focal adhesions (Figure 2) (Amano et al., 1996; Lessey et al., 2012; Burridge and Wittchen, 2013). Another downstream effector of Rho, focal adhesion kinase (FAK) is a non-receptor protein tyrosine kinase localized at focal adhesions and is involved in converting external mechanical input into chemical signals (Wang et al., 2001b). Upon phosphorylation at its autophosphorylation site, Y397, FAK is activated and localizes to focal adhesions, which occurs in a Rho-dependent manner (Clark et al., 1998). FAK and its associated signaling pathways act as mediators of cell cycle regulation (Zhao et al., 1998). Furthermore, FAK promotes cell motility, survival and proliferation, and drives tumor progression and metastasis (Sulzmaier et al., 2014).

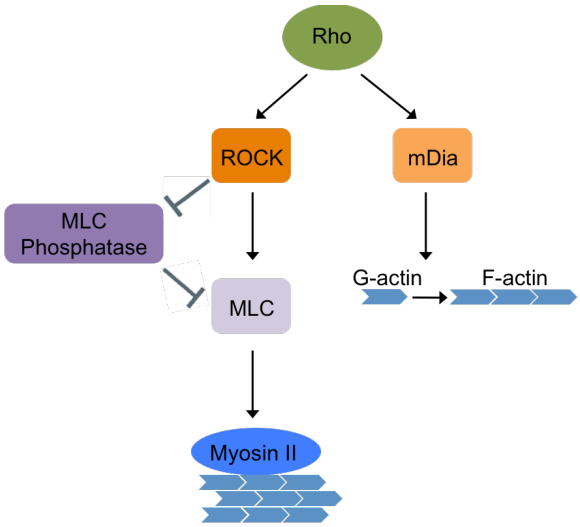


**Figure 2:** Rho GTPase signaling. Activated Rho mediates the formation of actin stress fibers through its downstream effector proteins ROCK (Rho-associated kinase) and mDia. ROCK regulates myosin light chain (MLC) activity either directly by activation of the protein or indirectly by inhibition of the MLC phosphatase. Activated MLC promotes assembly of myosin II with actin filaments and formation of actin stress fibers. mDia induces actin polymerization and formation of thin actin filaments. (Adapted from Lessey et al., 2012).

An injury or chronic inflammation may increase matrix stiffness and compromise the “mechanoreciprocity” between the cells and the ECM resulting in a sustained cytoskeletal tension, which in turn promotes the malignant transformation of a tissue (Paszek et al., 2005; Butcher et al., 2009). Matrix rigidity can expand flexible ECM proteins and uncover cryptic binding sites within them (Hynes, 2009). As a conseqeunce, the extended ECM proteins can bind to additional growth factors and receptors, which in turn enhances integrin expression (Yeung et al., 2005) and clustering, Rho/ROCK mediated cytoskeletal contractility, and subsequent focal adhesion and actin stress fiber formation at the cell-ECM contact sites. (Ridley and Hall, 1992; Chrzanowska-Wodnicka and Burridge, 1996; Bershadsky et al., 2003; Wozniak et al., 2003; Paszek et al., 2005; Vogel, 2006). The final response is increased FAK phosphorylation and cell proliferation (Wozniak et al., 2003).

When cells are grown on a stiff matrix they exhibit elevated Rho activity, increased number of focal adhesions, and higher tension compared to cells grown on a compliant ECM (Paszek et al., 2005). Rho stimulates cell cycle progression, increases cell proliferation, disrupts cell-cell junctions and cellular organization, and finally results in a “dedifferentiation phenotype” (Ridley and Hall, 1992; Chrzanowska-Wodnicka and Burridge, 1996; Paszek et al., 2005). Thus, activated Rho signaling through matrix stiffening facilitates tumor progression (Wozniak et al., 2003; Huang and Ingber, 2005; Paszek et al., 2005). On the contrary, a flexible matrix results in the downregulation of Rho and FAK activity, and subseqeunt differentiation of cells (Wozniak et al., 2003).

Similar to mechanical forces exerted exogenously on cells, it was shown that endogenous forces generated within the cells might activate mechanotransduction pathways and promote tumor growth and progression (Samuel et al., 2011). Conditional activation of ROCK in mouse skin results in generation of actomyosin contractile tension within the cell, which consequently elevates collagen deposition, increases tissue stiffness, and promotes β-catenin-mediated proliferation (Samuel et al., 2011). This study

underlines how an intermediate player of Rho GTPase signaling affects tissue homeostasis and tumor development (Samuel et al., 2011).

Rho GTPase signaling not only plays a role in cell proliferation and survival, but also in cell motility. The motility of eukaryotic cells is driven by the assembly and disassembly of actin filaments (Pollard and Borisy, 2003). Actin cytoskeleton reorganization enables cells to migrate in response to extracellular stimuli, and is required for the proper formation of organs and tissues during embryonic development (Olson and Sahai, 2009). In pathological situations like cancer, mechanical tension alters the mechanotransduction pathways and enhances the invasive behavior of tumor cells (Olson and Sahai, 2009).

Cells can move in different ways. They either migrate individually (mesenchymal and amoeboid/ rounded) or collectively as multicellular units maintaining their cell-cell contacts (Friedl and Wolf, 2009). The two distinct single-cell migration behaviors, mesenchymal and amoeboid are associated with different effectors of Rho GTPase signaling (Sahai and Marshall, 2003). Elevated Rho/ ROCK activity and consequent actomyosin contractile tension, as well as inhibition of matrix degrading enzymes induces amoeboid-like migration that is associated with invasion and metastasis (Sahai and Marshall, 2003; Friedl and Wolf, 2009). In contrast, low Rho activity is associated with amoeboid-to-mesenchymal transition (Friedl and Wolf, 2009). For instance, Sahai et al. showed that Smurf1 E3 ubiquitin ligase, which targets Rho for degradation is an important regulator of tumor cell migration (Sahai et al., 2007). Inhibition of Smurf1 leads to increased Rho activity changing the tumor cell morphology from mesenchymal to amoeboid and enhancing invasion into blood vessels (Sahai et al., 2007).

### 1.1.3 Megakaryoblastic leukemia protein 1 (MKL1): A link between the ECM and the nucleus

Megakaryoblastic leukemia protein 1 (MKL1), also known as megakaryocytic acute leukemia (MAL), myocardin-related transcription factor-A (MRTF-A) or basic SAP and coiled-coil (BSAC), belongs to the MRTF family and functions as a co-activator for serum response factor (SRF) to enhance SRF-dependent transcription (Wang et al., 2002; Scharenberg et al., 2010). SRF activates the expression of genes with CArG box-containing promoters and regulates several important biological processes including gastrulation and development, as well as actin cytoskeletal dynamics, survival and apoptosis at the cellular level (Olson and Nordheim, 2010).

MKL1 is expressed in a wide range of embryonic and adult tissues, with the most abundant expression in heart and liver (Wang et al., 2002). MKL1 knockout mice are viable, but females are unable to feed their offspring due to impaired mammary myoepithelial cell differentiation (Li et al., 2006; Sun et al., 2006). MKL1 was originally identified as a genomic fusion partner of RNA-binding motif protein 15 (RBM15), also known as OTT, in infant acute megakaryoblastic leukemia (AMKL), caused by chromosomal translocation t(1;22) (p13;q13) (Ma et al., 2001; Mercher et al., 2001). In addition to the involvement in AMKL, MKL1 has been implicated in actin-based cell adhesion, spreading, migration and invasion *in vitro* as well as in the colonization of tumor cells in an *in vivo* experimental metastasis assay (Medjkane et al., 2009). In support of the role of MKL1 in tumor progression, it was shown that suppressor of cancer cell invasion (SCAI), a negative regulator of invasive cell migration, binds to MKL1 and inhibits its transcriptional activity by forming a ternary complex with SRF (Brandt et al., 2009). Furthermore, MKL1 is involved in TGF-β-induced EMT via an interaction with Smad3 transcription factor (Morita et al., 2007). The MKL1-Smad3 complex has been reported to drive the expression of the *slug* gene, thereby inducing the dissociation of cell-cell contacts (Morita et al., 2007).

MKL1 shares common homology domains with other MRTF family members (Figure 3), including three highly conserved N-terminal Arg-Pro-X-X-X-Glu-Leu (RPEL) motifs, basic domains 1 and 2 (B1 and B2), glutamine-rich region (Q), SAP domain, leucine zipper-like region (LZ), and a C-terminal transactivation domain (TAD) (Scharenberg et al., 2010). MKL1 associates with SRF through its B1 domain and the adjacent Q domain; the RPEL domain mediates the interaction of MKL1 with globular actin (G-actin); basic regions, B1 and B2 are required for nuclear localization of MKL1 (Olson and Nordheim, 2010). Moreover, MKL1 contains a SAP domain, named after SAF-A/B, acinus and PIAS, a peptide motif found in several proteins known to contact DNA (Aravind and Koonin, 2000; Olson and Nordheim, 2010). Mutations in the SAP domain are shown to disrupt the ability of myocardin to activate a subset of SRF-dependent genes (Wang et al., 2001a), however deletion of this region had no obvious effect on the transcriptional activity of MKL1 and MKL1-SRF complex formation (Cen et al., 2003; Miralles et al., 2003). The LZ domain is involved in homo- and heterodimerization of myocardin and MKLs (Olson and Nordheim, 2010). The transcriptional activation domain, TAD is located at the C-terminal end of MKL1, and is required for the stimulation of SRF activity (Olson and Nordheim, 2010).

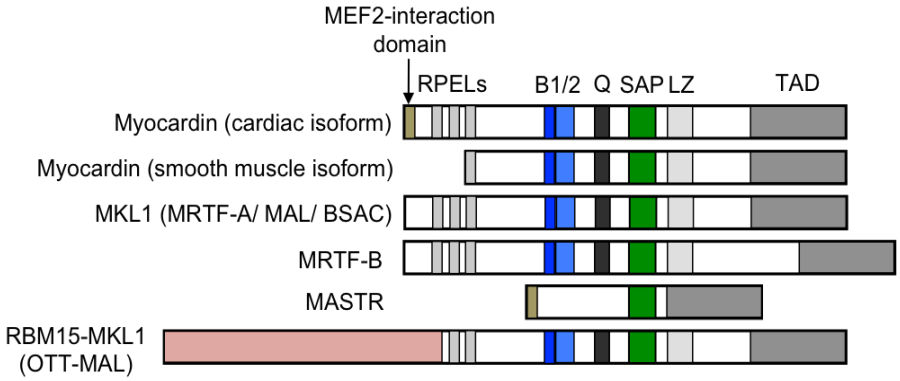


**Figure 3:** Structure of myocardin-related transcription factor (MRTF) family members. Functional homology domains are indicated. Abbreviations: RPEL: actin-binding motifs with Arg-Pro-X-X-X-Glu-Leu core consensus; B1 and B2: basic domains; Q: glutamine-rich domain; SAP: homology domain found in SAF-A/B, acinus, PIAS; LZ: leucine-zipper-like domain; TAD: transactivation domain. A cardiac-specific splice variant of myocardin (top row) contains a unique N-terminal sequence that is involved in the interaction with myocyte-specific enhancer factor 2 (MEF2) transcription factor, a MADS-box transcription factor related to serum response factor (SRF) (indicated by an arrow). This domain is present also in another member of MRTF family, MEF2-activating SAP transcriptional regulator (MASTR). MASTR lacks the basic domains and the glutamine-rich domain, which are involved in SRF interaction. The RBM15-MKL1 fusion protein observed in acute megakaryoblastic leukemia (AMKL) is shown at the bottom row. (Adapted from Olson and Nordheim, 2010).

The subcellular localization and following transcriptional activity of MKL1 is regulated by Rho GTPase signaling that transmits physical or biochemical extracellular signals to the actin cytoskeleton (Figure 4) (Butcher et al., 2009; Scharenberg et al., 2010). In unstimulated cells, MKL1 is sequestered in the cytoplasm by forming a stable complex with monomeric G-actin through its N-terminal RPEL motifs, but translocates into the nucleus upon serum-induced Rho GTPase pathway activation and subsequent F-actin formation (Ridley and Hall, 1992; Miralles et al., 2003; Olson and Nordheim, 2010). Nuclear G-actin also regulates the subcellular localization and the transcriptional activity of MKL1. Nuclear G-actin was shown to facilitate nuclear export of MKL1 and to prevent nuclear MKL1 from activating SRF target genes, unless actin binding is disrupted (Vartiainen et al., 2007). Thus, cellular G-actin regulates MKL1 at three levels: nuclear import, nuclear export and nuclear activation or inactivation of MKL1-SRF-dependent transcription (Vartiainen et al., 2007).

Every stimulus that activates Rho GTPase signaling, including mechanical force, triggers the nuclear accumulation and consequent transcriptional activity of MKL1. Not surprisingly, it was observed that MKL1 translocates from the cytoplasm to the nucleus when strain is applied to rat cardiac fibroblasts (Zhao et al., 2007) and to mouse embryonic fibroblasts (Maier et al., 2008) *in vitro* or in mechanically overloaded rat bladders *in vivo* (Hanna et al., 2009). Additionally, mechanical strain-induced expression of the ECM protein tenascin-C (TNC) depends on Rho GTPase/ actin signaling pathway (Chiquet et al., 2004; Sarasa-Renedo et al., 2006; Maier et al., 2008). Previous work from our group revealed that MKL1 regulates the mechanical strain-induced TNC expression in mouse fibroblasts as well as in normal and transformed mouse mammary epithelial cells (Asparuhova et al., 2011). TNC induction by MKL1 required the SAP domain of MKL1, but was independent of SRF interaction, demonstrating for the first time the role of MKL1 as a *bona fide* transcription factor (Asparuhova et al., 2011).

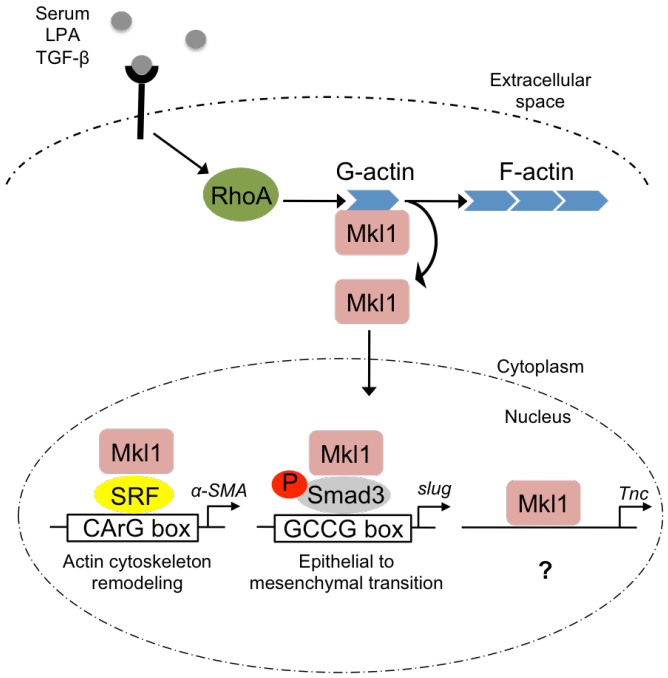


**Figure 4:** Megakaryoblastic leukemia protein 1 (MKL1) is a mediator of Rho GTPase/ actin signaling pathway and links the extracellular matrix to the nucleus. The subcellular localization and following transcriptional activity of MKL1 is regulated through its interaction with G-actin. Extracellular stimuli (e.g. lysophosphatidic acid (LPA), serum, transforming growth factor-β (TGF-β)) can activate Rho signaling. Activated Rho induces actin polymerization and results in the nuclear translocation of MKL1. MKL1 acts as transcriptional co-activator of serum response factor (SRF) and is involved in the regulation of cytoskeletal dynamics. Furthermore, MKL1 plays a role in epithelial to mesenchymal transition via an interaction with Smad3 transcription factor. In addition to its transcriptional coactivator function of SRF and Smad3, previous studies from our group revealed that MKL1 may act as a *bona fide* transcription factor mediating SRF-independent induction of tenascin-C (TNC) transcription (Asparuhova et al., 2011). (Adapted from Cen et al., 2004; Morita et al., 2007).

### 1.1.4 The role of the tumor stroma in cancer

In 1889, the English surgeon Stephen Paget proposed the “seed and soil” hypothesis to explain why disseminating tumor cells tend to metastasize to specific organs, independently of the vascular anatomy and the rate of blood flow (Paget, 1889). Paget compared the cells of the primary tumor to the seeds of a plant, and the affected organs to the soil, which provides the fertile environment for the metastatic tumor growth.

Today it has been widely accepted that cancer and metastasis are not only a result of genetic alterations or dysregulation of signaling pathways within the tumor cells, but also products of the reciprocal interaction between the tumor cells and the surrounding tumor stroma through cell-cell contacts and

paracrine signals (Figure 5) (Fidler, 2003; Mueller and Fusenig, 2004; Huang and Ingber, 2005; De Wever et al., 2008). The tumor stroma consists of fibroblasts, endothelial cells, pericytes, inflammatory cells, immunocytes, macrophages, and adipocytes, and provides the connective-tissue framework of the tumor (cf. Figure 1; Mueller and Fusenig, 2004; Kalluri and Zeisberg, 2006; De Wever et al., 2008; Joyce and Pollard, 2009; Psaila and Lyden, 2009). Malignant cells interact with their “niche”, the specialized local tissue microenvironment that supports tumor maintenance and growth at the primary tumor and at secondary metastatic sites (Psaila and Lyden, 2009).

Cancer cells secrete growth factors, including fibroblast growth factor (FGF), vascular endothelial growth factor (VEGF), platelet-derived growth factor, interleukins, colony-stimulating factors, and TGF-β, thus activate the stromal cells (Mueller and Fusenig, 2004; Joyce and Pollard, 2009). As a result, the “reactive tumor stroma”, also known as desmoplasia supports the tumor progression through the stimulation of cancer-cell survival, proliferation, migration and invasion, as well as the activation of angiogenesis and the inflammatory response (Fidler, 2003; Mueller and Fusenig, 2004; Joyce and Pollard, 2009). Moreover, the tumor cells can modulate the ECM to support their growth at the metastatic niche by secreting TNC (Oskarsson et al., 2011) and LOX (Erler et al., 2009).

Reactive tumor stroma harbors different activated cell types including carcinoma-associated fibroblasts (CAFs) (Kalluri and Zeisberg, 2006; De Wever et al., 2008). CAFs are mesenchymal cells that express different markers, such as α-smooth-muscle actin, vimentin, desmin and fibroblast activation protein (Mueller and Fusenig, 2004; Kalluri and Zeisberg, 2006). Like tumor cells, CAFs can change the composition of the ECM and promote tumor progression as well as metastasis by secreting ECM proteins including collagens, SPARC (secreted protein acidic and rich in cysteine also known as osteonectin), FN, periostin and tenascins (Kalluri and Zeisberg, 2006; Malanchi et al., 2012; Oskarson and Massague, 2012; Junttila and Sauvage, 2013; Oskarsson, 2013). Furthermore, CAFs secrete MMPs, which are involved in ECM degradation and remodeling, as well as growth factors and

cytokines such as insulin-like growth factor 1, hepatocyte growth factor, VEGF, stromal-cell-derived factor 1 and TGF-β, which promote endothelial cell proliferation and angiogenesis, tumor-cell survival, migration and invasion (Li et al., 2003; De Wever et al., 2004; Mueller and Fusenig, 2004; Sato et al., 2004; Kalluri and Zeisberg, 2006; Joyce and Pollard, 2009; Junttila and Sauvage, 2013). Through the secretion of inflammatory cytokines CAFs induce an immune response within the tumor stroma. The paracrine interaction between the inflammatory cells and tumor cells involving the secretion of colony-stimulating factor 1 (CSF1), epidermal growth factor and their receptors, induces the migration of cancer cells towards perivascular macrophages and the consequent intravasation into the blood circulation (Joyce and Pollard, 2009).

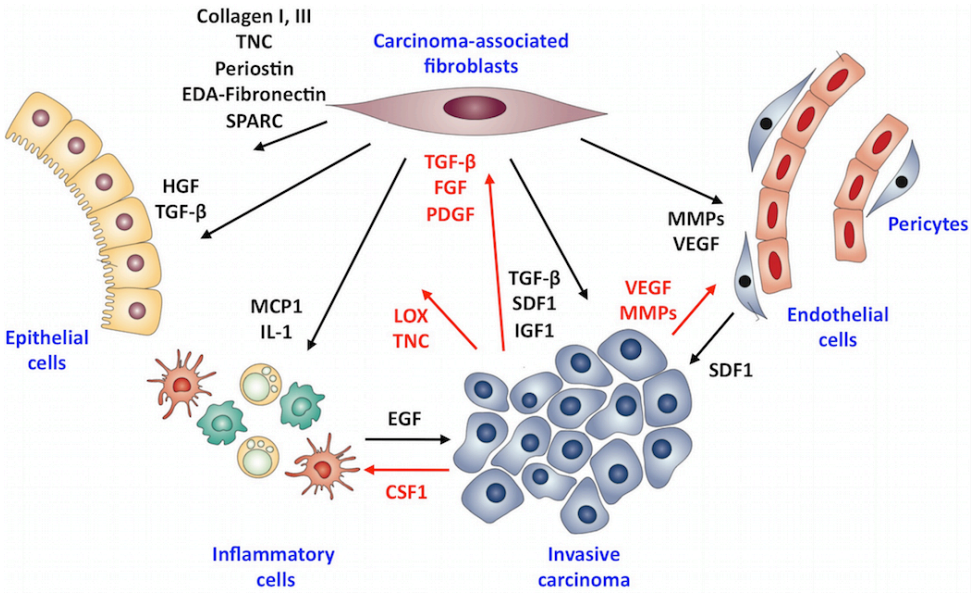


**Figure 5:** Reciprocal interactions within the tumor stroma contribute to tumor progression. Cancer cells modulate their microenvironment and activate the stroma through a variety of stroma-modulating proteins, including extracellular matrix (ECM) protein Tenascin-C (TNC), lysyl oxidase (LOX), metalloproteinases (MMPs), fibroblast growth factor (FGF), members of the vascular endothelial growth factor (VEGF) family, platelet-derived growth factor (PDGF), colony-stimulating factors (CSFs), and transforming growth factor-β (TGF-β). (Factors secreted by the tumor cells are indicated in red). Activated fibroblasts within the tumor stroma, carcinoma-associated fibroblasts (CAFs) communicate with cancer cells, endothelial cells, pericytes and inflammatory cells through secretion of ECM proteins (collagens, SPARC (secreted protein acidic and rich in cysteine), fibronectin that contains the extra domain a (EDA-fibronectin), periostin and TNC), growth factors (VEGF, insulin-like growth factor 1 (IGF1), hepatocyte growth factor (HGF), TGF-β and stromal-cell-derived factor 1 (SDF1)), inflammatory cytokines (monocyte chemotactic protein 1 (MCP1) and interleukin 1 (IL-1)), and MMPs. (Factors provided to tumor cells are indicated in black). In addition to CAFs, pericytes provide SDF1 to tumor cells to stimulate cancer-cell proliferation, migration and invasion. EGF: epithelial growth factor. (Adapted from Kalluri and Zeisberg, 2006).

The tumor microenvironment might serve as a potential therapeutic target. Combinatorial use of chemotoxic therapies with drugs that target the activated stroma might increase the efficiency of cancer treatment. Modulating tumor cell-stroma interaction through the inhibition of ECM receptors or by neutralizing paracrine growth factor and inflammatory cytokine signaling can reverse the malignant phenotype (Mueller and Fusenig, 2004; Junttila and Sauvage, 2013). For instance, in a breast cancer model, treatment of tumor cells with β1-integrin blocking antibody led to a morphological and functional reversion to a normal phenotype, and when these cells were injected into nude mice they had reduced number and size of tumors (Weaver et al., 1997). Furthermore, non-steroidal anti-inflammatory drugs have been used to inhibit the inflammatory cells and cytokines, and they have been shown to be an effective treatment regimen for colorectal cancer (Ricchi et al., 2003). On the other hand, MMP inhibitors, including tanomastat, marimastat and prinomastat, which were designed to maintain the ECM integrity were not beneficial over the standard-of-care treatments present in the clinic (Junttila and Sauvage, 2013).

Inhibition of angiogenesis by targeting VEGF signaling is an alternative approach for normalizing the tumor microenvironment (Goel and Mercurio, 2013). In high-grade glioma, a selective inhibitor of VEGF signaling downregulated tumor growth and tumor cell infiltration (Vajkoczy et al., 2000). A humanized monoclonal anti-VEGF antibody, bevacizumab (Avastin), is the first US Food and Drug Administration (FDA) approved molecule that targets VEGF pathway (Ferrara et al., 2004). In combination with other agents or as monotherapy, bevacizumab showed beneficial effects for the treatment of metastatic colorectal cancer, advanced non-small-cell lung cancer, metastatic renal cancer, ovarian cancer, advanced metastatic cervical cancer and recurrent glioblastoma multiforme (Junttila and Sauvage, 2013). However, recent preclinical studies have suggested that anti-angiogenic drugs targeting the VEGF pathway may accelerate metastasis and decrease the overall survival in mice indicating the development of an adaptive resistance (Ebos et al., 2009; Paez-Ribes et al., 2009). In line with these studies, some patients with recurrent malignant glioma treated with bevacizumab had more invasive

tumors (De Groot et al., 2010). On the other hand, a recent clinical study shows that VEGF receptor tyrosine kinase inhibitor, Sunitinib does not accelerate tumor growth and does not shorten patient survival (Blagoev et al., 2013). Alternatively, trastuzumab (herceptin), a monoclonal antibody against the cell surface receptor HER2 (human epidermal growth factor receptor-2) has been reported to reduce the diameter and volume of tumor blood vessels, as well as vascular permeability, and to slow down the tumor growth in an experimental breast cancer mouse model (Izumi et al., 2002). Besides, antibody-drug conjugates (ADCs) that enable targeted delivery of cytotoxic drugs with antibodies that selectively bind to tumor-associated antigens represent a promising strategy for increasing the therapeutic benefit for patients (Casi and Neri, 2012). Antigens expressed in the tumor stroma around the newly formed blood vessels are common targets in ADC technology. Antibodies against tumor vascular specific isoforms of FN (FN-EDB and FN-EDA) (Villa et al., 2008) and TNC (A1) (Brack et al., 2006) serve as promising candidates for the development of ADCs.

### 1.1.5 Radiation-induced modifications of the tumor microenvironment

Ionizing radiation therapy is used as a routine method in cancer treatment. Radiation causes DNA damage directly by ionization or indirectly by the generation of reactive oxygen species. As a result, tumor cells undergo p53-mediated apoptosis (Gudkov and Komarova, 2003). Furthermore, radiation induces apoptosis in tumor-associated endothelial cells, thus suppresses tumor angiogenesis and tumor growth (Ruegg et al., 2011). However, under certain circumstances, radiation exposure may alter the tissue microenvironment and contribute to metastasis. Radiation triggers several cellular mechanisms including ECM remodeling through the secretion of proteases, cytokines and growth factors, and recruitment of inflammatory cells (Barcellos-Hoff et al., 2005, Kuonen et al., 2012b). Furthermore, by suppressing angiogenesis, radiation results in hypoxia within the tumor tissue, which is associated with an aggressive tumor phenotype (Ruegg et al., 2011). Cancer cells that survive ionizing radiation can be radioresistant and cause tumor recurrence in cancer patients, and relapse after radiotherapy is often associated with increased local invasion, metastatic spread to lymph

nodes and distant organs, and poor prognosis (Ruegg et al., 2011; Li et al., 2014).

Experiments of different research groups revealed that the irradiated microenvironment induces the metastatic potential of tumor cells, a phenomenon that is known as “tumor bed effect” (Ruegg et al., 2011). When mammary epithelial cells were injected into the mammary fat pads of pre-irradiated mice, the tumor size and incidence was higher compared with non-irradiated hosts (Barcellos-Hoff and Ravani, 2000). Likewise, immortal myogenic cell lines have been reported to form tumors faster in irradiated than in non-irradiated host muscle (Morgan et al., 2002). Experimental tumors growing in irradiated tissues had a higher tendency to metastasize compared to tumors growing in a normal stroma (Milas et al., 1988). In another study, it was shown that ionizing radiation exposure induces senescence in human mammary stromal fibroblasts, alters the cytoskeletal network and upregulates ECM degrading MMP expression (Tsai et al., 2005). Furthermore, when breast carcinoma cells were grown with irradiated fibroblasts in three-dimensional co-culture they showed increased invasive growth (Tsai et al., 2005). Subcutaneous tumors growing within pre-irradiated mice had increased hypoxia and lung metastasis formation compared with tumors growing in non-irradiated control mice (Monnier et al., 2008). Cells derived from tumors grown in pre-irradiated beds preserved their metastatic capacity when injected into non-irradiated mice (Monnier et al., 2008). The study of Monnier et al. (2008) shows that pre-irradiated tumor stroma selects for tumor cells that have a high metastatic potential. CYR61/CCN1, the first member of the CCN matricellular protein family was identified as one of the genes linked to metastasis of tumor cells growing in a pre-irradiated bed (Monnier et al., 2008). Likewise, in an orthotopic breast cancer model, tumors growing in pre-irradiated mammary tissue had reduced angiogenesis and were more hypoxic, invasive, and metastatic to the lungs and to lymph nodes compared with control tumors (Kuonen et al., 2012a).

Previously it has been shown that prevention of apoptosis in endothelial cells attenuates the tumor response to radiotherapy (Garcia-Barros et al., 2003). Mauceri et al. (1998) reported that combined administration of ionizing radiation and anti-angiogenic treatment with angiostatin increases endothelial cell death *in vitro* and improves tumor management without increasing toxicity towards normal tissue (Mauceri et al., 1998). These results are clinically relevant. Anti-angiogenic drugs, such as bevacizumab that interfere with endothelial cell survival pathways and sensitize endothelial cells to ionizing radiation-induced death would improve the therapeutic response to radiotherapy (Wachsberger et al., 2004). On the other hand, anti-angiogenic therapies that reduce the blood supply might cause hypoxia within the tumor tissue and promote metastasis (Steeg, 2003).

Several signaling pathways have been reported to mediate tumor progression after radiotherapy (Kuonen et al., 2012b). The WNT/β-catenin pathway can be aberrantly activated by irradiation exposure, resulting in the transcription of β-catenin target genes (Kim et al., 2012). Aberrant activation of the WNT/β-catenin signaling pathway has been implicated in radioresistance in mammary progenitor cells (Chen et al., 2007) and in an orthotopic model of glioblastoma (Kim et al., 2012). Following irradiation, mammary progenitor cells displayed higher levels of β-catenin (Chen et al., 2007). Glioblastoma cells isolated from xenograft tumors after irradiation had a more aggressive phenotype compared with control tumor cells (Kim et al., 2012). Transcriptome analyses using glioblastoma xenograft tumors with or without *in vivo* ionizing radiation treatment revealed that Wnt pathway associated genes were activated upon irradiation (Kim et al., 2012). Among the differentially expressed genes, WNT1 inducible signaling pathway protein 1 (WISP1) showed the highest fold change (Kim et al., 2012). In line with these observations, upregulation of WISP1 was associated with poor clinical outcome in glioblastoma patients (Kim et al., 2012). A recent study shows that fractionated irradiation increases β-catenin activity and the expression of its target genes, including WISP1 in esophageal cancer cells (Li et al., 2014). WISP1 expression contributes to the development of fractionated irradiation-induced radioresistance (Li et al.,

2014). Future work will reveal further mechanistic details of how radiation contributes to tumor progression.

## 1.2 The family of CCN proteins

### 1.2.1 Functions and mechanism of action of CCN proteins:

ECM regulates cell behavior through different extracellular signaling molecules such as growth factors, cytokines, chemokines and extracellular enzymes, as well as directly by binding to and signaling through cell-surface receptors (Jun and Lau, 2011). A group of ECM proteins, known as matricellular proteins, are dynamically expressed and serve regulatory roles rather than contributing to the organization and structure of the vertebrate matrix (Bornstein and Sage, 2002; Jun and Lau, 2011). Thrombospondins, SPARC, hevin, osteopontin, tenascins, periostin, R-spondins, small leucine rich proteoglycans (SLRPs), the short fibulins including hemicentin, galectins, autotaxin, pigment epithelium derived factor (PEDF), plasminogen activator inhibitor-1 (PAI-1), and members of the CCN family are known matricellular proteins (Murphy-Ullrich and Sage, 2014). Matricellular proteins are usually expressed at high levels during development and in response to injury (Bornstein and Sage, 2002).

The acronym “CCN” is derived from the names of the first three members of the family: CYsteine-Rich 61 (CYR61) (O’Brien et al., 1990), Connective Tissue Growth Factor (CTGF) (Bradham et al., 1991) and Nephroblastoma OVer-expressed (NOV) (Joliot et al., 1992), which are named as CCN1, CCN2 and CCN3, respectively (Brigstock et al., 2003). Together with three WNT1 inducible signaling pathway proteins, WISP1/CCN4, WISP2/CCN5 and WISP3/CCN6 they comprise a family of six homologous proteins (Chapter 4.2, Supplementary Figure 1) (Pennica et al., 1998; Chen and Lau, 2009). CCN proteins contain a particularly high number of conserved cysteine residues, which corresponds to ~10% of the entire protein (Jun and Lau 2011).

Early studies raised the idea that CCN proteins are polypeptide growth factors (Bradham et al., 1991; Frazier et al., 1996). Later on, combined work within the CCN field defined CCNs as matricellular proteins that are involved in regulating cell-ECM interactions and cellular responses to extracellular stimuli (Leask and Abraham, 2006; Chen and Lau, 2009). CCN proteins regulate several cellular processes like cell adhesion, migration, proliferation, differentiation, apoptosis, survival, and senescence as well as ECM production and gene expression (Yeger and Perbal, 2007; Jun and Lau, 2011). At the organismal level, CCN proteins are implicated in embryogenesis, especially in cardiovascular, skeletal, renal and neuronal development (Chen and Lau, 2009; Jun and Lau, 2011). In postnatal development and in the adulthood, under normal situations CCN proteins are expressed at low levels in most tissues, however the expression increases upon inflammation, wound healing and fracture repair in bones and injury repair in many organs (Chen and Lau, 2009; Jun and Lau, 2011). Deregulation of CCN proteins results in various pathologies related to chronic inflammation and tissue injury, including arthritis, fibrosis and cancer, as well as cardiovascular diseases, diabetic nephropathy and retinopathy (Jun and Lau, 2011). The genes encoding CCN proteins are sensitive to growth factors, steroid hormones, and inflammatory cytokines such as interleukin 1 (IL-1) and tumor necrosis factor (TNF), as well as to environmental changes, like oxygen deprivation, ultraviolet light exposure, radiation, mechanical stress (e.g. mechanical stretch and tensile forces), and bacterial and viral infections (Chen and Lau, 2009; Jun and Lau, 2011).

Variants of CCN proteins have been detected in normal and pathological conditions, and some truncated CCNs were reported to serve as effective biomarkers for various diseases (Perbal, 2009). Alternative splicing (Hirschfeld et al., 2009; Perbal, 2009), proteolysis by MMPs (Dean et al., 2007) or post-translational modifications, such as glycosylation (Yang et al., 2011) are involved in the generation of different CCN isoforms with distinct biological functions.

CCN proteins mediate their activities through interaction with various cell surface receptors and co-receptors (Figure 6). These receptors include, many different integrins, heparan sulfate proteoglycans (e.g. syndecan 4), lipoprotein receptor-related proteins, and Notch (Segarani et al., 2001; Chen and Lau, 2009). Unlike many other ECM proteins, CCN proteins do not contain the canonical RGD sequence that is required for integrin binding. Instead, they possess non-canonical binding sites for adhesion receptors (Jun and Lau, 2011). CCN proteins can physically interact with other ECM proteins including FN (Chen et al., 2004; Hoshijima et al., 2006), perlecan (Nishida et al., 2003), vitronectin (Francischetti et al., 2010) and dermatan sulfate proteoglycans (e.g. decorin and biglycan) (Desnoyers et al., 2001). Moreover CCNs can modulate the activity and bioavailability of several growth factors and inflammatory cytokines through functional and/or physical interaction (Chen and Lau, 2009; Jun and Lau, 2011). Binding of CCN proteins to VEGF (Inoki et al., 2002), FGF-2 (Nishida et al., 2011), TGF-β (Abreu et al., 2002) and bone morphogenetic proteins (BMPs) (Abreu et al., 2002) has been reported.

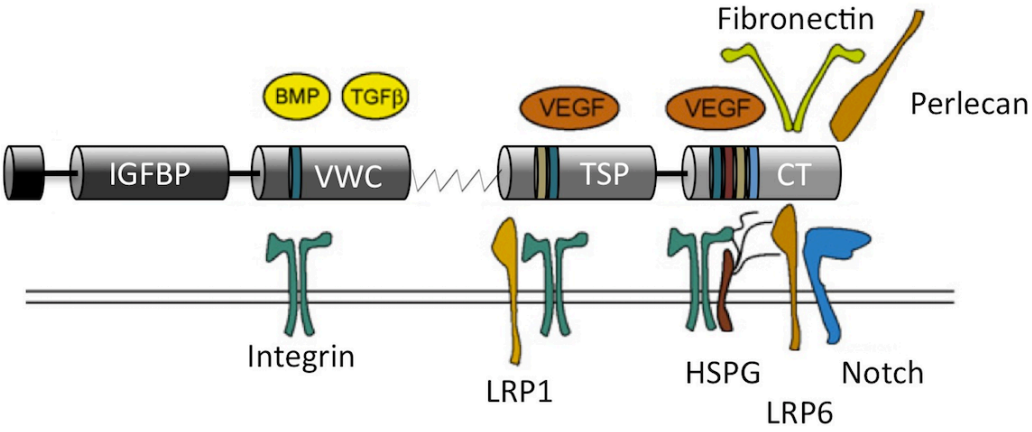


**Figure 6:** CCN proteins interact with various cell surface receptors and extracellular proteins. Interacting domains are shown. CCN2 binds to the extracellular matrix proteins, fibronectin and perlecan through its CT domain, as well as to growth factors such as bone morphogenetic proteins (BMPs) and transforming growth factor-β (TGF-β) through the VWC domain, and vascular endothelial growth factor (VEGF) through the TSP and CT domains. CCN3 has been shown to bind to Notch receptor through its CT domain. (Adapted from Chen and Lau, 2009).

### 1.2.2 CCN proteins in embryonic development

Targeted disruption of genes encoding CCN proteins in mice have been achieved. Among the different transgenic animals, the most commonly observed phenotype is defective cardiovascular and skeletal development (Chen and Lau, 2009; Jun and Lau, 2011). Targeted disruption of CCN1 results in embryonic lethality with severe cardiovascular defects in mice (Mo et al., 2002). CCN2-null mice are neonatal lethal due to respiratory defects that occur as a secondary cause of severe skeletal malformations (Ivkovic et al., 2003). Transgenic mice that produce mutant CCN3 lacking the VWC domain instead of the full length CCN3 have been constructed (Heath et al., 2008). Less than 50% of transgenic mice are viable and they show defects in the appendicular and axial skeleton, severe joint malformation, and abnormal remodeling of the endocardial cushions with associated cardiac septal defects (Heath et al., 2008). In another study, the entire CCN3 was inactivated by homologous recombination. CCN3-knockout (KO) animals were viable and mostly normal, exhibiting only modest and transient sexually dimorphic skeletal abnormalities (Canalis et al., 2010). WISP1/CCN4 KO mice show delayed wound healing and cartilage development compared to wildtype counterparts and they have lower expression levels of FN and Type I collagen (Seventh international workshop on the CCN family of genes, 2014) Moreover, dermal fibroblasts isolated from WISP1-KO mice show impaired cell proliferation and migration *in vitro*. Furthermore, WISP1 plays an important role in bone formation and maintenance. Conditional transgenic mice that overexpress human WISP1 in mineralized tissues have increased bone mineral density, trabecular thickness, and bone volume over wild-type controls (Ono et al., 2011). Mice were viable and no major abnormalities were observed, however female transgenics were unable to give birth (Ono et al., 2011). Alteration of CCN5 expression in either direction leads to embryonic lethality: both CCN5-null mice and transgenic mice overexpressing CCN5 do not implant properly and die at or before the gastrulation stage suggesting that CCN5 plays a critical role in early embryonic development (Russo and Castellot, 2010, mentioned as unpublished data). Loss-of-function mutations in the CCN6 gene in humans has been reported to cause autosomal recessive skeletal disease progressive pseudorheumatoid dysplasia, a

juvenile-onset degenerative disease of the joints (Hurvitz et al., 1999) However, CCN6-knockout mice or mice that overexpress CCN6 do not exhibit any observable phenotype compared to wildtype animals (Kutz et al., 2005).

### 1.2.3 CCN proteins in cancer and potential therapeutic approaches

Aberrant expression of CCN proteins have been identified in cancers of numerous organs and tissues, including breast, colorectal, gallbladder, gastric, ovarian, pancreatic, and prostate cancers, gliomas, hepatocellular carcinoma, non-small cell lung and squamous cell carcinoma, lymphoblastic leukemia, melanoma, and cartilaginous tumors (Chen and Lau, 2009).

CCN proteins can promote tumorigenesis and tumor progression by enhancing angiogenesis and stimulating tumor cell survival (Babic et al., 1998; Shimo et al., 2001; Chen and Lau, 2009). In particular, expression of CCN1 and CCN2 promotes tumor vascularization, EMT, and tumor cell survival through the induction of anti-apoptotic proteins (Jun and Lau, 2011). Furthermore, CCN2 has been identified as one of the genes overexpressed in human breast cancer cell lines with elevated osteolytic bone metastasis (Kang et al., 2003). In support of that, treatment of nude mice with an anti-CCN2 monoclonal antibody decreased osteolytic bone metastasis of human breast cancer cell xenografts (Shimo et al., 2006). Administration of a neutralizing CCN2-specific humanized monoclonal antibody, FG-3019 (FibroGen), attenuates tumor growth, lymph node metastasis, and tumor angiogenesis in xenograft (Dornhofer et al., 2006) and orthotopic (Aikawa et al., 2006) mouse models of pancreatic cancer. FG-3019 has been the subject of clinical trials in patients with idiopathic pulmonary fibrosis, liver fibrosis and pancreatic cancer (Yeger and Perbal, 2007). CCN3 expression has been associated with higher risk of developing metastasis and poor prognosis in Ewing's sarcoma (Perbal et al., 2009), melanoma (Vallacchi et al., 2008), and breast cancer (Ghayad et al., 2009). Likewise, aberrant WISP1/CCN4 expression has been associated with cancer. This is summarized and dicussed in our review entitled "CCN4/WISP1 (WNT1 inducible signaling pathway protein 1): a focus on its role in cancer" following this chapter.

Depending on the tumor type and tissue context, some tumor suppressive effects of CCN proteins have also been demonstrated (Jun and Lau, 2011). For instance, it was shown that CCN1 expression promotes growth arrest in non-small cell lung carcinoma cells *in vitro*, and when these cells are injected into the nude mice they form smaller tumors compared with the control cells (Tong et al., 2001). CCN2 inhibits metastasis and invasion of human lung adenocarcinoma (Chang et al., 2004), suppresses liver metastasis of colorectal cancer, and its expression is correlated with good prognosis (Lin et al., 2005). Ectopic expression of CCN3 inhibits the proliferation of glioma cells *in vitro* and tumor growth *in vivo* (Gupta et al., 2001). In the late nineties, WISP1/CCN4 was identified as Elm1 (expressed in low-metastatic cells) that can suppress the *in vivo* growth and metastatic potential of mouse melanoma cells (Hashimoto et al., 1998). CCN5, named COP1, has been reported to be a negative regulator of cell transformation (Zhang et al., 1998). Later, it has been shown that CCN5 reduces the proliferative and invasive phenotypes of poorly differentiated breast cancer cells and plays a role in maintaining the differentiated, non-invasive phenotype of these cells (Fritah et al., 2008). In breast adenocarcinoma, CCN5 mRNA and protein levels are reduced as the cancer progresses from a noninvasive to invasive type, and CCN5 expression is inversely correlated with lymph-node positivity (Banerjee et al., 2008). CCN6 has been reported to suppress *in vivo* tumor cell growth, invasion and angiogenesis, and it has been shown that loss of CCN6 expression contributes to inflammatory breast cancer phenotype (Kleer et al., 2002). Moreover, mice bearing CCN6 expressing tumors have a longer survival rate compared to the controls (Kleer et al., 2002).

### 1.2.4 CCN4/WISP1 (WNT1 inducible signaling pathway protein 1): A focus on its role in cancer

**Published Review**

The International Journal of Biochemistry & Cell Biology 2015, 62: 142-146

Molecules in Focus

Irem Gurbuz[a,b] and Ruth Chiquet-Ehrismann[a, b]

[a] Friedrich Miescher Institute for Biomedical Research, Novartis Research Foundation, Basel, Switzerland
[b] University of Basel, Faculty of Science, Basel, Switzerland

Corresponding author: Irem Gurbuz
Friedrich Miescher Institute for Biomedical Research
Maulbeerstrasse 66
CH-4058 Basel
Switzerland
Tel: +41 61 697 24 94
Email: irem.guerbuez@fmi.ch

The International Journal of Biochemistry & Cell Biology 62 (2015) 142–146

Contents lists available at ScienceDirect

The International Journal of Biochemistry & Cell Biology

journal homepage: www.elsevier.com/locate/biocel

Molecules in focus

# CCN4/WISP1 (WNT1 inducible signaling pathway protein 1): A focus on its role in cancer

Irem Gurbuz[a,b,*], Ruth Chiquet-Ehrismann[a,b]

[a] Friedrich Miescher Institute for Biomedical Research, Novartis Research Foundation, Basel, Switzerland
[b] University of Basel, Faculty of Science, Basel, Switzerland

ARTICLE INFO

*Article history:*
Received 30 October 2014
Received in revised form 6 March 2015
Accepted 9 March 2015
Available online 17 March 2015

*Keywords:*
WNT1 inducible signaling pathway protein 1
WISP
CCN
Cancer
Metastasis

ABSTRACT

The matricellular protein WISP1 is a member of the CCN protein family. It is induced by WNT1 and is a downstream target of β-catenin. WISP1 is expressed during embryonic development, wound healing and tissue repair. Aberrant WISP1 expression is associated with various pathologies including osteoarthritis, fibrosis and cancer. Its role in tumor progression and clinical outcome makes WISP1 an emerging candidate for the detection and treatment of tumors.



## 1. Introduction

The WNT1 inducible signaling pathway protein 1, also known as CCN4 or Elm1 is a cysteine-rich, matricellular protein that belongs to the CCN family (Hashimoto et al., 1998; Jun and Lau, 2011). The acronym "CCN" is derived from the names of the first three family members: CYsteine-Rich 61 (CYR61/CCN1), Connective Tissue Growth Factor (CTGF/CCN2) and Nephroblastoma OVer-expressed (NOV/CCN3) (Jun and Lau, 2011). WISP1 was originally identified as a downstream target of WNT1 and β-catenin, and contributes to β-catenin-mediated tumorigenesis (Pennica et al., 1998; Xu et al., 2000).

Deregulation of WISP1 signaling may result in various pathologies including osteoarthritis, fibrosis and cancer. In a previous review, the role of WISP1 in development and disease was discussed (Berschneider and Konigshoff, 2011). Here, we focus on the impact of WISP1 in tumor progression and summarize recent studies based on which WISP1 holds promise as a diagnostic marker and/or therapeutic target.

## 2. Structure

CCN proteins possess a conserved modular structure consisting of an amino-terminal secretory signal peptide followed by four structural domains: an insulin-like growth factor binding protein-like module (IGFBP), a von Willebrand factor type C repeat (VWC), a thrombospondin-homology type 1 repeat (TSP1), and a C-terminal cysteine-knot-containing (CT) domain (Jun and Lau, 2011). A non-conserved, protease-sensitive hinge region is located between VWC and TSP1 domains (Jun and Lau, 2011). Except CCN5, which lacks the CT module (Pennica et al., 1998), all CCN proteins contain the four complete structural modules (Fig. 1).

CCN protein variants that lack certain domains play distinct biological roles and have been implicated in several pathologies (Jun and Lau, 2011). Alternative splicing results in WISP1v lacking exon 3 and thus the VWC domain (Tanaka et al., 2001). This truncated variant has been detected in scirrhous gastric carcinoma (Tanaka et al., 2001) and invasive cholangiocarcinoma (Tanaka et al., 2003). Moreover, in addition to full length WISP1 and WISP1v, two hepatocellular carcinoma cell lines and a human chondrosarcoma-derived chondrocytic cell line express further shorter variants, WISP-1Δex3-4 (Cervello et al., 2004) and WISP1vx (Yanagita et al., 2007), respectively. Models of all described WISP1 variants are shown in Fig. 1.

The full length WISP1 protein consists of 367 aminoacids with a predicted molecular mass of 40 kDa, has 38 conserved cysteine

* Corresponding author at: Friedrich Miescher Institute for Biomedical Research, Maulbeerstrasse 66, CH-4058 Basel, Switzerland. Tel.: +41 61 697 24 94.
*E-mail address:* Irem.Guerbuez@fmi.ch (I. Gurbuz).

http://dx.doi.org/10.1016/j.biocel.2015.03.007

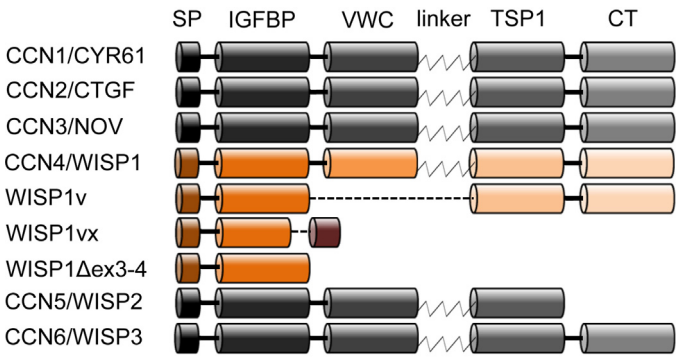


**Fig. 1.** Modular structure of CCN proteins. Full length CCN4/WISP1 and truncated variants are shown in orange. WISP1v is a gene product formed by alternative splicing that lacks exon 3, hence the VWC domain (Tanaka et al., 2001). WISP1vx lacks VWC and TSP1 domains and part of the IGFBP domain (23 bp shorter than the full-length exon). Owing to a frame-shift, the IGFBP/CT fusion coding frame is not translated properly after the alternative splice site. The protein product is a single IGFBP module, in which eight C-terminal amino acid residues are removed, and an extra 14 residues are added in their place (Yanagita et al., 2007). WISP1 Δex3-4 splice variant is a product of joining of exons 2 and 5 with a frameshift that led to a premature stop. As a result, the predicted protein has only the first module (Cervello et al., 2004). SP: signal peptide, IGFBP: insulin growth factor binding protein, VWC: van Willebrand Factor C, TSP1: thrombospondin type 1 repeat, CT: C-terminal domain. (For interpretation of the references to color in this figure legend, the reader is referred to the web version of this article.)

residues and four potential N-linked glycosylation sites (Pennica et al., 1998; Berschneider and Konigshoff, 2011). Indeed, it was observed that WISP1 is glycosylated and that the pattern of glycosylation differs between cancer cells and normal fibroblasts (discussed in Soon et al., 2003). Furthermore, overexpression of WISP1 in mammalian cells and external addition of the recombinant WISP1 produced in *Escherichia coli* (*E.coli*), lacking mammalian post-translational modifications, had different biological effects on cells (Inkson et al., 2008). According to these results, post-translational modifications seem to affect WISP1 function.

## 3. Regulation and biological function

WISP1 expression is regulated by different signaling pathways and is sensitive to different biochemical cues as well as extracellular perturbations. Previous work from our group showed that WISP1 is induced by megakaryoblastic leukemia protein 1 (Mkl1) in a serum response factor-independent, SAP domain-dependent manner and it was found to be part of a gene signature implicated in cell proliferation and motility elevated in breast cancer patients with poor survival (Gurbuz et al., 2014). Many genes of this signature, including WISP1 were shown to be mechano-responsive in cyclically stretched mouse mammary epithelial cells (Gurbuz et al., 2014). Furthermore, WISP1 was induced by mechanical stretch in lung alveolar epithelial cells (Heise et al., 2011). Additionally, cellular processes that modulate Wnt/β-catenin signaling regulate the expression of the downstream target genes, including WISP1. In a rat model of alcohol-induced liver disease, it was found that chronic alcohol feeding induces Wnt/β-catenin signaling and WISP1 upregulation, which in turn increases hepatocyte proliferation and promotes tumorigenesis (Mercer et al., 2014). A recent study shows that overexpression of WISP1 contributes to the development of fractionated irradiation-induced radioresistance in esophageal cancer cells *in vitro* and *in vivo*, and links WISP1 to radiation, a phenomenon that is known to activate Wnt/β-catenin signaling (Li et al., 2014).

CCN family members regulate complex biological processes during embryogenesis, wound healing and tissue repair (Berschneider and Konigshoff, 2011). WISP1 expression has been observed in the developing skeleton and during bone healing in the adulthood (French et al., 2004). WISP1 mRNA was detected in the adult heart, kidney, lung, pancreas, placenta, ovary, small intestine, and spleen. Low or no expression was seen in the brain, liver, skeletal muscle, colon, peripheral blood leukocytes, prostate, testis, or thymus (Pennica et al., 1998). WISP1 knockout (KO) mice show delayed wound healing and cartilage development compared to wildtype mice (Seventh international workshop on the CCN family of genes, 2014). Many reports support a function of WISP1 in tumor cell proliferation, migration and survival *in vitro*, as well as tumor growth and metastasis *in vivo*.

Recombinant WISP1 (Source: *E. coli*) treatment is shown to promote mitosis in irradiated esophageal cancer cells (Li et al., 2014) and in human bone marrow stromal cells (hBMSCs; Inkson et al., 2008). Likewise, recombinant WISP1 treatment (Source: mouse myeloma cells) induces proliferation of alveolar epithelial cells and adenocarcinomic human alveolar basal epithelial cells (Konigshoff et al., 2009). Overexpression of WISP1 variants increases the growth rate of mouse embryonic fibroblasts (Tanaka et al., 2001), rat kidney fibroblasts (Xu et al., 2000), hBMSCs (Inkson et al., 2008) and human esophageal cancer cells (Nagai et al., 2011). Dermal fibroblasts isolated from KO mice show impaired cell proliferation and migration *in vitro* (Seventh international workshop on the CCN family of genes, 2014). This seems to be different for melanoma cells. Mouse melanoma cells expressing a high level of WISP1 showed slightly slower *in vitro* and *in vivo* growth rates than cells expressing a low level of the protein (Hashimoto et al., 1998). Furthermore, a recent study shows that supplementation of recombinant WISP1 (Source: mouse myeloma cells) in the culture medium has an inhibitory effect on melanoma cell growth while migration is not affected (Shao et al., 2011). The number of migrated gastric carcinoma cells (Tanaka et al., 2001) and cholangiocarcinoma cells (Tanaka et al., 2003) increased with exposure to WISP1v. Human prostate cancer cells (Ono et al., 2013) and chondrosarcoma cells (Hou et al., 2011) show increased migration and invasion toward WISP1 recombinant protein (Source: *E. coli*), which suggests that WISP1 could have chemotactic properties and might influence the homing of cancer cells in case of metastasis. In support of these results, it was reported that recombinant WISP1 treatment (Source: mouse myeloma cells) induces epithelial to mesenchymal transition by regulating marker gene expression and by increasing cell migration (Konigshoff et al., 2009). In contrast, WISP1 overexpression in lung cancer cells leads to an inhibition of *in vitro* cell invasion and motility, as well as lung metastasis (Soon et al., 2003).

How exactly WISP1 modulates cellular function and through which receptors it transmits signals is unknown. Different integrins have been identified as functional receptors for some CCN proteins (Jun and Lau, 2011). Recent studies have confirmed the functional and physical interaction of WISP1 with integrins. It was shown that WISP1 physically interacts with α5β1 Integrin, and that its overexpression increases α5 expression in bone marrow stromal cells (Ono et al., 2011). Two other binding partners of WISP1 are decorin and biglycan, members of a family of small leucine-rich proteoglycans present in the extracellular matrix of connective tissue (Desnoyers et al., 2001).

## 4. Expression in cancer and role in prognosis

CNN proteins are aberrantly expressed in numerous diseases, including cancer (Jun and Lau, 2011). Generally, WISP1 expression has been associated with the promotion of tumor progression, and in a range of tumor types high WISP1 expression has been identified within the tumor tissue compared to the healthy organ (summarized in Table 1). Likewise, transcript profiling studies available from the Oncomine database reveal increased WISP1 transcript levels in a wide variety of cancers (Fig. 2). Moreover, WISP1 correlates with poor prognosis in the majority of cancer incidences.

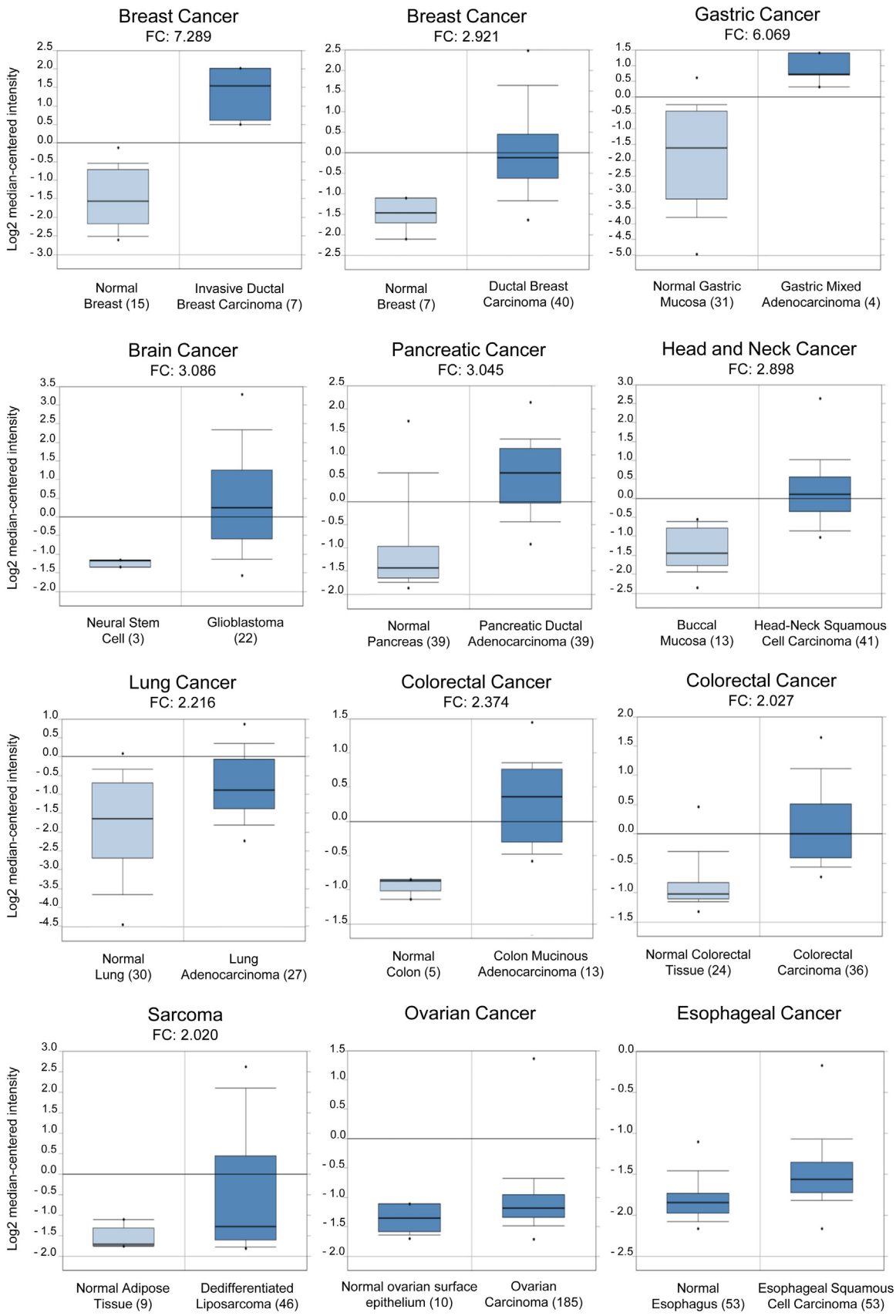


**Fig. 2.** Aberrant WISP1 expression has been identified in different tumor types. Oncomine differential gene expression analysis (Normal vs Cancer, Human Genome U133 Affymetrix Array data, Affymetrix Probe ID: 206796_at, www.oncomine.org) revealed that WISP1 mRNA expression levels are higher within tumor tissue compared with normal tissue in most of the cancer incidences. Results are represented with a box plot: the thick line represents the median value. Minimal and maximal values are plotted as dots. Fold changes (FC) between normal and tumor tissues are indicated. Number of samples analyzed is shown within brackets.

**Table 1**

| Cancer type | Expression level tumor versus normal | Correlation of WISP1 level with prognosis | Reference |
|---|---|---|---|
| Breast Cancer | Higher<br>Not known<br>Higher | Bad<br>Good<br>Not known | Xie et al. (2001), Davies et al. (2007), Klinke (2014) |
| Gastric Adenocarcinoma | Higher | Not known | Bizama et al. (2014) |
| Brain Cancer | Higher | Bad | Xie et al. (2004) |
| Pancreatic Cancer | Higher | Not known | Cao et al. (2004), Badea et al. (2008) |
| Head and Neck Cancer | Higher | Not known | Chuang et al. (2013) |
| Lung Adenocarcinoma | Higher | Not known | Chen et al. (2007), Yang et al. (2014) |
| Colorectal Cancer | Higher | Good<br>Bad | Khor et al. (2006), Davies et al. (2010) |
| Rectal Cancer | Higher | Bad | Tian et al. (2007) |
| Colon Adenocarcinoma | Higher | Not known | Pennica et al. (1998) |
| Chondrosarcoma | Higher | Not known | Hou et al. (2011) |
| Endometrial Endometrioid Carcinoma | Higher | Bad | Tang et al. (2011) |
| Esophageal Cancer | Higher | Bad | Nagai et al. (2011) |
| Scirrhous Carcinoma | Higher | Not known | Tanaka et al. (2001) |
| Cholangiocarcinoma | Higher | Bad | Tanaka et al. (2003) |
| Prostate Cancer | Higher | Good | Ono et al. (2013) |
| Melanoma | Lower | Not known | Shao et al. (2011) |
| Aggressive Fibromatosis | Higher | Bad | Skubitz and Skubitz (2004), Misemer et al. (2013) |

Publication details only provided for reports that are not listed under References: Badea et al. (2008) Hepatogastroenterology 55(88): 2016–2027; Bizama et al. (2014) Int J Cancer 134(4): 755–764; Cao et al. (2004) Cancer Biol Ther 3(11): 1081–1089; Chen et al. (2007) PLoS One 2(6): e534; Chuang et al. (2013). PloS One 8(10): e78022; Klinke (2014) PLoS Comput Biol 10(1): e1003409; Misemer et al. (2014) Cancer Med 3(1): 81–90; Skubitz and Skubitz (2004) J Lab Clin Med 143(2): 89–98; Tang et al. (2011) J Obstet Gynaecol Res 37(6): 606–612; Xie et al. (2004) Clin Cancer Res 10(6): 2072–2081; Yang et al. (2014) Cancer Gene Ther 21(2): 74–82.

Exceptionally, WISP1 levels in the primary prostate cancer stroma and in the patient's sera decreases with increasing severity of the cancer (Ono et al., 2013). In some cancers a role for WISP1 levels in prognosis is controversial. For example, two independent studies show that higher level of WISP1 is associated with poor histological differentiation, tumor aggressiveness and poor clinical outcome in colorectal and rectal carcinomas (Tian et al., 2007; Davies et al., 2010). In contrast, Khor et al. (2006) links WISP1 expression to well-differentiated colorectal tumors. A similar discrepancy is seen when analyzing WISP1 expression in breast cancer. Davies et al. (2007) show that the transcript levels are lower in node-positive and high-grade tumors and in patients with poor clinical outcome. These results contradict a previously published study where it was shown that high WISP1 mRNA levels correlate with an advanced stage of breast cancer (Xie et al., 2001).

The crosstalk between tumor cells and the tumor stroma has a remarkable impact on tumor progression. Cancer cells secrete growth factors and proteases to activate surrounding stromal cells to form a supportive environment for tumor progression (Mueller and Fusenig, 2004). Activated fibroblasts, also known as carcinoma-associated fibroblasts (CAFs), in turn modulate the tumor microenvironment by secreting extracellular matrix proteins and matrix degrading enzymes (Mueller and Fusenig, 2004). WISP1 is upregulated in CAFs compared with fibroblasts in the adjacent normal tissue in colon cancer (Rupp et al., 2014) and in breast cancer (Bauer et al., 2010). In many cancers and in WNT1 transgenic mice, WISP1 is localized to the tumor stroma surrounding the cancer cells (Pennica et al., 1998; Tanaka et al., 2001, 2003; Bauer et al., 2010; Ono et al., 2013; Rupp et al., 2014). WISP1 overexpressing rat kidney fibroblasts are not able to form colonies in the soft agar, however when they are injected into nude mice they form tumors (Xu et al., 2000). These results suggest that the paracrine interactions may have a positive regulatory effect on tumor growth and progression. In contrast, Shao et al. (2011) show that WISP1 expression is stronger in quiescent fibroblasts compared with melanoma cells and "melanoma activated fibroblasts", which suggest a negative regulatory effect of paracrine WISP1 signaling in melanoma.

## 5. Possible applications in cancer diagnosis and therapy

The differential expression status of WISP1 between the tumor tissue and normal healthy tissue, as well as the correlation of its expression with clinical outcome makes WISP1 a promising target for the evaluation of clinical diagnosis and prognosis of cancers.

In particular, WISP1 could be exploited to predict different stages of prostate cancer and thus serve as an alternative biomarker to Prostate Specific Antigen (Ono et al., 2013). In early stages of prostate cancer, WISP1 was detected not only in tissue biopsies but also in sera from patients (Ono et al., 2013). In the future, WISP1 might be used as a tumor marker that is easy to detect by a simple blood test.

In addition to its diagnostic potential, WISP1 can be utilized as a therapeutic target. Targeting WISP1 by neutralizing antibodies negatively regulates progression of certain cancers, including prostate cancer and recurrent esophageal carcinoma after radiotherapy. In mouse xenograft models of human prostate cancer cells, treatment with WISP1 neutralizing antibodies reduces tumor growth as well as metastasis to bone (Ono et al., 2013). In another study, depletion of WISP1 by neutralizing antibodies cause mitotic catastrophe in radioresistant esophageal cancer cells without affecting normal cancer cells (Li et al., 2014). Blocking WISP1 interaction with its partners, such as cancer-associated integrins, might be another therapeutic strategy to inhibit WISP1-mediated tumor progression. Furthermore, finding ways to down-regulate its expression might open new treatment opportunities. Since WISP1 expression is known to be induced by Wnt/β-catenin signaling as well as by mechanical signals mediated by Mkl1, drugs constraining these pathways may help to alleviate WISP1-mediated effects on cancer progression.

## Acknowledgments

We apologize to those whose primary work we were unable to include in this review due to constraints on length and scope. This work was supported by the Swiss National Science Foundation

grants number NF31003A_120235 and NF31003A_135584 as well as from the Swiss Cancer League grant number KFS-2980-08-2012.

## References


Bauer M, Su G, Casper C, He R, Rehrauer W, Friedl A. Heterogeneity of gene expression in stromal fibroblasts of human breast carcinomas and normal breast. Oncogene 2010;29:1732–40.

Berschneider B, Konigshoff M. WNT1 inducible signaling pathway protein 1 (WISP1): a novel mediator linking development and disease. Int J Biochem Cell Biol 2011;43:306–9.

Cervello M, Giannitrapani L, Labbozzetta M, Notarbartolo M, D'Alessandro N, Lampiasi N, et al. Expression of WISPs and of their novel alternative variants in human hepatocellular carcinoma cells. Ann NY Acad Sci 2004;1028:432–9.

Davies SR, Watkins G, Mansel RE, Jiang WG. Differential expression and prognostic implications of the CCN family members WISP-1, WISP-2, and WISP-3 in human breast cancer. Ann Surg Oncol 2007;14:1909–18.

Davies SR, Davies ML, Sanders A, Parr C, Torkington J, Jiang WG. Differential expression of the CCN family member WISP-1, WISP-2 and WISP-3 in human colorectal cancer and the prognostic implications. Int J Oncol 2010;36:1129–36.

Desnoyers L, Arnott D, Pennica D. WISP-1 binds to decorin and biglycan. J Biol Chem 2001;276:47599–607.

French DM, Kaul RJ, D'Souza AL, Crowley CW, Bao M, Frantz GD, et al. WISP-1 is an osteoblastic regulator expressed during skeletal development and fracture repair. Am J Pathol 2004;165:855–67.

Gurbuz I, Ferralli J, Roloff T, Chiquet-Ehrismann R, Asparuhova MB. SAP domain-dependent Mkl1 signaling stimulates proliferation and cell migration by induction of a distinct gene set indicative of poor prognosis in breast cancer patients. Mol Cancer 2014;13:22.

Hashimoto Y, Shindo-Okada N, Tani M, Nagamachi Y, Takeuchi K, Shiroishi T, et al. Expression of the Elm1 gene, a novel gene of the CCN (connective tissue growth factor, Cyr61/Cef10, and neuroblastoma overexpressed gene) family, suppresses In vivo tumor growth and metastasis of K-1735 murine melanoma cells. J Exp Med 1998;187:289–96.

Heise RL, Stober V, Cheluvaraju C, Hollingsworth JW, Garantziotis S. Mechanical stretch induces epithelial–mesenchymal transition in alveolar epithelia via hyaluronan activation of innate immunity. J Biol Chem 2011;286:17435–44.

Hou CH, Chiang YC, Fong YC, Tang CH. WISP-1 increases MMP-2 expression and cell motility in human chondrosarcoma cells. Biochem Pharmacol 2011;81:1286–95.

Inkson CA, Ono M, Kuznetsov SA, Fisher LW, Robey PG, Young MF. TGF-beta1 and WISP-1/CCN-4 can regulate each other's activity to cooperatively control osteoblast function. J Cell Biochem 2008;104:1865–78.

Jun JI, Lau LF. Taking aim at the extracellular matrix: CCN proteins as emerging therapeutic targets. Nat Rev Drug Discov 2011;10:945–63.

Khor TO, Gul YA, Ithnin H, Seow HF. A comparative study of the expression of Wnt-1, WISP-1, survivin and cyclin-D1 in colorectal carcinoma. Int J Colorectal Dis 2006;21:291–300.

Konigshoff M, Kramer M, Balsara N, Wilhelm J, Amarie OV, Jahn A, et al. WNT1-inducible signaling protein-1 mediates pulmonary fibrosis in mice and is upregulated in humans with idiopathic pulmonary fibrosis. J Clin Investig 2009;119:772–87.

Li WF, Zhang L, Li HY, Zheng SS, Zhao L. WISP-1 contributes to fractionated irradiation-induced radioresistance in esophageal carcinoma cell lines and mice. PLoS ONE 2014;9:e94751.

Mercer KE, Hennings L, Sharma N, Lai K, Cleves MA, Wynne RA, et al. Alcohol consumption promotes diethylnitrosamine-induced hepatocarcinogenesis in male mice through activation of the Wnt/beta-catenin signaling pathway. Cancer Prev Res 2014;7:675–85.

Mueller MM, Fusenig NE. Friends or foes – bipolar effects of the tumour stroma in cancer. Nat Rev Cancer 2004;4:839–49.

Nagai Y, Watanabe M, Ishikawa S, Karashima R, Kurashige J, Iwagami S, et al. Clinical significance of Wnt-induced secreted protein-1 (WISP-1/CCN4) in esophageal squamous cell carcinoma. Anticancer Res 2011;31:991–7.

Ono M, Inkson CA, Kilts TM, Young MF. WISP-1/CCN4 regulates osteogenesis by enhancing BMP-2 activity. J Bone Miner Res 2011;26:193–208.

Ono M, Inkson CA, Sonn R, Kilts TM, de Castro LF, Maeda A, et al. WISP1/CCN4: a potential target for inhibiting prostate cancer growth and spread to bone. PLoS ONE 2013;8:e71709.

Pennica D, Swanson TA, Welsh JW, Roy MA, Lawrence DA, Lee J, et al. WISP genes are members of the connective tissue growth factor family that are up-regulated in wnt-1-transformed cells and aberrantly expressed in human colon tumors. Proc Natl Acad Sci U S A 1998;95:14717–22.

Rupp C, Scherzer M, Rudisch A, Unger C, Haslinger C, Schweifer N, et al. IGFBP7, a novel tumor stroma marker, with growth-promoting effects in colon cancer through a paracrine tumor-stroma interaction. Oncogene Adv Online Publ 2014., http://dx.doi.org/10.1038/onc.2014.18.

Seventh international workshop on the CCN family of genes. J Cell Commun Signal 2014;8:77–92.

Shao H, Cai L, Grichnik JM, Livingstone AS, Velazquez OC, Liu ZJ. Activation of Notch1 signaling in stromal fibroblasts inhibits melanoma growth by upregulating WISP-1. Oncogene 2011;30:4316–26.

Soon LL, Yie TA, Shvarts A, Levine AJ, Su F, Tchou-Wong KM. Overexpression of WISP-1 down-regulated motility and invasion of lung cancer cells through inhibition of Rac activation. J Biol Chem 2003;278:11465–70.

Tanaka S, Sugimachi K, Saeki H, Kinoshita J, Ohga T, Shimada M, et al. A novel variant of WISP1 lacking a Von Willebrand type C module overexpressed in scirrhous gastric carcinoma. Oncogene 2001;20:5525–32.

Tanaka S, Sugimachi K, Kameyama T, Maehara S, Shirabe K, Shimada M, et al. Human WISP1v, a member of the CCN family, is associated with invasive cholangiocarcinoma. Hepatology 2003;37:1122–9.

Tian C, Zhou ZG, Meng WJ, Sun XF, Yu YY, Li L, et al. Overexpression of connective tissue growth factor WISP-1 in Chinese primary rectal cancer patients. World J Gastroenterol 2007;13:3878–82.

Xie D, Nakachi K, Wang H, Elashoff R, Koeffler HP. Elevated levels of connective tissue growth factor, WISP-1, and CYR61 in primary breast cancers associated with more advanced features. Cancer Res 2001;61:8917–23.

Xu L, Corcoran RB, Welsh JW, Pennica D, Levine AJ. WISP-1 is a Wnt-1- and beta-catenin-responsive oncogene. Genes Dev 2000;14:585–95.

Yanagita T, Kubota S, Kawaki H, Kawata K, Kondo S, Takano-Yamamoto T, et al. Expression and physiological role of CCN4/Wnt-induced secreted protein 1 mRNA splicing variants in chondrocytes. FEBS J 2007;274:1655–65.

### 1.3 Aim of the thesis:

Our lab is interested in understanding extracellular matrix (ECM)-cell interactions and the role of these interactions in cancer progression. Megakaryoblastic leukemia 1 (MKL1) belongs to myocardin related transcription factor family and functions as a co-activator for serum response factor (SRF) (Scharenberg et al., 2010). It plays role in diverse biological processes, including cell adhesion, spreading and motility (Medjkane et al., 2008). It has been shown that MKL1 is involved in tumor cell invasion and metastasis (Medjkane et al., 2008), and in transforming growth factor-β (TGF-β)-induced epithelial-mesenchymal transition (EMT) (Morita et al., 2007). Through Rho GTPase/ actin signaling pathway, MKL1 forms a link between the ECM and the nucleus and functions as a mediator of mechanotransduction. Previous work from our group revealed a novel function of MKL1 and showed that MKL1 may act as a *bona fide* transcription factor mediating SRF-independent, SAP-domain-dependent induction of Tenascin-C (TNC) transcription (Asparuhova et al., 2011). In the present study our goal is to identify additional SAP-domain dependent MKL1 target genes that are co-regulated with TNC and to investigate whether such genes are implicated in cancer progression. For our analyses we used mutant MKL1 constructs that were transfected into HC11 mouse mammary epithelial cells (Figure 7) (Asparuhova et al., 2011).

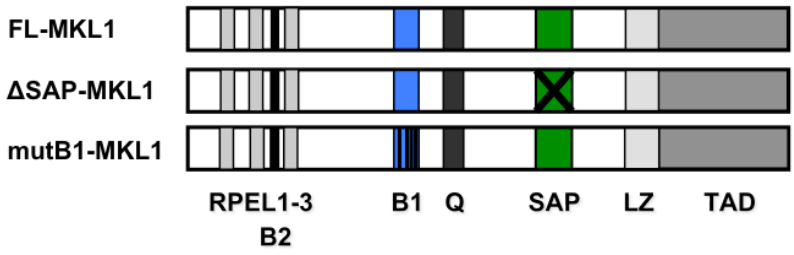


**Figure 7:** Mouse MKL1 constructs used in the study. The full-length constract contains all functional domains. mutB1 construct has a mutated B1 domain, which is involved in serum response factor interaction. ΔSAP constract lacks the SAP domain, which is the homology domain found in SAF-A/B, Acinus, PIAS. SAP domain is involved in DNA binding. (Adapted from Asparuhova et al., 2011).

## CHAPTER 2: RESULTS

### 2.1 Published Manuscript

"SAP domain-dependent Mkl1 signaling stimulates proliferation and cell migration by induction of a distinct gene set indicative of poor prognosis in breast cancer patients"

Irem Gurbuz, Jacqueline Ferralli, Tim Roloff, Ruth Chiquet-Ehrismann and Maria B Asparuhova

Molecular Cancer 2014, 13:22.

**My contribution:**

For this study, together with Maria B Asparuhova I designed and analyzed cell functional assays. I performed 5-bromo-2′-deoxyuridine (BrdU) incorporation assay to test the proliferation rate of HC11 cell strains. To investigate the cell motility, I performed Boyden Chamber migration assay. With the inputs of Jacqueline Ferralli and Maria B Asparuhova, I planned, performed and analyzed mechanical strain application experiments. Furthermore, I performed all qRT-PCR analyses and immunoblot experiments to test mRNA expression and protein expression, respectively. Finally, I contributed to the preparation of the manuscript.

MOLECULAR CANCER

RESEARCH Open Access

# SAP domain-dependent Mkl1 signaling stimulates proliferation and cell migration by induction of a distinct gene set indicative of poor prognosis in breast cancer patients

Irem Gurbuz[1,2], Jacqueline Ferralli[1], Tim Roloff[1], Ruth Chiquet-Ehrismann[1,2*] and Maria B Asparuhova[1]

## Abstract

**Background:** The main cause of death of breast cancer patients is not the primary tumor itself but the metastatic disease. Identifying breast cancer-specific signatures for metastasis and learning more about the nature of the genes involved in the metastatic process would 1) improve our understanding of the mechanisms of cancer progression and 2) reveal new therapeutic targets. Previous studies showed that the transcriptional regulator megakaryoblastic leukemia-1 (Mkl1) induces tenascin-C expression in normal and transformed mammary epithelial cells. Tenascin-C is known to be expressed in metastatic niches, is highly induced in cancer stroma and promotes breast cancer metastasis to the lung.

**Methods:** Using HC11 mammary epithelial cells overexpressing different Mkl1 constructs, we devised a subtractive transcript profiling screen to identify the mechanism by which Mkl1 induces a gene set co-regulated with tenascin-C. We performed computational analysis of the Mkl1 target genes and used cell biological experiments to confirm the effect of these gene products on cell behavior. To analyze whether this gene set is prognostic of accelerated cancer progression in human patients, we used the bioinformatics tool GOBO that allowed us to investigate a large breast tumor data set linked to patient data.

**Results:** We discovered a breast cancer-specific set of genes including tenascin-C, which is regulated by Mkl1 in a SAP domain-dependent, serum response factor-independent manner and is strongly implicated in cell proliferation, cell motility and cancer. Downregulation of this set of transcripts by overexpression of Mkl1 lacking the SAP domain inhibited cell growth and cell migration. Many of these genes are direct Mkl1 targets since their promoter-reporter constructs were induced by Mkl1 in a SAP domain-dependent manner. Transcripts, most strongly reduced in the absence of the SAP domain were mechanoresponsive. Finally, expression of this gene set is associated with high-proliferative poor-outcome classes in human breast cancer and a strongly reduced survival rate for patients independent of tumor grade.

**Conclusions:** This study highlights a crucial role for the transcriptional regulator Mkl1 and its SAP domain during breast cancer progression. We identified a novel gene set that correlates with bad prognosis and thus may help in deciding the rigor of therapy.

**Keywords:** Myocardin-related transcription factor-A (MRTF-A), Metastasis, Cancer progression, Prognosis, Gene regulation, Mechanical strain

* Correspondence: Ruth.Chiquet@fmi.ch
[1]Friedrich Miescher Institute for Biomedical Research, Maulbeerstrasse 66, Basel CH-4058, Switzerland
[2]Faculty of Science, University of Basel, Klingelbergstrasse 50, Basel CH-4056, Switzerland

## Background

Most breast cancer patients die from tumor metastases and not from the primary tumor itself. Thus, the identification of genes and signaling pathways influencing the metastatic process are of utmost importance. Once the mechanisms leading to metastasis are uncovered, they can in the future serve as a rational basis for prognosis and intervention. From the beginning of its discovery, tenascin-C has been strongly associated with tumorigenesis and cancer progression in many different types of tumors (reviewed in [1,2]). Tenascin-C was not only enriched in breast cancer tissue [3,4], but its high expression was part of a gene signature of breast cancers metastasizing to the lung [5]. There is strong evidence that tenascin-C contributes to the metastatic behavior of breast cancer cells [6] by providing a niche for their settlement in the lung [7,8]. The source of tenascin-C can be the tumor cells themselves as well as the stromal cells of the cancer microenvironment. Downregulation of tenascin-C by miR-335 or shRNA in human cancer cells in a mouse xenograft model inhibits metastasis formation [7], and in tenascin-C-deficient mice, metastasis formation of tenascin-C positive cancer cells is also suppressed [9].

There are many signaling pathways inducing tenascin-C expression (reviewed in [10]). Among these, mechanical strain application *in vivo* as well as to cells in culture is a potent stimulus to induce tenascin-C expression in fibroblasts [11,12]. We have recently shown that induction of tenascin-C by cyclic mechanical strain requires the action of Mkl1 [13]. Mkl1 is a member of the myocardin-related transcription factor family (MRTF) and a well-known transcriptional co-activator of serum response factor (SRF) [14-16]. SRF target genes, which are regulated upon recruitment of MRTF cofactors, encode proteins involved in actin cytoskeletal function that can either be structural (for example, actin) or related to actin dynamics (for example, talin 1) (reviewed in [17,18]). However, Mkl1-mediated stretch-induced tenascin-C expression in fibroblasts did not require SRF, but instead depended on the potential DNA-binding SAP domain of Mkl1. This implies a novel mode of Mkl1 action as a *bona fide* transcription factor in mechanotransduction [13]. Interestingly, normal and transformed mouse mammary epithelial cells also appear to be highly sensitive to Mkl1 signaling, responding to Mkl1 overexpression with several fold induction of tenascin-C [13].

The present study was designed to find SAP-dependent Mkl1 target genes co-regulated with tenascin-C and to analyze whether such genes could be indicative of specific physiological states of cells that might be controlled by mechanotransduction. For our study, we made use of the HC11 mammary epithelial cell line. HC11 cells are capable of both self-renewal and differentiation and can be cultured for unlimited time in an undifferentiated state [19], the condition we used in our study. HC11 cells can reconstitute the ductal epithelium of a cleared mammary fat pad *in vivo* with ductal, alveolar and myoepithelial cells, illustrating their stem cell abilities [19,20]. In addition, HC11 cells contain a mutated p53 gene that not only increases the replicative potential of stem cells but confers predisposition to mammary carcinoma [21]. Undifferentiated HC11 cells share transcriptome signatures with human breast cancer [22], supporting the relevance of this model for breast cancer-related studies. We therefore concluded our study by investigating whether the genes co-regulated with tenascin-C would also be implicated in breast cancer progression.

## Results

### Screen for SAP-dependent Mkl1 target genes

We devised a screening method to identify genes co-regulated with tenascin-C by Mkl1 in a SAP domain-dependent manner without involvement of SRF. For this purpose, we used HC11 mammary epithelial cells that react strongly to the overexpression of Mkl1 with induction of tenascin-C expression [13]. We compared three HC11 strains that either overexpress the C-terminal red fluorescent protein (RFP)-tagged full length Mkl1 (HC11-FL), Mkl1-RFP with a mutated SRF-interaction site (HC11-mutB1) or Mkl1-RFP with a deletion of the SAP domain (HC11-ΔSAP). None of the three Mkl1 variants appear to be toxic to the cells, as we have not observed any changes in viability or cell morphology. HC11-FL cells were shown to overexpress Mkl1 7.1-fold above the endogenous Mkl1 present in parental HC11 cells [13], and were used as control cells in our study. All cell strains were FACS sorted to express similar levels of Mkl1-RFP proteins. These cells were used for transcript profiling and gene lists of interest were established as shown in Figure 1A, B. A scatter plot (Figure 1A) of all transcripts expressed in HC11-mutB1 versus HC11-FL control cells (y-axis) and all transcripts expressed in HC11-ΔSAP versus HC11-FL control cells (x-axis) shows that a large majority of transcripts does not differ significantly between the three cell strains (log fold change (FC) ≈ 0; black dots). Setting the threshold to a 2-fold reduction (logFC = -1; grey lines), three gene sets can be distinguished: 1) blue dots represent genes that are lower in HC11-mutB1 than in HC11-FL control cells, but are unaffected in HC11-ΔSAP cells, thus representing typical SRF/Mkl1 target genes; 2) green dots represent genes that are lower in HC11-ΔSAP than in HC11-FL control cells, but are unaffected in HC11-mutB1 cells (this gene set includes tenascin-C); and 3) red dots indicate genes with reduced expression in both HC11-mutB1 and HC11-ΔSAP cells compared to HC11-FL control cells.

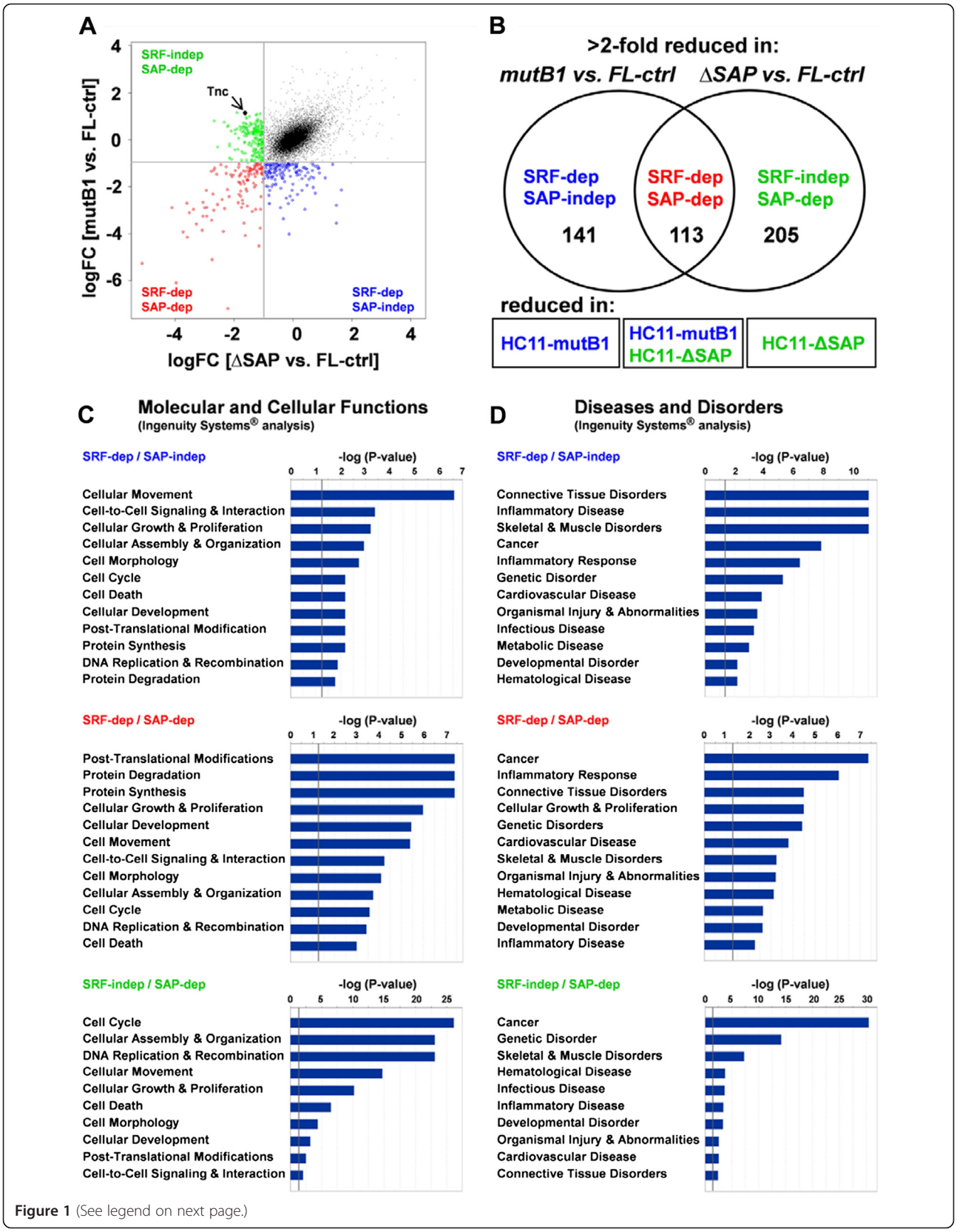


**Figure 1** (See legend on next page.)

(See figure on previous page.)
**Figure 1 Screen for SAP-dependent Mkl1 target genes and their implication in cancer. (A)** Scatter plot and **(B)** Venn diagram representing classification of Mkl1 target genes into three groups: SRF-dependent/SAP-independent (blue), SRF-dependent/SAP-dependent (red) and SRF-independent/SAP-dependent (green). The scatter plot **(A)** represents the log fold change (logFC) in gene expression in HC11-ΔSAP versus HC11-FL control cells (x-axis; ΔSAP vs. FL) and between HC11-mutB1 versus HC11-FL control cells (y-axis; mutB1 vs. FL). Each dot represents a probeset, and the one for tenascin-C is highlighted (Tnc). The vertical and horizontal lines in the chart denote the 2-fold change cutoff (logFC = -1). The Venn diagram **(B)** represents the number of probesets for transcripts, which are more than 2-fold reduced in either HC11-mutB1 or HC11-ΔSAP cells when compared to HC11-FL control cells. Boxes below the Venn diagram indicate the cell strains that have reduced levels of the respective transcripts. **(C, D)** Functional analysis for the three Mkl1-regulated gene sets performed using the IPA software. The high-level functional **(C)** and disease **(D)** categories are displayed along the x-axis of each bar chart. The y-axis displays the –log of the P-value determined by right-tailed Fisher's exact test. The P-value is a measure of the likelihood that the association between a set of genes in each dataset and a related function or disease is due to random association. The grey vertical line denotes the cutoff for significance (P = 0.05; -logP = 1.3).

Thus, this approach enabled us to form three gene sets that were distinct from the large majority of transcripts and were dependent for expression on the B1 site of Mkl1, the SAP domain, or both. The three groups presented by a Venn diagram (Figure 1B) contain 141 probesets for transcripts that depended on the function of the B1 site but not the SAP domain for their induction, 113 probesets for transcripts that depended on both of these Mkl1 domains and a third group of 205 probesets for transcripts co-regulated with tenascin-C that did not require an interaction of Mkl1 with SRF but depended on the SAP domain for induction (complete probeset lists and annotations are found in Additional file 1: Table S1, Additional file 2: Table S2 and Additional file 3: Table S3). This analysis revealed that the SAP-dependent mechanism of tenascin-C regulation by Mkl1 is shared by a large cohort of genes. Below the Venn diagram, we indicated which cells were deficient in the respective transcripts. Thus, the typical SRF/Mkl1 target genes are reduced in HC11-mutB1 cells, while the SRF-independent/SAP-dependent genes are reduced in HC11-ΔSAP cells. The intermediate group that requires both Mkl1 activities is reduced in both the HC11-mutB1 and HC11-ΔSAP cells.

### The SAP-dependent Mkl1 target genes are implicated in cancer

Functional analysis of the three gene lists using the IPA software revealed different molecular and cellular functions (Figure 1C) and different disease associations (Figure 1D) for the three types of gene signatures. Thus, the SRF-dependent/SAP-independent signature implicated a function of these genes in cellular movement and the linked diseases included connective tissue disorders, inflammatory disease and skeletal and muscle disorders, which are the main features known to be regulated by SRF/Mkl1 interaction [23-25]. The SRF-dependent/SAP-dependent group of genes includes as major functions post-translational modification, protein degradation and protein synthesis, and the top disease association is cancer. Finally, the genes of the SRF-independent/SAP-dependent group were associated with extremely high significance with cell cycle and cancer (-logP ≥ 25 and ≥ 30, respectively), while the SRF/Mkl1 target genes were associated with the same two categories at low significance only (-logP ≥ 2 and ≥ 7, respectively). These data imply that SAP-dependent induction of transcription by Mkl1 may counteract the known differentiation-promoting effect of SRF/Mkl1-induced transcription. A list of SAP-dependent genes with published cancer-related functions, whose transcripts were downregulated more than 3-fold in HC11-ΔSAP compared to HC11-FL control cells, is presented in Table 1. To confirm that these transcripts are indeed differentially expressed in the different HC11 cell strains, qRT-PCR analysis was performed using cDNA from three different batches of the respective HC11 strains. Differences in gene expression between HC11-ΔSAP and control cells are presented in Table 1 and in more detail in Additional file 4: Figure S1. The qRT-PCR results agreed with the data obtained by transcript profiling. We also tested the SAP-dependent gene expression in the HC11 strains when grown in the presence of serum. It is interesting to note that in the presence of 3% FCS, these transcripts remained strongly reduced in HC11-ΔSAP compared to control cells (Table 1). Thus, the induction of these genes seems to depend mainly on whether the SAP domain is present in the transfected Mkl1 construct.

In addition, we monitored changes in the expression of some of the SRF-independent/SAP-dependent Mkl1 targets on a protein level. In agreement with the changes seen at the transcript level, we confirmed the reduction of tenascin-C, Wisp1 and Nox4 proteins in cells overexpressing the ΔSAP-Mkl1 construct compared to the HC11-FL control and HC11-mutB1 cells (Additional file 4: Figure S2). Using zymography, we found that Mmp2, a gene that was not affected by Mkl1 overexpression at the transcript level was highly expressed in all three cell strains, whereas Mmp3 and/or 12, which belonged to the SRF-dependent/SAP-dependent gene set, were almost completely lacking in HC11-mutB1 as well as HC11-ΔSAP cells, corresponding to the data obtained by transcript profiling.

**Table 1 SAP-dependent Mkl1 target genes**

| Gene | Description | Fold Reduction in HC11-ΔSAP vs. HC11-FL cells | | | Functions |
|---|---|---|---|---|---|
| | | Microarrays in 0.03% FCS | qRT-PCR in 0.03% FCS | qRT-PCR in 3% FCS | |
| **SRF-independent genes** | | | | | |
| Tnc | Tenascin C, ECM protein | 3.07*** | 3.50*** | 26.34*** | Cell adhesion, cell migration, wound healing and tissue remodeling, cancer cell invasion and metastasis [10] |
| Anln | Anillin, actin binding protein | 3.10*** | 1.93*** | 1.38** | Cell cycle regulation [26], cell motility and cancer progression [26-28] |
| Nox4 | NADPH oxidase 4 | 3.31*** | 94.19** | 332.70*** | Cell growth, differentiation and migration [29], tumor angiogenesis [30] |
| Adamts16 | Metallopeptidase, ECM protein | 3.63*** | 5.70*** | 14.84** | Cell growth and motility [31], role in arthritis [32] and cancer [31] |
| Krt5 | Keratin 5, intermediate filament protein | 3.73*** | 2.74*** | 8.02*** | Protein synthesis, epithelial cell growth and differentiation [33,34] |
| p15 (PAF) | 2810417H13Rik, PCNA-associated factor | 3.91*** | 1.89*** | 1.34*** | DNA repair and cell cycle regulation, cell survival and proliferation, tumorigenesis [35-37], hematopoiesis [38] |
| Ass1 | Argininosuccinate synthetase 1 | 4.23*** | 3.89** | 2.72** | Regulation of nitric oxide production and cell viability [39,40] |
| Cd34 | CD34 antigen, stem cell antigen | 4.25*** | 10.61*** | 1.72*** | Vessel development and function [41], tumor growth [42,43] |
| Wisp1 | WNT1 inducible signaling pathway protein 1, ECM protein | 4.41*** | 2.54** | 4.06** | Cell proliferation and survival, ECM deposition and turnover, EMT, tumorigenesis, tissue remodeling [44] |
| Mcm6 | Minichromosome maintenance complex component 6 | 4.42*** | 2.83*** | 1.30*** | Cell cycle regulation [45] |
| Car12 | Carbonic anyhydrase 12 | 4.58*** | 16.11*** | 26.07** | Cell survival under hypoxic conditions, tumor-associated cell migration and invasion [46,47] |
| Htatip2 | Hyaluronectin, TIP30, transcriptional regulator | 5.89*** | 548.59*** | 245.27*** | Regulation of apoptosis [48], tumor growth and metastasis [49] |
| Kif26b | Kinesin family member 26B | 6.33*** | 8.36*** | 61.22*** | Regulation of adhesion and cell polarity in kidney development [50] |
| **SRF-dependent genes** | | | | | |
| Lox | Lysyl oxidase, ECM protein | 4.61*** | 4.70** | 12.04*** | ECM turnover, connective tissue remodeling and repair, tumor progression and metastasis [51,52] |
| Mmp12 | Matrix metallopeptidase 12, metalloelastase | 12.01*** | 23.49*** | 4.90** | ECM degradation in tissue remodeling [49] and tumorigenesis [53] |
| Mmp3 | Matrix metallopeptidase 3, stromelysin-1 | 15.64*** | 14.70*** | 2.08** | ECM degradation in tissue remodeling [49] and tumorigenesis [54] |

*Abbreviations:* ECM extracellular matrix protein, PCNA proliferating cell nuclear antigen, EMT epithelial-to-mesenchymal transition.
***P < 0.001, **P < 0.01, Student's *t* test.

### SRF-independent/SAP-dependent transcripts represent direct Mkl1 target genes

Since we have previously shown that the SAP domain of Mkl1 interacts with the proximal promoter of tenascin-C to induce its transcription [13], we tested whether this was also the case for other transcripts of the same group. The promoters of the SRF-independent/SAP-dependent genes listed in Table 1 encompassing at least 500 bp upstream of the transcription start site (TSS) were fused to the secreted alkaline phosphatase (SEAP) reporter gene of pSEAP2-Basic. We tested the induction of each promoter-reporter construct by co-transfection with FL-Mkl1 (Figure 2A). This revealed that the majority of the new promoters tested (8 out of 12) were induced at least 2-fold by Mkl1 in comparison to co-transfection with an inactive Mkl1 devoid of the transactivation domain, indicating that these are indeed direct Mkl1 target genes. The promoter constructs that did not respond to Mkl1 overexpression may represent genes that are indirectly regulated by Mkl1, or the relevant promoter regions were not contained in the constructs tested. Next, we investigated whether the induction was SAP-dependent and SRF-independent by comparing the reporter activity after co-transfection with mutB1- versus ΔSAP-Mkl1 variants (Figure 2B). Indeed, the promoter-reporter constructs induced by FL-Mkl1 were also strongly induced by mutB1-Mkl1, but not by ΔSAP-Mkl1. In contrast, the promoter construct for Acta2, a gene from the SRF-dependent/SAP-independent gene set was strongly induced by ΔSAP-Mkl1 but not by mutB1-Mkl1, as

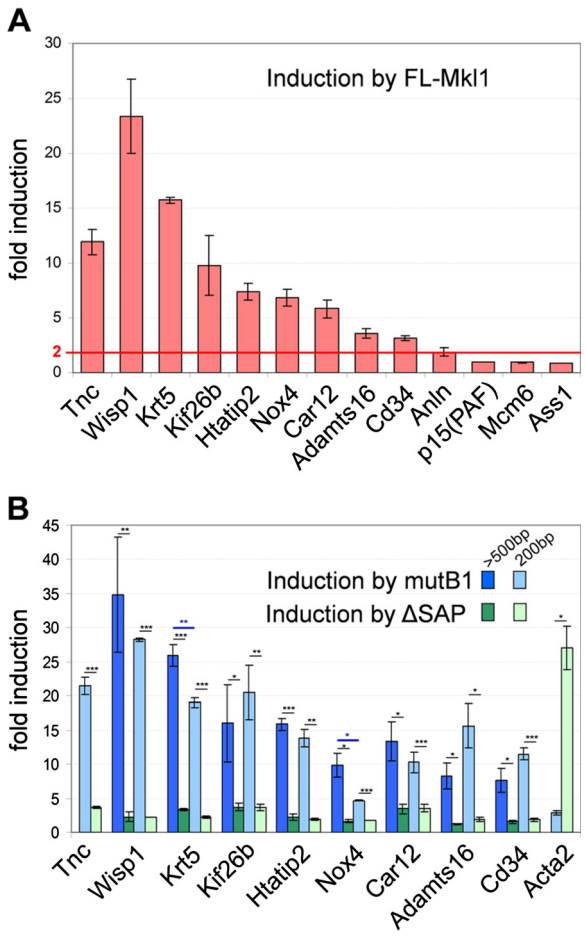


**Figure 2 SRF-independent/SAP-dependent transcripts represent direct Mkl1 target genes requiring the SAP domain of Mkl1 to induce transcription from their proximal promoter. (A)** The indicated promoter constructs that contained at least 500 bp upstream of the transcription start site (TSS) and were linked to the secreted alkaline phosphatase (SEAP) reporter gene, were cotransfected in HC11 cells together with an inactive Mkl1 devoid of the transactivation domain [13] or the FL-Mkl1 construct. SEAP activity is expressed as fold induction above the level obtained with the inactive Mkl1. In addition to Tnc, for 8 out of the 12 new promoters tested, induction greater than 2-fold (indicated by the red line) was obtained. Values are means ± SEM from three to seven independent experiments. **(B)** HC11 cells were cotransfected with the indicated promoter constructs that were either > 500 bp or shortened to 200 bp upstream of the TSS, and with vectors encoding the indicated mutant Mkl1 constructs. SEAP activity is normalized and expressed as in **(A)**. Means ± SEM from at least three independent experiments and significant differences between either mutB1- and ΔSAP-Mkl1-transactivated promoter constructs or between the longer and shorter promoter constructs transactivated by mutB1-Mkl1, ***P < 0.001, **P < 0.01, *P < 0.05 are shown.

expected for a typical SRF/Mkl1 target gene [18,55,56]. All promoters that revealed SAP-dependency were shortened to 200 bp upstream of the TSS to test whether this was sufficient to relay the Mkl1 response, as it has been seen previously for tenascin-C [13]. With the exception of Krt5 and Nox4, for which some activity was lost by shortening the promoters, the 200 bp proximal promoters of all other genes tested were induced equally well as the longer constructs (Figure 2B). Thus, we conclude that there are many genes that are regulated similarly as tenascin-C requiring the SAP domain of Mkl1 to induce transcription from their proximal promoter.

### The different HC11 cell strains proliferate at different rates and show distinct migration behaviors

Next, we tested whether the differential gene expression seen in the different HC11 strains overexpressing either FL-, mutB1- or ΔSAP-Mkl1 constructs have functional consequences on their behavior. Since most of the SAP-dependent transcripts are proposed to have a function in cancer, we decided to analyze two main functions important for cancer progression: proliferation and cell migration. An approximately equal overexpression of the different Mkl1 protein variants in the HC11 cell lines was confirmed by Western blot analysis (Figure 3A). An HC11 cell strain stably transfected with an empty vector [13] expressing only endogenous Mkl1 (below the detection limit in Figure 3A) was also included in these studies. The proliferation rates of the HC11 strains were analyzed using a 5-bromo-2′-deoxyuridine (BrdU) incorporation assay. The incorporated BrdU was measured immediately after plating (0 h) as well as at 24, 48, 72 and 96 h. Compared to empty vector-, FL- or mutB1-transfected HC11 strains, there was a significant decrease in BrdU uptake into newly synthesized DNA in HC11-ΔSAP cells over the entire time period tested (Figure 3B). To investigate cell motility, we used a transfilter migration assay. Similarly to the effect on cellular proliferation, the expression of ΔSAP-Mkl1 significantly inhibited HC11 cell migration by 2.7-fold compared to endogenous or full length Mkl1 expression, and more than 3.5-fold compared to mutB1-Mkl1 expression (Figure 3C).

Thus, overexpression of FL-Mkl1 protein in HC11 cells did not affect their behavior. However, overexpression of ΔSAP-Mkl1 led to a significant reduction in the proliferative and migratory ability of HC11 epithelial cells, either through a dominant-negative effect of ΔSAP-Mkl1 on SRF-mediated action and/or a positive impact of the SAP-dependent Mkl1 target genes on these functions important for cancer progression.

### SAP-dependent Mkl1 target genes are mechanoresponsive

We have previously found that the SAP-dependent induction of tenascin-C was triggered by applying mechanical strain to fibroblasts. Mammary epithelial cells are also exposed to mechanical strains, both during normal development, pregnancy and lactation, as well as under pathological conditions such as in cancer. Therefore, we

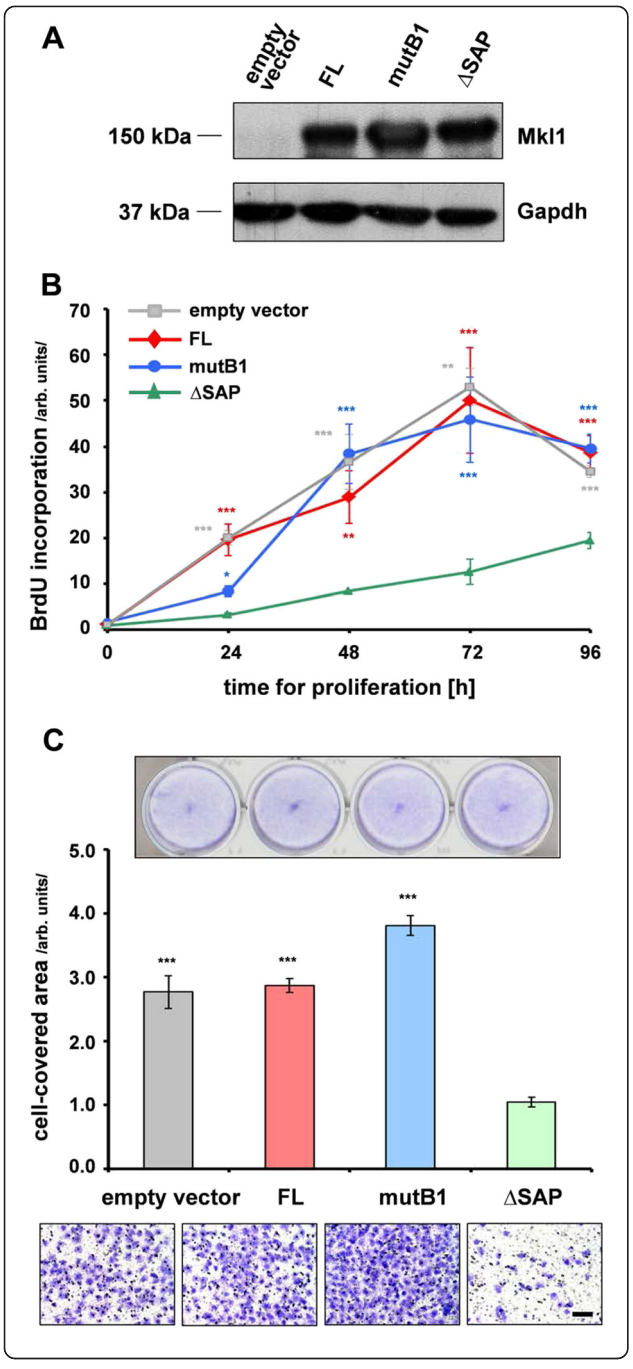


**Figure 3 The different HC11 cell strains proliferate at different rates and show distinct migration behaviors. (A)** Immunoblot with mAb65F13 of Mkl1 proteins in whole-cell extracts from the empty vector-, FL-, mutB1- or ΔSAP-transfected HC11 strains. Anti-Gapdh served as loading control. Endogenous Mkl1 protein was below the detection limit in empty vector cells. **(B)** SAP-dependent proliferation of HC11 mammary epithelial cells. Proliferation rates of the four HC11 cell strains were assessed by BrdU incorporation into newly synthesized DNA immediately after plating (0 h) as well as at 24, 48, 72 and 96 h. Means ± SD from three independent experiments and significant differences to the HC11-ΔSAP cells, ***P < 0.001, **P < 0.01, *P < 0.05 are shown. **(C)** SAP-dependent migration of HC11 mammary epithelial cells. Cell migration of the four HC11 strains was evaluated by Transwell migration assay using filters with 8 μm pore size. Quantification of the cell migration was measured by the area on the lower side of the filter covered with cells. Above the bar graph, a photo of fixed and stained cells seeded in parallel in a 24-well plate is shown as a seeding control, and representative photos of fixed and stained cells of each of the cell strains that have migrated to the lower side of the filter, are shown below (bar, 200 μm). Data and statistical significance are expressed as in **(B)**.

tested whether tenascin-C and other members of the SAP-dependent Mkl1-induced gene set are mechanoresponsive in HC11 cells. We tested two paradigms: 1) static strain that was shown to induce c-fos, a very prominent mechanoresponsive gene in HC11 cells [57] that we used as a control, and 2) cyclic strain. While we were able to confirm induction of c-fos by applying static strain at 20% for 1 h, there was no induction of tenascin-C under these conditions compared to cells at rest (Figure 4A). However, using 15% cyclic strain at a frequency of 0.3 Hz for 1 h, we found that not only the control gene c-fos but 11 out of 16 SAP-dependent genes, including tenascin-C were significantly upregulated above the expression levels obtained in resting cells (Figure 4). Even though significant, the induction of tenascin-C was minimal (Figure 4A) compared to 18-fold upregulation for Adamts16 or 10-fold upregulation for Lox (Figure 4B), both of which are enzymes involved in extracellular matrix (ECM) remodeling and cancer progression [31,58]. Being mechanoresponsive, the SAP-dependent Mkl1 target genes might be activated in stiff tumor tissue, which further confirms their relation with cancer.

### The SRF-independent/SAP-dependent genes represent a bad prognostic signature for breast cancer patients

In order to investigate whether the SRF-independent/SAP-dependent genes were prognostic of accelerated cancer progression in human patients, we used the bioinformatics tool Gene expression-based Outcome for Breast cancer Online (GOBO) that allowed us to investigate a breast tumor data set containing 1881 samples analyzed by Affymetrix Human Genome U133A arrays. GOBO is designed to assess gene expression levels and association with outcome of single genes or gene sets in multiple subgroups of

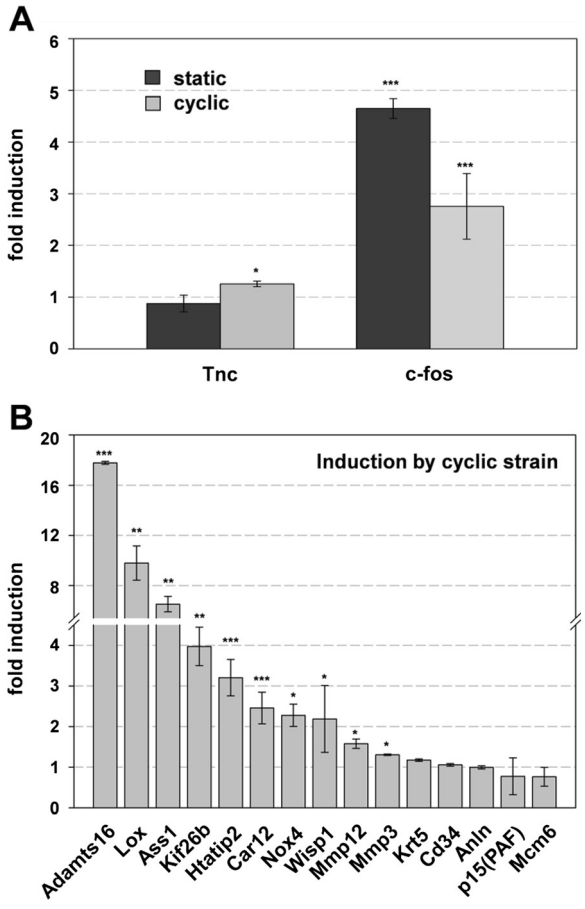


**Figure 4 SAP-dependent Mkl1 target genes are mechanoresponsive. (A)** Effect of static (20%) and cyclic (15%, 0.3 Hz) strain on Tnc and c-fos mRNA levels. HC11 cells were cultured on either growth factor reduced matrigel matrix- or fibronectin-coated silicone membranes in 0.03% serum-containing medium for 24 h before applying static or cyclic strain for 1 h. Cells cultured under the same conditions and not exposed to mechanical stimulation were used as a resting control. The two types of coating gave identical results under the indicated experimental conditions. Total RNA was extracted and qRT-PCR was performed for Tnc and c-fos mRNA levels. Values normalized to Gapdh are expressed relative to the values of resting cells. Data represent means ± SD from three independent experiments. Significant differences to the resting control, ***P < 0.001, **P < 0.01, *P < 0.05. **(B)** SAP-dependent genes respond to cyclic strain. HC11 cells were stretched and mRNA analyses were performed as described in **(A)**. Data and statistical significance are expressed as in **(A)**.

this breast cancer data set [59]. Here, we analyzed two sets of genes, namely the SRF/Mkl1-induced gene set (SRF-dependent/SAP-independent) and the SAP-dependent gene set (SRF-independent/SAP-dependent) containing tenascin-C. The analysis was performed across tumor samples stratified according to PAM50 subtypes [60], estrogen receptor (ER)-status and histological grade. In contrast to the SRF/Mkl1 target genes that were predominantly associated with tumors classified as normal-like and with lower histological grades (1 and 2) (Figure 5A), elevated expression of SAP-dependent genes was associated with extremely high significance (P < 0.00001) with typical high-proliferative poor outcome classes in breast cancer, such as basal-like, HER2-enriched, luminal B, ER-negative and histological grade 3 tumors (Figure 5B). Next, a functional correlation analysis to find a possible interconnection between the SAP-dependent Mkl1 target genes was performed using the GOBO tool (Additional file 4: Figure S3). This analysis explores the correlation of expression of individual genes in our gene sets with eight different co-expressed gene modules emulating breast cancer-specific as well as general tumor biological processes [61]. Interestingly, whereas the gene set of SRF/Mkl1 targets did not show a significant correlation with any of these modules, the genes in the SAP-dependent gene set were correlated with a very high significance (P < 0.00001) with two proliferation modules – mitotic checkpoint and mitotic progression. Both modules contain genes related to central mitotic processes involved in either the regulation of the M-phase and the mitotic checkpoint or in carrying out the M-phase. Finally, the association of our gene sets with outcome using distant metastasis free survival (DMFS) as an endpoint and 10-year censoring was analyzed. The survival analysis was performed in all tumors for which DMFS follow-up is available (1379 cases), as well as in 21 groups that were stratified based on gene expression subtypes (PAM50 classifier), ER-status, lymph node (LN)-status, histological grade, and treatment status. Samples in the whole cancer data set (1881 patients) were stratified into three quantiles, low, intermediate and high, based on SRF-dependent/SAP-independent or SRF-independent/SAP-dependent gene expression. Interestingly, high expression of SRF/Mkl1-induced genes was associated with a better clinical outcome for all tumors, as well as for LN-negative and untreated tumors compared to low and intermediate expression of these genes (Figure 6A). In contrast, both high and intermediate expression of the SAP-dependent genes was associated with bad clinical outcome in all tumors, and particularly in LN-negative, systemically untreated, ER-positive, Grade 1 and 2 tumors (Figure 6B). Similar results were obtained for the typical breast cancer gene CCNB1 by Ringnér et al. [59]. The Kaplan-Meier survival analyses were supported by the corresponding multivariate analyses (Figure 7A, B). The hazard ratio for the variate Grade shows statistical significance, proving that the influence of high SAP-dependent gene expression on patient survival is independent of tumor grade. Among all tumors for which DMFS data are available, a hazard ratio of 0.44 (95% CI = 0.28-0.68; P = 0.0003) for the low SRF-independent/SAP-dependent tercile was detected compared to the high SRF-independent/SAP-dependent tercile (Figure 7B, all tumors). This indicates that patients

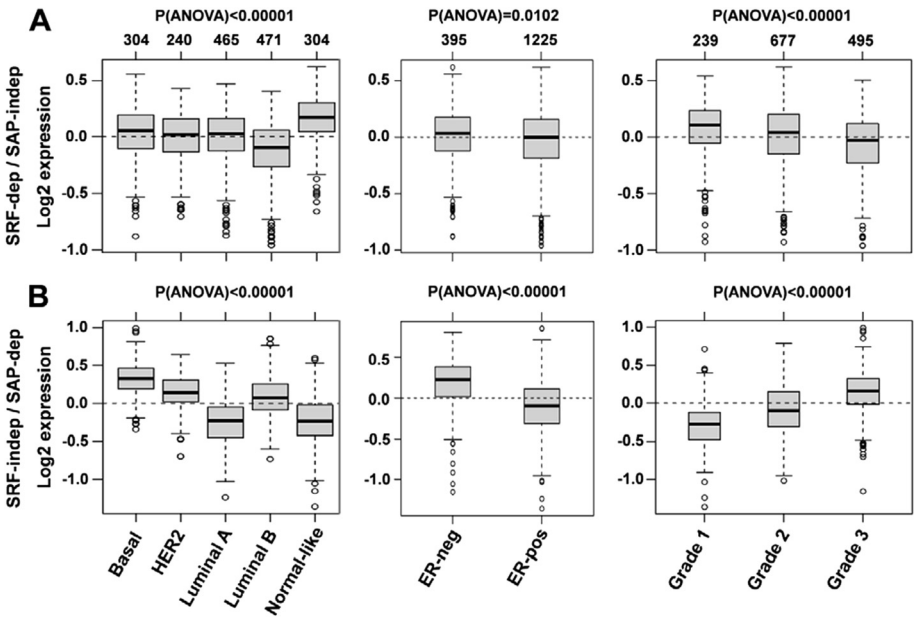


**Figure 5 SAP-dependent Mkl1 target genes are associated with typical high-proliferative poor outcome classes in breast cancer.** The expression levels for the SRF-dependent/SAP-independent **(A)** and SRF-independent/SAP-dependent **(B)** gene sets are analyzed across the 1881-sample breast cancer data set stratified according to PAM50 subtypes (left panels), estrogen receptor (ER)-status (middle panels) and histological grade (right panels), and represented by box plots using the GOBO bioinformatics tool. The number of tumors in each breast cancer subtype and the significant difference in gene expression (P-value calculated using ANOVA) between them are shown above the box plots.

with tumors expressing high levels of the SAP-dependent genes are more than twice as likely to develop metastatic disease. Similar hazard ratios, in the range of 0.28-0.44 for the low tercile compared to the high tercile were also detected among subgroups of untreated, LN-negative, ER-positive, Grade 1 and 2 tumors (Figure 7B). Thus, the association of high SRF-independent/SAP-dependent gene expression with reduced DMFS among patients not receiving adjuvant therapy, as well as among LN-negative, ER-positive, Grade 1 and 2 patients indicates that increased expression of the SAP-dependent Mkl1 target genes plays a significant role in the natural metastatic progression of non-aggressive towards highly aggressive breast cancer in human patients.

## Discussion

Given the heterogeneity of mutations in tumor cells, it becomes increasingly clear that not only individual genes but pathways govern the course of tumorigenesis and cancer progression [62]. We have recently shown that induction of tenascin-C by cyclic mechanical strain required the action of the potential DNA-binding SAP domain of Mkl1 independently of an interaction of Mkl1 with SRF [13]. Now, we report a screen for genes co-regulated with tenascin-C by the same SAP-dependent and SRF-independent mechanism in mammary epithelial cells. This screen reveals a set of SAP domain-dependent Mkl1 target genes with a strong implication in cell proliferation, cell motility and cancer.

To date only a few studies have shown that Mkl1 is implicated in cancer-related processes (reviewed in [63]) and most of them have concentrated on the SRF/Mkl1 signaling for the induction of individual genes [64-67]. The first study reporting that depletion of Mkl1/2 proteins reduced motility, invasion and colonization of metastatic tumor cells in an experimental *in vivo* metastasis assay [64] was further supported by the discovery of the Mkl1-binding protein, suppressor of cancer cell invasion (SCAI), which inhibited SRF/Mkl1-mediated expression of β1 integrin [68]. Since then, several studies describing opposing biological effects for Mkl1 appeared. For instance, several antiproliferative SRF/Mkl1 target genes including mig6/errfi-1, a negative regulator of the EGFR-MAPK pathway, were identified [65], or the tumor suppressor gene Eplin-α was described as a direct target of the SRF/Mkl1 pathway [66]. Furthermore, expression of a constitutively active form of Mkl1 in oncogenic ras- or src-transformed rat intestinal epithelial cells injected into the spleen of nude mice significantly suppressed tumor formation and reduced liver metastases by rescuing the expression of the SRF/Mkl1 targets tropomyosin and caldesmon [67]. In line with these findings, we could show that high expression of SRF/Mkl1 target genes is associated with an improved clinical outcome in breast cancer patients. However, the opposite is the case for high expression

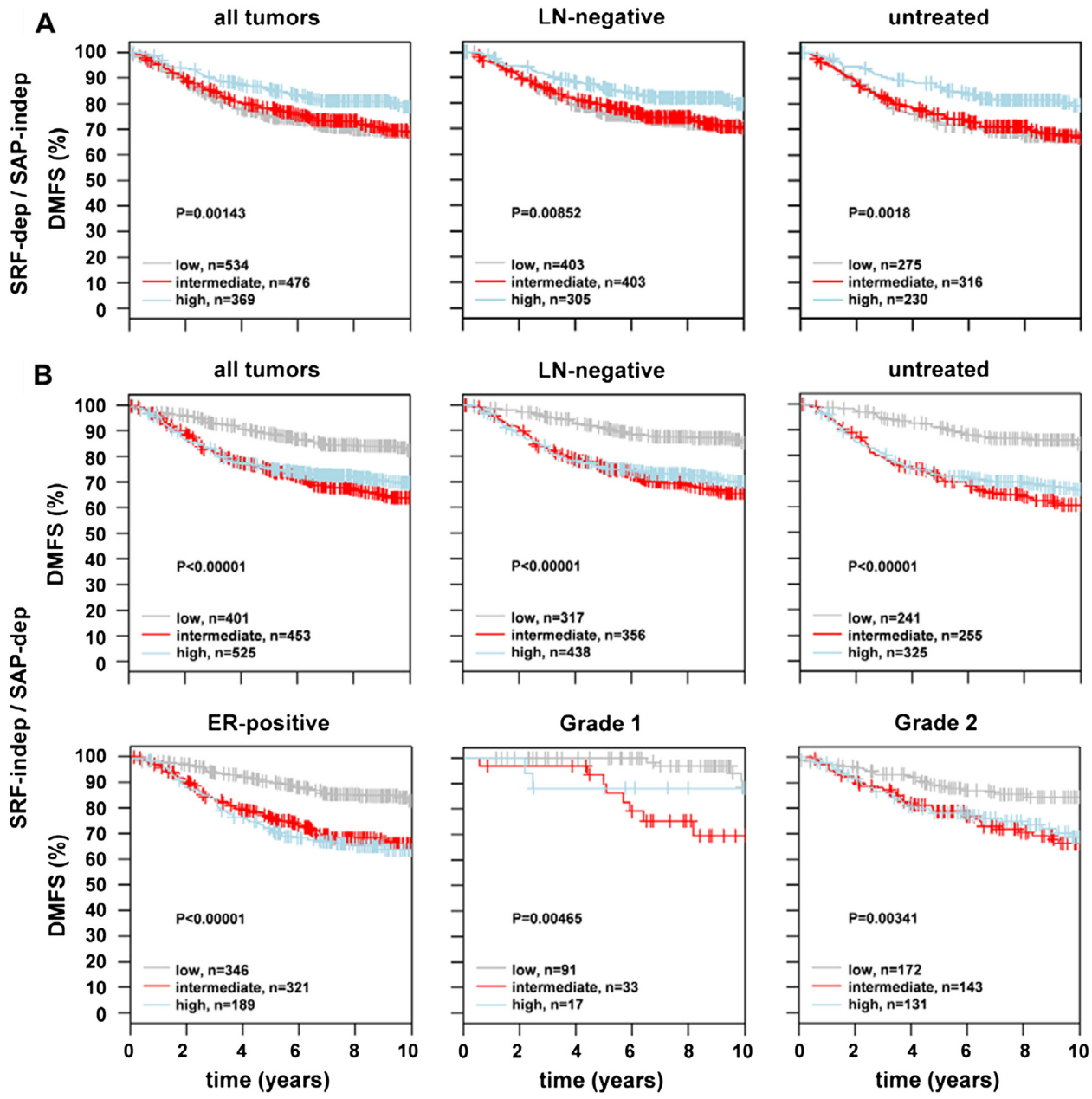


**Figure 6 The SRF-independent/SAP-dependent genes represent a bad prognostic signature for breast cancer patients.** Tumors in the 1881-sample breast cancer data set were stratified into three quantiles, low, intermediate and high, based on SRF-dependent/SAP-independent **(A)** or SRF-independent/SAP-dependent **(B)** gene expression. **(A)** Kaplan-Meier survival analysis using distant metastasis free survival (DMFS) as endpoint and 10-year censoring for all tumors (n = 1379; left panels), or in the subgroups of lymph node (LN)-negative (n = 1111; middle panels) and untreated tumors (n = 821; right panels) was performed using the GOBO bioinformatics tool, interrogating the group of SRF-dependent/SAP-independent target genes. P-value is calculated using log-rank test. **(B)** Kaplan-Meier survival analysis for tumors with expression of SRF-independent/SAP-dependent Mkl1 target genes was performed as in **(A)**. Association with clinical outcome was assessed in the subgroups of ER-positive (n = 856; left panel), Grade 1 (n = 141, middle panel) and Grade 2 (n = 446; right panel) tumors in addition to all tumors and the subgroups used in **(A)**. P-value is calculated using log-rank test.

of SAP-dependent Mkl1 target genes. These genes are associated with poor clinical outcome predominantly in less aggressive tumors such as LN-negative, ER-positive, Grade 1 and 2 tumors, which makes them valuable predictors of breast cancer progression. A scheme that depicts our model for Mkl1 action in breast cancer is presented in Figure 8. In this model Mkl1 is transactivating SRF-target genes in less aggressive tumors, while in the course of cancer progression and metastatic behavior Mkl1 is activating a new group of genes in a SAP-dependent manner either by direct

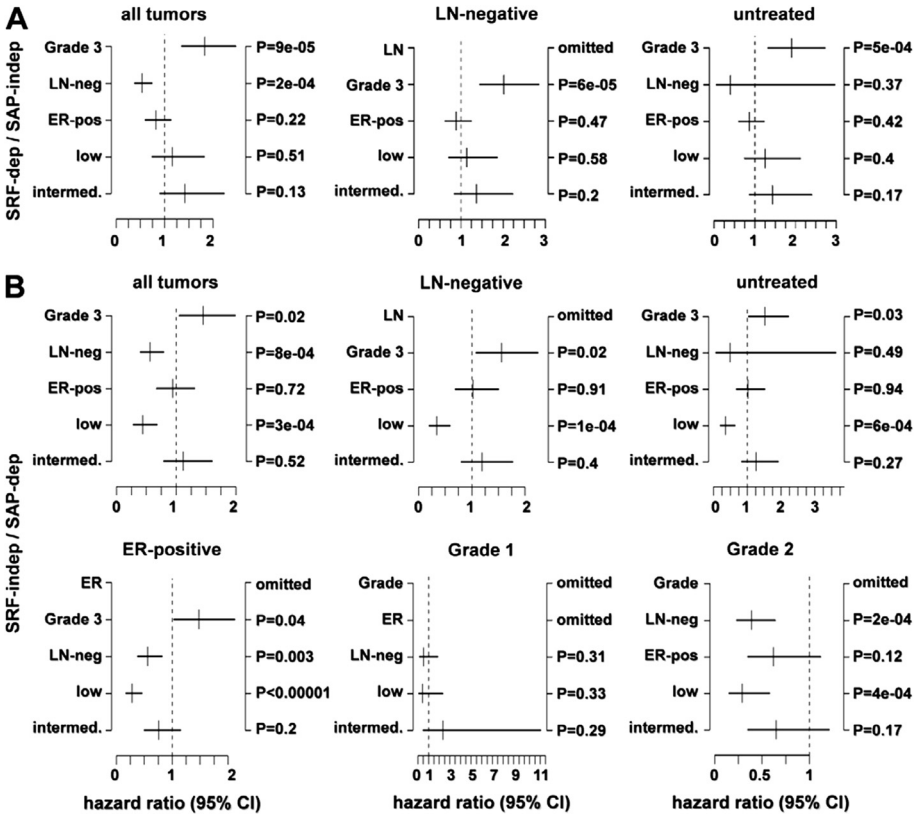


**Figure 7 Elevated expression of SAP-dependent Mkl1 target genes is a poor prognosis factor in breast cancer independent of histological grade.** Multivariate analysis supporting the Kaplan-Maier survival analysis (shown in Figure 6) for the SRF-dependent/SAP-independent **(A)** and SRF-independent/SAP-dependent **(B)** gene sets, was performed using the GOBO bioinformatics tool. The analysis was executed for all tumors (n = 1379) and in the subgroups of LN-negative (n = 1111) and untreated tumors (n = 821) **(A, B)**, as well as in the subgroups of ER-positive (n = 856), Grade 1 (n = 141) and Grade 2 (n = 446) tumors **(B)**, using LN-status, ER-status, and stratified histological grade (histological grade 1 and 2 vs. 3) as covariates, DMFS as endpoint and 10-year censoring. The hazard ratio and the 95% confidence interval (CI) are plotted for each of these covariates. Specified covariates may be omitted in certain comparisons, e.g. ER-status is omitted when analyzing ER-positive tumors only, or when not all of the investigated cases have clinical follow-up or clinical information for the specified covariate.

interaction with the promoters of these genes or by interaction with additional DNA-binding factors.

Interestingly, in parental HC11 cells many of the genes that we found in the SAP-dependent gene set that foster cell proliferation and migration and may cause poor survival of breast cancer patients are also induced by mechanical strain. A recent study has demonstrated that inhibition of cell spreading due to a lack of matrix stiffness is overcome by externally applied stretch, suggesting that similar mechanotransduction mechanisms sense stiffness and stretch [69]. Tumor stroma is typically stiffer than normal stroma. In breast cancer, diseased tissue can be 10 times stiffer than normal breast [70,71]. It is known that abnormal ECM stiffness plays an important role in cancer progression [72,73], but the mechanisms by which stiffness influences cancer progression are still under investigation. If we assume that we have discovered a general reaction of mammary epithelial cells to mechanical strain, we envisage that epithelial cells in a stiff, mechanically dynamic tumor environment may react by inducing a SAP-dependent Mkl1 gene set that in turn affects tumor progression. Furthermore, the products of these genes, many of which are involved in ECM turnover and function, for example Lox [58], Mmps [74], Adamts16 [31] or Wisp1 [44] might themselves manipulate the tumor microenvironment, thereby influencing tumor cell survival by a positive tumorigenic feedback loop.

Finding how to switch the mode of action of Mkl1 between SRF transactivation versus its SAP-dependent transcriptional activity is a subject of ongoing research in our lab that in future may help with the development of new therapeutic interventions for breast cancer. Post-translational modifications such as sumoylation are known to influence Mkl1 transcriptional activity [75] and phosphorylation has been shown to influence interaction of Mkl1 with nuclear actin resulting in transcriptional changes [76,77]. Further characterization of these and

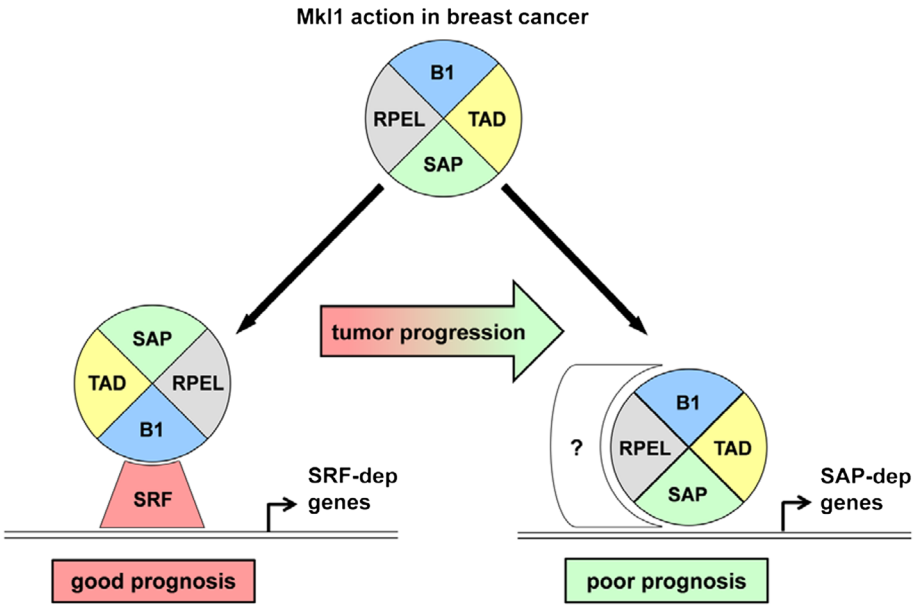


**Figure 8 Schematic representation of the Mkl1 action in breast cancer.** A circular Mkl1 model is depicted with four of its domains: RPEL, actin binding motifs with RPxxxEL core consensus; B1, basic domain involved in SRF-binding; SAP, homology domain found in the nuclear proteins SAF-A/B, Acinus, PIAS; TAD, transactivation domain. Serum response factor is drawn as a red shape and putative unidentified DNA-binding proteins as white shape with a question mark. Mkl1 exerts two distinct modes of action: one of them is through the B1 domain required for serum response factor (SRF)-binding activity and induction of SRF/Mkl1 target gene expression; the other one is strongly dependent on the SAP domain and triggers the expression of a specific set of pro-proliferative and pro-migratory genes that we called SAP-dependent Mkl1 target genes. High expression of SRF-dependent genes is associated with good clinical outcome for breast cancer patients, whereas elevated expression of SAP-dependent targets correlates with poor prognosis and indicates a significant role for these genes in breast cancer progression.

other post-transcriptional changes of Mkl1 deserve special attention when trying to answer the above question.

## Conclusions

In the current study, we discovered a breast cancer-specific set of genes that is highly interesting as a prognostic marker and therapeutic target for several reasons. (1) The expression of this gene set is regulated by Mkl1 and its SAP domain and is independent of SRF. (2) The SAP-dependent, SRF-independent Mkl1signaling is triggered by mechanical strain and may thus be activated in stiff tumors with a high stromal content and high interstitial tissue pressure. (3) This gene set is composed of interesting members some of which represent novel candidates for playing a functional role in cancer and others that have already been implicated in cancer-related functions, as for example tenascin-C, a metastatic niche component important for lung colonization [8], or Lox as a gene mediating collagen crosslinking responsible for fibrosis-enhanced metastasis [58]. (4) The SAP-dependent Mkl1 target genes are associated with a poor clinical outcome in breast cancer patients, not receiving adjuvant therapy or having a cancer classified as non-aggressive such as LN-negative, ER-positive, Grade 1 or 2 tumors. This makes these genes potential valuable prognostic markers in selecting patients who may benefit from an immediate and/or more aggressive therapy.

## Methods

### Cell culture

Full length Mkl1 (FL-Mkl1) and the two Mkl1 mutants, mutB1-Mkl1 comprising alanine substitutions of four amino acids (underlined) in the B1 domain of Mkl1 (KKA KELKPKVKKLKYHQYIPPDQKQD) [78] and ΔSAP-Mkl1 with a deletion of the SAP domain [15], were constructed based on transcript variant 1 (GenBank accession number NM_153049) as previously described [13]. All Mkl1 variants were expressed as C-terminal RFP-tagged fusions. An empty vector expressing RFP alone was previously described [13].

HC11 mammary epithelial cells, kindly provided by Dr. N. Hynes (Basel, Switzerland), were grown in RPMI-1640 medium supplemented with 10% FCS, 5 μg/ml insulin (Sigma, Buchs, Switzerland) and 10 ng/ml epidermal growth factor (EGF; Invitrogen, Zug, Switzerland). In most of the experiments, the HC11 cells were starved in 0.03% FCS/RPMI without EGF. To obtain HC11 cells stably expressing FL-Mkl1-RFP (HC11-FL), mutB1-Mkl1-RFP (HC11-mutB1), ΔSAP-Mkl1-RFP (HC11-ΔSAP) or RFP alone (HC11-empty vector), cells were transfected using FuGENE® 6 (Roche, Basel, Switzerland) and selected

with Geneticin (1 mg/ml; Roche) for 14 days before fluorescence-activated cell sorting (FACS) of RFP-positive cells on a Vantage SE (Becton Dickinson, Basel, Switzerland). Cell viability of the four HC11 cell strains was assessed by the CellTiter-Blue viability assay (Promega, Duebendorf, Switzerland).

### Cell proliferation assay

Proliferation rates of the HC11 cell strains were determined using BrdU incorporation assay (Roche). After 24 h of starvation, cells were plated in triplicate on Black 96-well microtiter plates (PerkinElmer, Schwerzenbach, Switzerland) at $5 \times 10^3$ cells/well in 3% FCS/RPMI and allowed to proliferate for 0, 24, 48, 72 and 96 h before labeling with BrdU for 2 h. BrdU incorporation into newly synthesized DNA was determined according to the manufacturer's protocol using a Luminometer Mithras LB940 (Berthold Technologies, Regensdorf, Switzerland). Experimental values were normalized to the values of HC11-ΔSAP cells at the time point 0. Data represent means ± SD from three independent experiments.

### Cell migration assay

Cell migration was assayed using transwell polycarbonate membrane inserts (6.5 mm; Corning, Amsterdam, The Netherlands) with 8 μm pores as described [79]. After 24 h of starvation, $5 \times 10^4$ cells were plated in the top insert chamber with 100 μl serum-free RPMI. The lower chamber was filled with 600 μl 10% FCS/RPMI. Cells were allowed to migrate across the filter for 22 h at 37°C before fixation and crystal violet-staining. Images of duplicate inserts were acquired on a Nikon Eclipse E600 using 10× magnification and a color CCD camera. Migration was quantified by measuring the area covered by migrated cells using the Fiji distribution of ImageJ [80]. Data represent means ± SD from three independent experiments.

### Mechanical stimulation of cells

$2 \times 10^5$ HC11 cells/well were seeded in BioFlex® 6-well culture plates (Flexcell International, Hillsborough, NC, USA) coated with either growth factor reduced-Matrigel (BD Biosciences, Basel, Switzerland) or fibronectin [11]. Cultures were starved for 24 h before applying either equibiaxial cyclic strain (15%, 0.3 Hz) or static strain (20%) at 37°C for 1 h using Flexcell FX-4000 (Flexcell International). Cells cultured under the same conditions and not exposed to strain were used as a resting control. After mechanical stimulation, cells were lysed and total RNA was isolated using the RNeasy Mini Kit (Qiagen, Basel, Switzerland).

### Transcript profiling and bioinformatics analysis

HC11 cell strains stably expressing Mkl1 variants were starved for 48 h before total RNA was extracted, converted into labeled cDNA and hybridized to Affymetrix GeneChip Mouse Gene 1.0 ST arrays. RMA-normalized expression values were calculated with the Affy package from Bioconductor 2.4 [81], and differentially expressed genes were identified using moderated *t*-statistics calculated with the empirical Bayes method as implemented in the Bioconductor limma package [82]. To be considered as differentially expressed between HC11-FL and HC11-mutB1 or HC11-ΔSAP cells, genes had to pass the filters: adjusted P-value ≤ 0.01 (with Benjamin-Hochberg false discovery correction), a minimum absolute linear fold change difference of 2.0 and a minimum average expression value of 4.0 (log2). Microarray data files are available from the Gene Expression Omnibus (GEO; http://www.ncbi.nlm.nih.gov/geo/), accession number GSE44907. Using the above parameters, gene lists of the two contrasts (mutB1/FL and ΔSAP/FL) were compared resulting in the formation of three gene groups: SRF-dependent/SAP-independent, SRF-dependent/SAP-dependent and SRF-independent/SAP-dependent. The three gene sets were analyzed using the bioinformatics softwares: 1) IPA (Ingenuity® Systems; www.ingenuity.com); and 2) GOBO (http://co.bmc.lu.se/gobo) [59]. In order to use the latter tool, Affymetrix GeneChip Mouse Gene 1.0 ST IDs were mapped to Affymetrix Human Genome U133A IDs using Biomart for Ensembl build 66. The module "Gene Set Analysis Tumors" was used to investigate the expression pattern and to perform survival and functional correlation analyses for the SRF-dependent/SAP-independent and SRF-independent/SAP-dependent gene sets across 1881 breast cancers characterized by Affymetrix Human Genome U133A arrays.

### RNA analyses by qRT-PCR

Total RNA was isolated from HC11 cell strains after 24 h of incubation either in 0.03 or 3% FCS/RPMI. RNA was reverse transcribed and relative tenascin-C and c-fos mRNA levels were detected as described [12,13]. Relative mRNA levels for the genes listed in Table 1, normalized to Gapdh, were measured using Platinum® SYBR® Green qPCR SuperMix-UDG with ROX (Invitrogen) and the primers listed in Additional file 4: Table S4. Real-time PCR was performed in a StepOnePlus Real-Time PCR System (Applied Biosystems, Rotkreuz, Switzerland) using a standard cycling profile. All samples were run in duplicate. Data were analyzed by the ΔCt method [83] and presented as fold changes in mRNA expression levels between HC11-FL and HC11-ΔSAP cells. RNA from stretched cells was analyzed by qRT-PCR using the efficiency ΔΔCt method [84] that included a further normalization to the resting control. Data represent means ± SD from three independent experiments.

### Protein analyses by immunoblotting and zymography

After 24 h of starvation, whole-cell extracts from the three HC11 strains were prepared in RIPA buffer and immunoblotting was performed as described [12,13]. The following primary antibodies were used: mAb65F13 anti-Mkl1 [12], MTn12 anti-Tnc [85], anti-Wisp1/CCN4 (clone 214203, R&D Systems), anti-Nox4 (NB110-58851, Novus Biologicals), anti-Vcl (clone hVIN-1, Sigma) and anti-Gapdh (ab9485, Abcam).

After reaching 90% confluency, HC11 strains were starved for 48 h before conditioned medium was collected, concentrated and analyzed by zymography as described [86].

### Promoter-reporter assays

The tenascin-C promoter used in this study was described as TNC 247 bp [13]. Promoters of Acta2 [87] and all SRF-independent/SAP-dependent genes described in Table 1 were PCR-amplified from genomic DNA and corresponded to the sequences listed in Additional file 4: Table S5. Each promoter contained ≥ 500 bp 5′ of the TSS and was cloned into the pSEAP2-Basic (Clontech, Saint-Germain-en-Laye, France). For some promoters also 200 bp proximal promoter sequences were cloned as described above. All clones were verified by DNA sequencing.

HC11 cells in 6-well plates were cotransfected with 1 μg of the SEAP reporter vectors, 1 μg of pcDNA3 vectors encoding Mkl1 variants [13], and 200 ng of the secreted luciferase MetLuc vector (Clontech) used to normalize for transfection efficiency. Cells were cultured in 0.03% FCS/RPMI for 24 h before enzymatic activity measurements were performed as described [13]. Experimental values represent averages of three independent experiments, each performed in duplicate.

### Statistical analysis

Numerical results were expressed as means ± SD. Statistical analysis was completed using GraphPad InStat Software, version 3.05. The two-tailed Student's *t* test was used to evaluate differences between two groups. Multiple comparisons were performed using one-way analysis of variance (ANOVA). Values of P less than 0.05 were considered statistically significant. Statistics for bioinformatics analyses is given in figure legends.

## Additional files

**Additional file 1: Table S1.** SRF-dependent/SAP-independent probeset list.

**Additional file 2: Table S2.** SRF-dependent/SAP-dependent probeset list.

**Additional file 3: Table S3.** SRF-independent/SAP-dependent probeset list.

**Additional file 4: Table S4.** Primer sequences. **Table S5.** Promoter constructs. **Figure S1.** Quantification of SAP-dependent Mkl1 target gene expression using qRT-PCR analysis. **Figure S2.** Differential expression of newly discovered Mkl1 target genes in HC11 strains overexpressing either FL-, mutB1- or ΔSAP-Mkl1 constructs (protein analyses performed by immunoblotting and zymography). **Figure S3.** SAP-dependent Mkl1 target genes are correlated with a very high significance ($P < 0.00001$) with the two proliferation modules – mitotic checkpoint and mitotic progression (a functional correlation analysis performed using the GOBO bioinformatics tool).

### Competing interests

The authors declare that they have no competing interests.

### Authors' contributions

MBA and RCE conceived the project. MBA designed the experiments. MBA and TR performed transcript profiling of HC11 cell strains and bioinformatics analysis. Promoter-reporter studies were designed by RCE and performed by JF. IG and JF performed Western blot and zymographic analysis, and mechanical strain experiments. IG performed qRT-PCR experiments, cell proliferation and cell migration assays. MBA and RCE interpreted the data and wrote the paper. All authors discussed the results, read and approved the final manuscript.

### Acknowledgements

We thank Hubertus Kohler for FACS service, Stephane Thiry for microarray hybridization, and Matthias Chiquet and Richard P. Tucker for critical reading of the manuscript. This work was supported by grants from the Cancer League of Basel, the Swiss Cancer League and the Swiss National Science Foundation 3100A0-120235 and 31003A_135584 to R.C.E.

Received: 28 June 2013 Accepted: 30 January 2014
Published: 5 February 2014

### References

1. Orend G, Chiquet-Ehrismann R: **Tenascin-C induced signaling in cancer.** *Cancer Lett* 2006, **244:**143–163.
2. Brellier F, Chiquet-Ehrismann R: **How do tenascins influence the birth and life of a malignant cell?** *J Cell Mol Med* 2012, **16:**32–40.
3. Jahkola T, Toivonen T, Virtanen I, von Smitten K, Nordling S, von Boguslawski K, Haglund C, Nevanlinna H, Blomqvist C: **Tenascin-C expression in invasion border of early breast cancer: a predictor of local and distant recurrence.** *Br J Cancer* 1998, **78:**1507–1513.
4. Tsunoda T, Inada H, Kalembeyi I, Imanaka-Yoshida K, Sakakibara M, Okada R, Katsuta K, Sakakura T, Majima Y, Yoshida T: **Involvement of large tenascin-C splice variants in breast cancer progression.** *Am J Pathol* 2003, **162:**1857–1867.
5. Minn AJ, Gupta GP, Siegel PM, Bos PD, Shu W, Giri DD, Viale A, Olshen AB, Gerald WL, Massague J: **Genes that mediate breast cancer metastasis to lung.** *Nature* 2005, **436:**518–524.
6. Calvo A, Catena R, Noble MS, Carbott D, Gil-Bazo I, Gonzalez-Moreno O, Huh JI, Sharp R, Qiu TH, Anver MR, *et al*: **Identification of VEGF-regulated genes associated with increased lung metastatic potential: functional involvement of tenascin-C in tumor growth and lung metastasis.** *Oncogene* 2008, **27:**5373–5384.
7. Tavazoie SF, Alarcon C, Oskarsson T, Padua D, Wang Q, Bos PD, Gerald WL, Massague J: **Endogenous human microRNAs that suppress breast cancer metastasis.** *Nature* 2008, **451:**147–152.
8. Oskarsson T, Acharyya S, Zhang XHF, Vanharanta S, Tavazoie SF, Morris PG, Downey RJ, Manova-Todorova K, Brogi E, Massague J: **Breast cancer cells produce tenascin C as a metastatic niche component to colonize the lungs.** *Nat Med* 2011, **17:**867–874.
9. O'Connell JT, Sugimoto H, Cooke VG, MacDonald BA, Mehta AI, LeBleu VS, Dewar R, Rocha RM, Brentani RR, Resnick MB, *et al*: **VEGF-A and Tenascin-C produced by S100A4+ stromal cells are important for metastatic colonization.** *Proc Natl Acad Sci USA* 2011, **108:**16002–16007.
10. Chiquet-Ehrismann R, Tucker RP: **Tenascins and the importance of adhesion modulation.** *Cold Spring Harb Perspect Biol* 2011. doi:10.1101/cshperspect.a004960.

11. Chiquet M, Sarasa-Renedo A, Tunc-Civelek V: **Induction of tenascin-C by cyclic tensile strain versus growth factors: distinct contributions by Rho/ROCK and MAPK signaling pathways.** *Biochim Biophys Acta* 2004, **1693:**193–204.
12. Maier S, Lutz R, Gelman L, Sarasa-Renedo A, Schenk S, Grashoff C, Chiquet M: **Tenascin-C induction by cyclic strain requires integrin-linked kinase.** *Biochim Biophys Acta* 2008, **1783:**1150–1162.
13. Asparuhova MB, Ferralli J, Chiquet M, Chiquet-Ehrismann R: **The transcriptional regulator megakaryoblastic leukemia-1 mediates serum response factor-independent activation of tenascin-C transcription by mechanical stress.** *FASEB J* 2011, **25:**3477–3488.
14. Wang DZ, Li S, Hockemeyer D, Sutherland L, Wang Z, Schratt G, Richardson JA, Nordheim A, Olson EN: **Potentiation of serum response factor activity by a family of myocardin-related transcription factors.** *Proc Natl Acad Sci USA* 2002, **99:**14855–14860.
15. Cen B, Selvaraj A, Burgess RC, Hitzler JK, Ma Z, Morris SW, Prywes R: **Megakaryoblastic leukemia 1, a potent transcriptional coactivator for serum response factor (SRF), is required for serum induction of SRF target genes.** *Mol Cell Biol* 2003, **23:**6597–6608.
16. Miralles F, Posern G, Zaromytidou AI, Treisman R: **Actin dynamics control SRF activity by regulation of its coactivator MAL.** *Cell* 2003, **113:**329–342.
17. Olson EN, Nordheim A: **Linking actin dynamics and gene transcription to drive cellular motile functions.** *Nat Rev Mol Cell Biol* 2010, **11:**353–365.
18. Miano JM, Long X, Fujiwara K: **Serum response factor: master regulator of the actin cytoskeleton and contractile apparatus.** *Am J Physiol Cell Physiol* 2007, **292:**C70–C81.
19. Ball R, Friis R, Schoenenberger C, Doppler W, Groner B: **Prolactin regulation of beta-casein gene expression and of a cytosolic 120-kd protein in a cloned mouse mammary epithelial cell line.** *EMBO J* 1988, **7:**2089–2095.
20. Humphreys R, Rosen J: **Stably transfected HC11 cells provide an in vitro and in vivo model system for studying Wnt gene function.** *Cell Growth Differ* 1997, **8:**839–849.
21. Cicalese A, Bonizzi G, Pasi CE, Faretta M, Ronzoni S, Giulini B, Brisken C, Minucci S, Di Fiore PP, Pelicci PG: **The tumor suppressor p53 regulates polarity of self-renewing divisions in mammary stem cells.** *Cell* 2009, **138:**1083–1095.
22. Williams C, Helguero L, Edvardsson K, Haldosen LA, Gustafsson JA: **Gene expression in murine mammary epithelial stem cell-like cells shows similarities to human breast cancer gene expression.** *Breast Cancer Res* 2009, **11:**R26.
23. Cen B, Selvaraj A, Prywes R: **Myocardin/MKL family of SRF coactivators: key regulators of immediate early and muscle specific gene expression.** *J Cell Biochem* 2004, **93:**74–82.
24. Wang DZ, Olson EN: **Control of smooth muscle development by the myocardin family of transcriptional coactivators.** *Curr Opin Genet Dev* 2004, **14:**558–566.
25. Pipes GCT, Creemers EE, Olson EN: **The myocardin family of transcriptional coactivators: versatile regulators of cell growth, migration, and myogenesis.** *Genes Dev* 2006, **20:**1545–1556.
26. Piekny AJ, Maddox AS: **The myriad roles of Anillin during cytokinesis.** *Semin Cell Dev Biol* 2010, **21:**881–891.
27. Hall PA, Todd CB, Hyland PL, McDade SS, Grabsch H, Dattani M, *et al*: **The septin-binding protein anillin is overexpressed in diverse human tumors.** *Clin Cancer Res* 2005, **11:**6780–6786.
28. Suzuki C, Daigo Y, Ishikawa N, Kato T, Hayama S, Ito T, *et al*: **ANLN plays a critical role in human lung carcinogenesis through the activation of RhoA and by involvement in the phosphoinositide 3-kinase/AKT pathway.** *Cancer Res* 2005, **65:**11314–11325.
29. Reddy MM, Fernandes MS, Salgia R, Levine RL, Griffin JD, Sattler M: **NADPH oxidases regulate cell growth and migration in myeloid cells transformed by oncogenic tyrosine kinases.** *Leukemia* 2011, **25:**281–289.
30. Ushio-Fukai M, Nakamura Y: **Reactive oxygen species and angiogenesis: NADPH oxidase as target for cancer therapy.** *Cancer Lett* 2008, **266:**37–52.
31. Sakamoto N, Oue N, Noguchi T, Sentani K, Anami K, Sanada Y, *et al*: **Serial analysis of gene expression of esophageal squamous cell carcinoma: ADAMTS16 is upregulated in esophageal squamous cell carcinoma.** *Cancer Sci* 2010, **101:**1038–1044.
32. Davidson RK, Waters JG, Kevorkian L, Darrah C, Cooper A, Donell ST, *et al*: **Expression profiling of metalloproteinases and their inhibitors in synovium and cartilage.** *Arthritis Res Ther* 2006, **8:**R124.
33. Kim S, Wong P, Coulombe PA: **A keratin cytoskeletal protein regulates protein synthesis and epithelial cell growth.** *Nature* 2006, **441:**362–365.
34. Alam H, Sehgal L, Kundu ST, Dalal SN, Vaidya MM: **Novel function of keratins 5 and 14 in proliferation and differentiation of stratified epithelial cells.** *Mol Biol Cell* 2011, **22:**4068–4078.
35. Hosokawa M, Takehara A, Matsuda K, Eguchi H, Ohigashi H, Ishikawa O, *et al*: **Oncogenic role of KIAA0101 interacting with proliferating cell nuclear antigen in pancreatic cancer.** *Cancer Res* 2007, **67:**2568–2576.
36. Xu L, Geman D, Winslow R: **Large-scale integration of cancer microarray data identifies a robust common cancer signature.** *BMC Bioinforma* 2007, **8:**275.
37. Turchi L, Fareh M, Aberdam E, Kitajima S, Simpson F, Wicking C, *et al*: **ATF3 and p15PAF are novel gatekeepers of genomic integrity upon UV stress.** *Cell Death Differ* 2009, **16:**728–737.
38. Amrani YM, Gill J, Matevossian A, Alonzo ES, Yang C, Shieh JH, *et al*: **The Paf oncogene is essential for hematopoietic stem cell function and development.** *J Exp Med* 2011, **208:**1757–1765.
39. Zhao Y, Zhang J, Li H, Li Y, Ren J, Luo M, *et al*: **An NADPH sensor protein (HSCARG) down-regulates nitric oxide synthesis by association with argininosuccinate synthetase and is essential for epithelial cell viability.** *J Biol Chem* 2008, **283:**11004–11013.
40. Mun GI, Kim IS, Lee BH, Boo YC: **Endothelial argininosuccinate synthetase 1 regulates nitric oxide production and monocyte adhesion under static and laminar shear stress conditions.** *J Biol Chem* 2011, **286:**2536–2542.
41. Blanchet MR, Gold M, Maltby S, Bennett J, Petri B, Kubes P, *et al*: **Loss of CD34 Leads To exacerbated autoimmune arthritis through increased vascular permeability.** *J Immunol* 2010, **184:**1292–1299.
42. Trempus CS, Morris RJ, Ehinger M, Elmore A, Bortner CD, Ito M, *et al*: **CD34 Expression by hair follicle stem cells is required for skin tumor development in mice.** *Cancer Res* 2007, **67:**4173–4181.
43. Maltby S, Freeman S, Gold MJ, Baker JH, Minchinton AI, Gold MR, *et al*: **Opposing roles for CD34 in B16 melanoma tumor growth alter early stage vasculature and late stage immune cell infiltration.** *PLoS One* 2011, **6:**e18160.
44. Berschneider B, Koenigshoff M: **WNT1 inducible signaling pathway protein 1 (WISP1): A novel mediator linking development and disease.** *Int J Biochem Cell Biol* 2011, **43:**306–309.
45. Noseda M, Karsan A: **Notch and minichromosome maintenance (MCM) proteins: integration of two ancestral pathways in cell cycle control.** *Cell Cycle* 2006, **5:**2704–2709.
46. Hsieh MJ, Chen KS, Chiou HL, Hsieh YS: **Carbonic anhydrase XII promotes invasion and migration ability of MDA-MB-231 breast cancer cells through the p38 MAPK signaling pathway.** *Eur J Cell Biol* 2010, **89:**598–606.
47. Neri D, Supuran CT: **Interfering with pH regulation in tumours as a therapeutic strategy.** *Nat Rev Drug Discov* 2011, **10:**767–777.
48. Whitman S, Wang X, Shalaby R, Shtivelman E: **Alternatively spliced products CC3 and TC3 have opposing effects on apoptosis.** *Mol Cell Biol* 2000, **20:**583–593.
49. Paris S, Sesboue R, Chauzy C, Maingonnat C, Delpech B: **Hyaluronectin modulation of lung metastasis in nude mice.** *Eur J Cancer* 2006, **42:**3253–3259.
50. Uchiyama Y, Sakaguchi M, Terabayashi T, Inenaga T, Inoue S, Kobayashi C, *et al*: **Kif26b, a kinesin family gene, regulates adhesion of the embryonic kidney mesenchyme.** *Proc Natl Acad Sci USA* 2010, **107:**9240–9245.
51. Lucero H, Kagan H: **Lysyl oxidase: an oxidative enzyme and effector of cell function.** *Cell Mol Life Sci* 2006, **63:**2304–2316.
52. Rodriguez C, Rodriguez-Sinovas A, Martinez-Gonzalez J: **Lysyl oxidase as a potential therapeutic target.** *Drug News Perspect* 2008, **21:**218–224.
53. Shiomi T, Lemaitre V, D'Armiento J, Okada Y: **Matrix metalloproteinases, a disintegrin and metalloproteinases, and a disintegrin and metalloproteinases with thrombospondin motifs in non-neoplastic diseases.** *Pathol Int* 2010, **60:**477–496.
54. Hua H, Li M, Luo T, Yin Y, Jiang Y: **Matrix metalloproteinases in tumorigenesis: an evolving paradigm.** *Cell Mol Life Sci* 2011, **68:**3853–3868.
55. Elberg G, Chen L, Elberg D, Chan MD, Logan CJ, Turman MA: **MKL1 mediates TGF-β1-induced α-smooth muscle actin expression in human renal epithelial cells.** *Am J Physiol Renal Physiol* 2008, **294:**F1116–F1128.
56. Long X, Cowan SL, Miano JM: **Mitogen-activated protein kinase 14 is a novel negative regulatory switch for the vascular smooth muscle cell contractile gene program.** *Arterioscler Thromb Vasc Biol* 2013, **33:**378–386.
57. Quaglino A, Salierno M, Pellegrotti J, Rubinstein N, Kordon E: **Mechanical strain induces involution-associated events in mammary epithelial cells.** *BMC Cell Biol* 2009, **10:**55.

58. Cox TR, Bird D, Baker AM, Barker HE, Ho MWY, Lang G, Erler JT: **LOX-mediated collagen crosslinking is responsible for fibrosis-enhanced metastasis.** *Cancer Res* 2013, **73:**1721–1732.
59. Ringner M, Fredlund E, Hakkinen J, Borg Å, Staaf J: **GOBO: gene expression-based outcome for breast cancer online.** *PLoS One* 2011, **6:**e17911.
60. Parker JS, Mullins M, Cheang MCU, Leung S, Voduc D, Vickery T, Davies S, Fauron C, He X, Hu Z, *et al*: **Supervised risk predictor of breast cancer based on intrinsic subtypes.** *J Clin Oncol* 2009, **27:**1160–1167.
61. Fredlund E, Staaf J, Rantala J, Kallioniemi O, Borg A, Ringner M: **The gene expression landscape of breast cancer is shaped by tumor protein p53 status and epithelial-mesenchymal transition.** *Breast Cancer Res* 2012, **14:**R113.
62. Minn AJ, Bevilacqua E, Yun J, Rosner MR: **Identification of novel metastasis suppressor signaling pathways for breast cancer.** *Cell Cycle* 2012, **11:**2452–2457.
63. Scharenberg MA, Chiquet-Ehrismann R, Asparuhova MB: **Megakaryoblastic leukemia protein-1 (MKL1): Increasing evidence for an involvement in cancer progression and metastasis.** *Int J Biochem Cell Biol* 2010, **42:**1911–1914.
64. Medjkane S, Perez-Sanchez C, Gaggioli C, Sahai E, Treisman R: **Myocardin-related transcription factors and SRF are required for cytoskeletal dynamics and experimental metastasis.** *Nat Cell Biol* 2009, **11:**257–268.
65. Descot A, Hoffmann R, Shaposhnikov D, Reschke M, Ullrich A, Posern G: **Negative regulation of the EGFR-MAPK cascade by actin-MAL-mediated Mig6/Errfi-1 induction.** *Mol Cell* 2009, **35:**291–304.
66. Leitner L, Shaposhnikov D, Descot A, Hoffmann R, Posern G: **Epithelial protein lost in neoplasm alpha (Eplin-alpha) is transcriptionally regulated by G-actin and MAL/MRTF coactivators.** *Mol Cancer* 2010, **9:**60.
67. Yoshio T, Morita T, Tsujii M, Hayashi N, Sobue K: **MRTF-A/B suppress the oncogenic properties of v-ras- and v-src-mediated transformants.** *Carcinogenesis* 2010, **31:**1185–1193.
68. Brandt DT, Baarlink C, Kitzing TM, Kremmer E, Ivaska J, Nollau P, Grosse R: **SCAI acts as a suppressor of cancer cell invasion through the transcriptional control of beta1-integrin.** *Nat Cell Biol* 2009, **11:**557–568.
69. Throm Quinlan A, Sierad L, Capulli A, Firstenberg L, Billiar K: **Combining dynamic stretch and tunable stiffness to probe cell mechanobiology in vitro.** *PLoS One* 2011, **6:**e23272.
70. Levental KR, Yu H, Kass L, Lakins JN, Egeblad M, Erler JT, Fong SFT, Csiszar K, Giaccia A, Weninger W, *et al*: **Matrix crosslinking forces tumor progression by enhancing integrin signaling.** *Cell* 2009, **139:**891–906.
71. Lopez JI, Kang I, You WK, McDonald DM, Weaver VM: **In situ force mapping of mammary gland transformation.** *Integr Biol (Camb)* 2011, **3:**910–921.
72. Cox TR, Erler JT: **Remodeling and homeostasis of the extracellular matrix: implications for fibrotic diseases and cancer.** *Dis Model Mech* 2011, **4:**165–178.
73. Lu P, Weaver VM, Werb Z: **The extracellular matrix: A dynamic niche in cancer progression.** *J Cell Biol* 2012, **196:**395–406.
74. Kessenbrock K, Plaks V, Werb Z: **Matrix metalloproteinases: Regulators of the tumor microenvironment.** *Cell* 2010, **141:**52–67.
75. Nakagawa K, Kuzumaki N: **Transcriptional activity of megakaryoblastic leukemia 1 (MKL1) is repressed by SUMO modification.** *Genes Cells* 2005, **10:**835–850.
76. Muehlich S, Wang R, Lee SM, Lewis TC, Dai C, Prywes R: **Serum-induced phosphorylation of the serum response factor coactivator MKL1 by the extracellular signal-regulated kinase 1/2 pathway inhibits its nuclear localization.** *Mol Cell Biol* 2008, **28:**6302–6313.
77. Muehlich S, Hampl V, Khalid S, Singer S, Frank N, Breuhahn K, Gudermann T, Prywes R: **The transcriptional coactivators megakaryoblastic leukemia 1/2 mediate the effects of loss of the tumor suppressor deleted in liver cancer 1.** *Oncogene* 2012, **31:**3913–3923.
78. Zaromytidou AI, Miralles F, Treisman R: **MAL and ternary complex factor use different mechanisms to contact a common surface on the serum response factor DNA-binding domain.** *Mol Cell Biol* 2006, **26:**4134–4148.
79. Brellier F, Ruggiero S, Zwolanek D, Martina E, Hess D, Brown-Luedi M, Hartmann U, Koch M, Merlo A, Lino M, Chiquet-Ehrismann R: **SMOC1 is a tenascin-C interacting protein over-expressed in brain tumors.** *Matrix Biol* 2011, **30:**225–233.
80. Schindelin J, Arganda-Carreras I, Frise E, Kaynig V, Longair M, Pietzsch T, Preibisch S, Rueden C, Saalfeld S, Schmid B, *et al*: **Fiji: an open-source platform for biological-image analysis.** *Nat Methods* 2012, **9:**676–682.
81. Gentleman R, Carey V, Bates D, Bolstad B, Dettling M, Dudoit S, Ellis B, Gautier L, Ge Y, Gentry J, *et al*: **Bioconductor: open software development for computational biology and bioinformatics.** *Genome Biol* 2004, **5:**R80.
82. Smyth GK, Speed T: **Normalization of cDNA microarray data.** *Methods* 2003, **31:**265–273.
83. Schmittgen TD, Livak KJ: **Analyzing real-time PCR data by the comparative CT method.** *Nat Protoc* 2008, **3:**1101–1108.
84. Livak KJ, Schmittgen TD: **Analysis of relative gene expression data using real-time quantitative PCR and the 2(-Delta Delta C(T)) Method.** *Methods* 2001, **25:**402–408.
85. Aufderheide E, Ekblom P: **Tenascin during gut development: appearance in the mesenchyme, shift in molecular forms, and dependence on epithelial-mesenchymal interactions.** *J Cell Biol* 1988, **107:**2341–2349.
86. Li DQ, Meller D, Liu Y, Tseng SCG: **Overexpression of MMP-1 and MMP-3 by Cultured Conjunctivochalasis Fibroblasts.** *Invest Ophthalmol Vis Sci* 2000, **41:**404–410.
87. Min BH, Foster DN, Strauch AR: **The 5′-flanking region of the mouse vascular smooth muscle alpha-actin gene contains evolutionarily conserved sequence motifs within a functional promoter.** *J Biol Chem* 1990, **265:**16667–16675.

doi:10.1186/1476-4598-13-22
**Cite this article as:** Gurbuz *et al.*: SAP domain-dependent Mkl1 signaling stimulates proliferation and cell migration by induction of a distinct gene set indicative of poor prognosis in breast cancer patients. *Molecular Cancer* 2014 **13**:22.

### 2.1.1 Supplementary information

**Additional file for:**

"SAP domain-dependent Mkl1 signaling stimulates proliferation and cell migration by induction of a distinct gene set indicative of poor prognosis in breast cancer patients"

**Content:**

**Table S4. Primer Sequences.**

| Gene symbol | Gene bank accession number | Primer pair (fwd/rev) | Amplicon size (bp) |
|---|---|---|---|
| Anln | NM_028390.3 | 5’-CAGTGGTGACGCTCTGACAT-3'<br>5’-GGGACTGGCCATAACTGAAG-3' | 220 |
| Nox4 | NM_015760.4 | 5’-CATTCCAGTGGTTTGCAGATT-3'<br>5’-AACTGGGTCCACAGCAGAAA-3' | 249 |
| Adamts16 | NM_172053.2 | 5’-TTGGAGAGAAAGCCAAGCTC-3'<br>5’-GGGCCTTCATCACCGTACT-3' | 181 |
| Krt5 | NM_027011.2 | 5’-CAGGACCTGGTGGAGGACTA-3'<br>5’-CCATGGAAAGGACCACAGAT-3' | 241 |
| p15(PAF) | NM_026515.2 | 5’-GGGAATTCTTCAGGCTGTCC-3'<br>5’-CAACAAGCCAATTGGACAAA-3' | 227 |
| Ass1 | NM_007494.3 | 5’-CACCACATCCCTGGAACTCT-3'<br>5’-ATGAGCGTGGTAAAGGATGG-3' | 151 |
| Cd34 | NM_001111059.1 | 5’-AGGCTGATGCTGGTGCTAGT-3'<br>5’-ACTCCAGAGGTGACCAATGC-3' | 235 |
| Wisp1 | NM_018865.2 | 5’-GCTCTACCACCTGTGGCCTA-3'<br>5’-ACAGCCTGCGAGAGTGAAGT-3' | 194 |
| Mcm6 | NM_008567.1 | 5’-CATGTCCCGCTTTGATCTCT-3'<br>5’-CTGGCGGAGACGTTTGTACT-3' | 232 |
| Car12 | NM_178396.4 | 5’-GTTCGATGAGAGGCTGGTGT-3'<br>5’-CCTCAGCCTCCTTCTTGATG-3' | 215 |
| Htatip2 | NM_016865.3 | 5’-GCTGGATGTCTATGCTTCTGC-3'<br>5’-TCAACCTTGGCTTCCACTTC-3' | 243 |
| Kif26b | NM_001161665.1 | 5’-AAGAAGCAGCCAGGTTCCTC-3'<br>5’-AATGCCCAGGTTCTGCATAG-3' | 214 |
| Lox | NM_010728.2 | 5’-CAGGGATTGAGTCCTGGATG-3'<br>5’-ACTGGGAACTGGGCTTCTTT-3' | 242 |
| Mmp12 | NM_008605.3 | 5’-CATCCCATCTGGTATTCAAGC-3'<br>5’-ATGAGCTCCTGCCTCACATC-3' | 249 |
| Mmp3 | NM_010809.1 | 5’-CATCACCAATGTGCAGCTCT-3'<br>5’-CTCCTCGTGCCCTCGTATAG-3' | 248 |
| Gapdh | NM_008084.2 | 5’-CTTGTGCAGTGCCAGCCTC-3'<br>5’-GCCGTGAGTGGAGTCATACTG-3' | 189 |

**Table S5. Promoter constructs.**

| Promoter | Accession number | Nucleotide position |
|---|---|---|
| mTNC 247bp | NT_039260.7 | 3336826-3336433 |
| Wisp1 >500bp | NT_039621.7 | 28008443-28009129 |
| Wisp1 200bp | NT_039621.7 | 28008801-28009129 |
| Krt5 >500bp | NT_039621.7 | 62829844-62829249 |
| Krt5 200bp | NT_039621.7 | 62829551-62829249 |
| Kif26b >500bp | NT_039185.7 | 22360019-22360523 |
| Kif26b 200bp | NT_039185.7 | 22360158-22360523 |
| Htatip2 >500bp | NT_039424.7 | 10657737-10658750 |
| Htatip2 200bp | NT_039424.7 | 10658493-10658750 |
| Nox4 >500bp | NT_039433.7 | 4994940-4995484 |
| Nox4 200bp | NT_039433.7 | 4995123-4995484 |
| Car12 >500bp | NT_039474.7 | 12981551-12982239 |
| Car12 200bp | NT_039474.7 | 12981860-12982239 |
| Adamts16 >500bp | NT_039589.7 | 16522290-16521672 |
| Adamts16 200bp | NT_039589.7 | 16522032-16521672 |
| Cd34 >500bp | NT_039190.7 | 2888907-2889501 |
| Cd34 343bp | NT_039190.7 | 2889159-2889501 |
| Anln >500bp | NT_039472.7 | 8976459-8975867 |
| p15(PAF) >500bp | NT_039474.7 | 12158197-12158785 |
| Mcm6 >500bp | NT_078297.6 | 42913044-42912468 |
| Ass1 >500bp | NT_039206.7 | 8927941-8928521 |
| Acta2 562bp | NT_039687.7 | 27442283-27441676 |

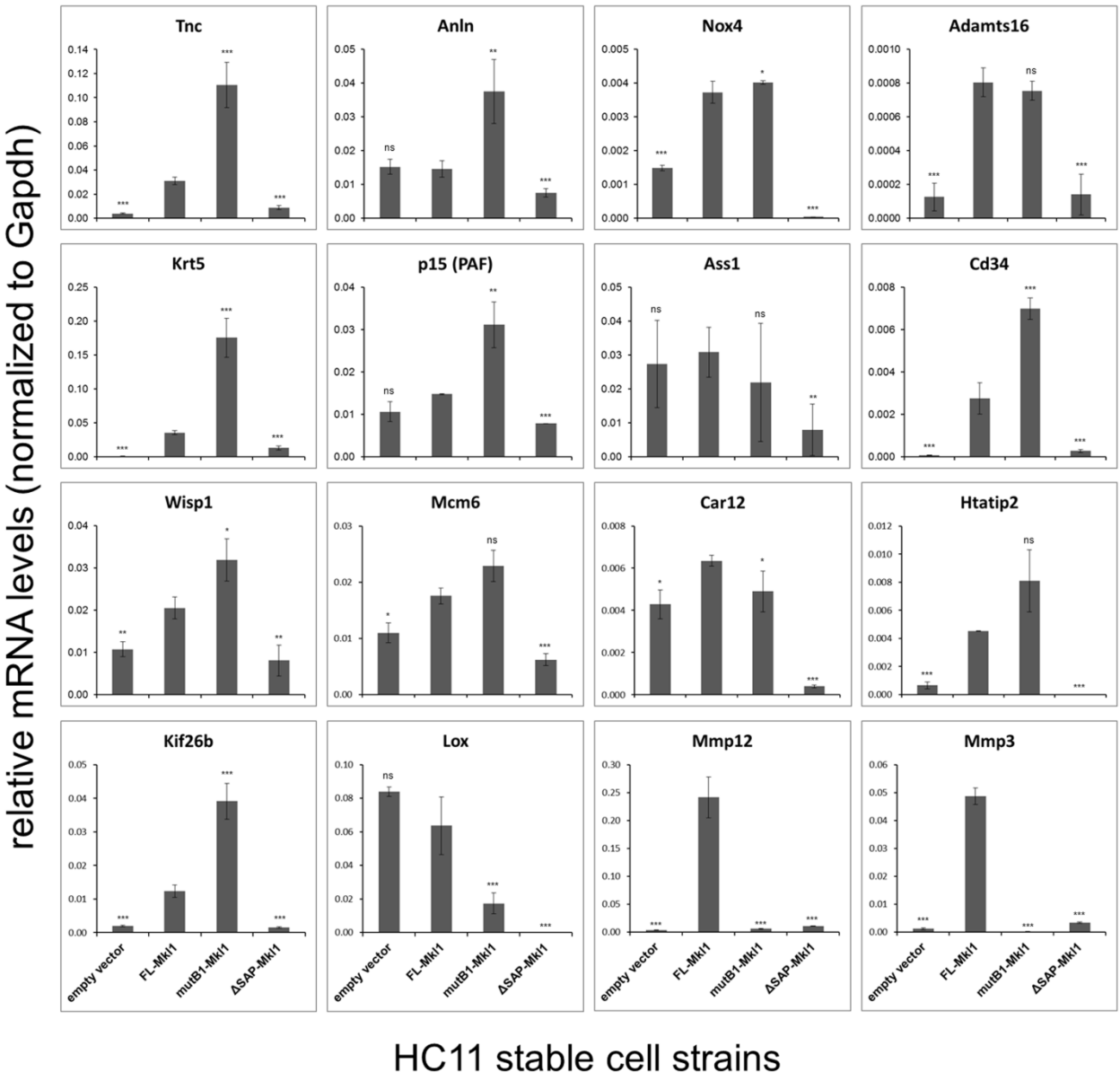


**Figure S1. Quantification of SAP-dependent Mkl1 target gene expression using qRT-PCR analysis.** Relative mRNA levels for the genes listed in Table 1, normalized to Gapdh, were analyzed in HC11 cells stably transfected with either empty vector or with vectors encoding FL-, mutB1- or ΔSAP-Mkl1 proteins. The results agreed with the data obtained by transcript profiling (Figure 1). Induction of these genes strongly depends on the SAP domain of Mkl1 as well as on the B1 domain for Lox, Mmp12 and Mmp3 genes, which belong to the SRF-dependent/SAP-dependent gene set. Means ± SD from three independent experiments and significant differences to the HC11-FL cells, ***P < 0.001, **P < 0.01, *P < 0.05 are shown.

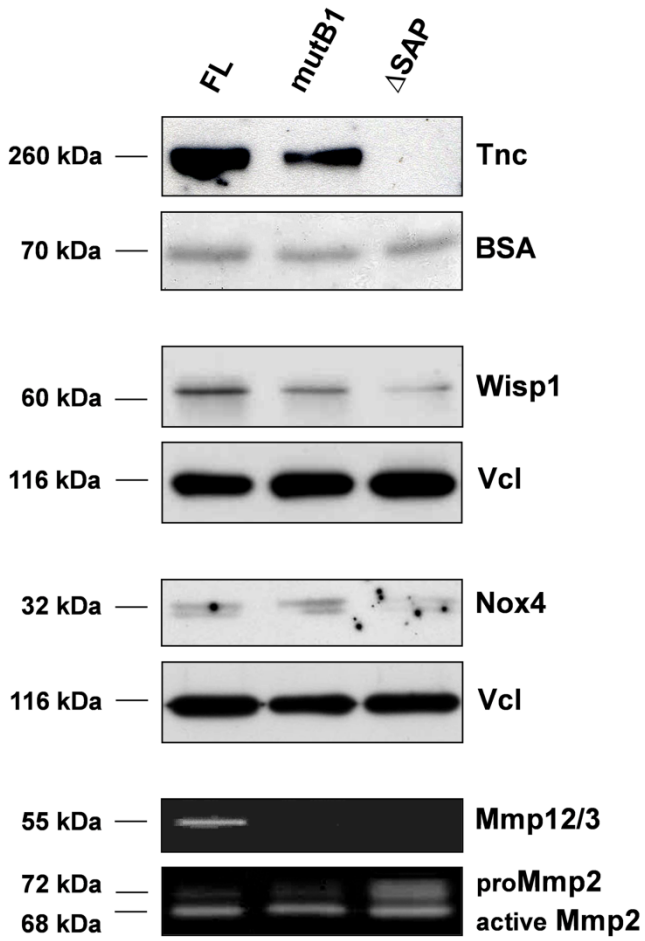


**Figure S2. Differential expression of newly discovered Mkl1 target genes in HC11 strains overexpressing either FL-, mutB1- or ΔSAP-Mkl1 constructs.** Western blot analysis of Tnc, Wisp1 and Nox4, and zymographic analysis for Mmp12/3 show SAP-dependent protein expression in HC11 epithelial cells. Secreted Tnc protein was detected in cell culture media using the MTn12 anti-Tnc antibody, and bovine serum albumin (BSA) from the medium visualized by Ponceau S staining served as loading control. Wisp1 and Nox4 proteins were detected in whole-cell extracts from the three HC11 cell strains, HC11-FL, HC11-mutB1 and HC11-ΔSAP using respective antibodies. Anti-Vcl served as loading control. Conditioned media from the three HC11 cell strains was subjected to casein or gelatin zymography for detection of the matrix metalloproteinases Mmp12/3 and Mmp2, respectively. For Mmp2, both an inactive (proMmp2) and active form was detected and served as loading control. Relevant bands and molecular weight markers (in kDa) are indicated on the right and left of each panel, respectively.

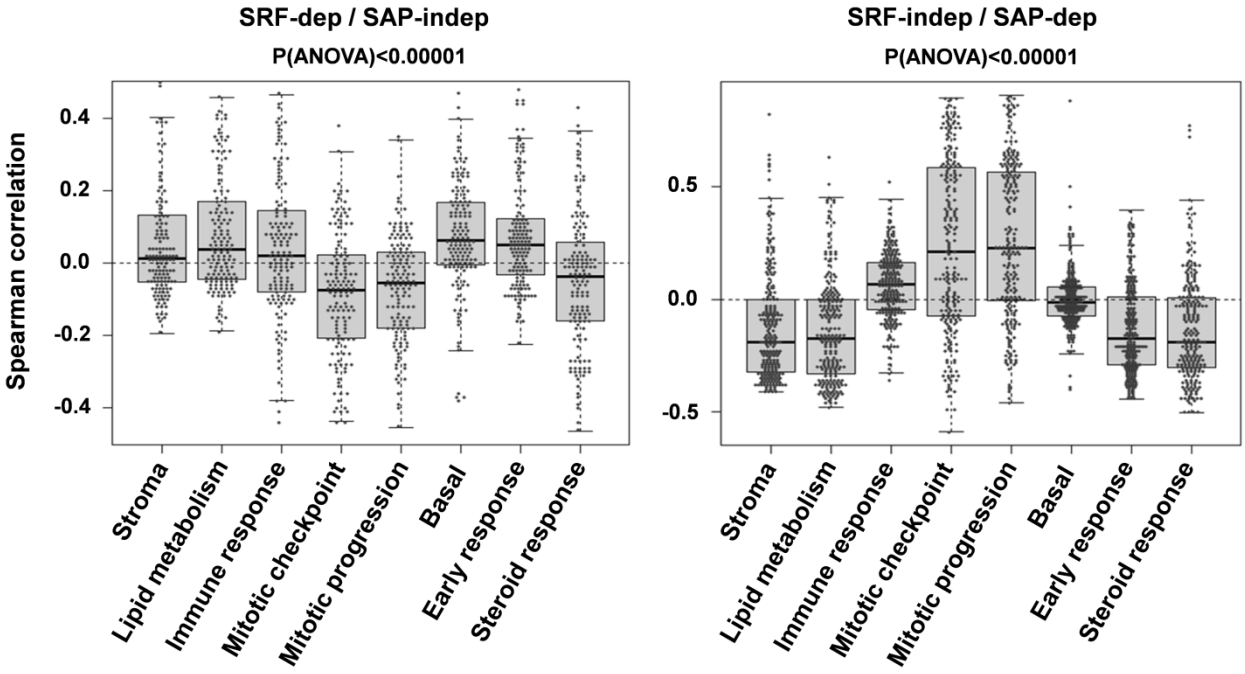


**Figure S3. SAP-dependent Mkl1 target genes are correlated with a very high significance (P < 0.00001) with the two proliferation modules – mitotic checkpoint and mitotic progression.** Functional correlation of genes in the SRF-dependent/SAP-independent (left panel) and SRF-independent/SAP-dependent (right panel) gene sets to different gene expression modules emulating breast cancer-specific biological processes [33] was performed using the GOBO bioinformatics tool. For each gene module and gene in the two gene data sets, a Spearman correlation value is computed by comparing the expression pattern across all samples for a specific gene to the corresponding rank sum for each sample in the specific module. Dots indicate actual correlation values.

## 2.2 Unpublished Results

### 2.2.1 WISP1 mRNA expression in transformed mouse mammary epithelial cell lines

Isogenic mouse breast cancer cell lines, 67NR, 168FARN, 4T07, 4T1 can form primary tumors with equivalent kinetics but differ in their ability to metastasize when implanted into the mammary glands of BALB/c mice (Aslakson and Miller, 1992) (Figure 1). 67NR cells can form primary tumors, but tumor cells do not intravasate and metastasize. 168FARN cells are slightly metastatic and can be detected in the lymph nodes, but rarely in other tissues such as the lungs. This observation suggest that 168FARN cells can disseminate from the primary tumor site and enter the blood stream, however they do not extravasate efficiently. Cells of the 4TO7 line are able to spread to the lungs, but cannot form visible metastatic nodules. Moreover, when the primary 4T07 tumor is removed, clonogenic cells within the lungs disappear suggesting that they fail to colonize distant sites. 4T1 cells are fully metastatic and can form macroscopic lung nodules (Aslakson and Miller, 1992).

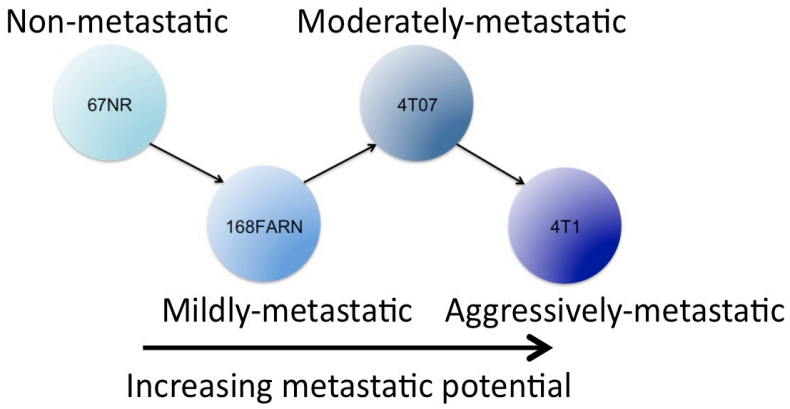

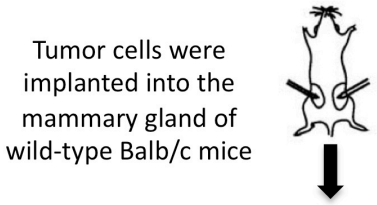


| | 67NR | 168FARN | 4T07 | 4T1 |
|---|---|---|---|---|
| Tumor formation | + | + | + | + |
| Metastasis | – | Micrometastases Lymph node | Micrometastases Lymph node, blood, lung | Lymph node, Blood, visible lung nodules |

**Figure 1:** The breast cancer metastasis model comprising four isogenic mouse mammary tumor cell lines that differ in their ability to metastasize when implanted into the mammary fat pad. (Schematic representations were adapted from Yang et al., 2004 and Ho et al., 2009).

We analyzed the endogenous WISP1 mRNA levels in the parental isogenic tumor cells, 67NR, 168FARN, 4T07 and 4T1. Compared with the non-metastatic 67NR cells, 168FARN and 4T07 cells exhibit ~6 fold higher WISP1 mRNA expression. Strikingly, WISP1 mRNA levels in the aggressively metastatic 4T1 cells were ~18 fold higher compared with 67NR cells. This result shows that the endogenous WISP1 levels correlate with the metastatic potential of mouse mammary tumor cell lines (Figure 2).

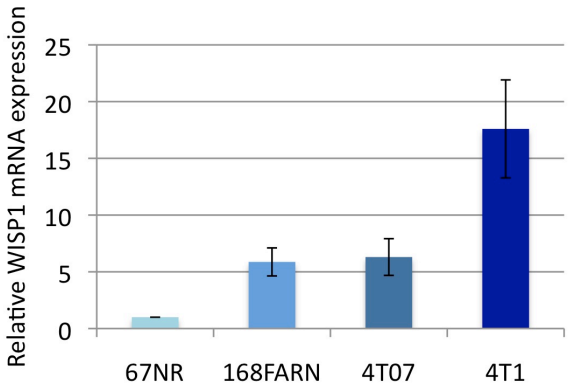


**Figure 2:** qRT-PCR analysis of WISP1 mRNA expression in isogenic mouse mammary epithelial tumor cell lines with different metastatic potential. WISP1 mRNA levels in all cell lines were normalized towards WISP1 mRNA levels in 67NR cells. Data represent means ± SD from technical replicates

### 2.2.2 Change in WISP1 mRNA expression in response to WNT ligand Wnt3A stimulation

The normal mouse mammary epithelial cell line HC11 is derived from COMMA-1D mouse mammary epithelial cells that were isolated from mammary tissue of mid-pregnancy Balb/c mice (Danielson et al., 1984; Ball et al., 1988). HC11 cells resemble mammary stem cells or progenitor cells and possess unlimited proliferation capacity. They are able to differentiate into milk-producing cells *in vitro* (Ball et al., 1988) and to reconstitute the ductal epithelium of a cleared mammary fat pad with myoepithelial, alveolar and ductal luminal cells *in vivo* (Humphreys et al., 1997).

WISP1 is a downstream target of the canonical WNT/β-catenin signaling pathway (Pennica et al., 1998; Xu et al., 2000). Hence, stimuli activating the WNT/β-catenin signaling pathway are expected to increase the expression of the target genes, including WISP1. Activation of WNT/β-catenin signaling is linked to different pathologies including fibrosis and cancer (Clevers 2006; Konigshoff et al., 2009). Previously, Konigshoff and colleagues have shown that either the treatment of mice with the recombinant Wnt3A or induction of experimental lung fibrosis in mice result in WNT/β-catenin pathway activation (Konigshoff et al., 2009). Furthermore, they reported that WISP1 expression in primary alveolar epithelial type II (ATII) cells increases upon Wnt3A stimulation *in vitro* (Konigshoff et al., 2009).

To test whether activation of WNT/β-catenin signaling results in upregulation of WISP1 in mouse mammary epithelial cells, we stimulated the cells with WNT ligand Wnt3A for 12 and 24 hours. For Wnt3A stimulation, cell culture media of L cells stably overexpressing Wnt3A was used. The presence of Wnt3A protein was confirmed by immunoblotting (Figure 3A). As seen in figure 3B, compared to untreated control cells, WISP1 mRNA levels in HC11 normal mouse mammary epithelial cells stimulated with Wnt3A didn't increase. On the contrary, we observed a slight decrease of WISP1 expression in HC11 cells in response to Wnt3A treatment. However, WISP1 expression in mouse mammary tumor cells did increase upon Wnt3A treatment. In 168FARN cells the change in WISP1 mRNA levels after both 12

hours and 24 hours treatment was minor. WISP1 expression in 67NR, 4T07 and 4T1 cells slightly increased after 12 hours of Wnt3A stimulation (less than 1.5 fold). The upregulation of WISP1 expression was more prominent after 24 hours of Wnt3A treatment (1.5 fold for 67NR cells, more than 2 fold for 4T07 cells and 2 fold for 4T1 cells). Thus, although we could not observe activation of WNT/β-catenin signaling and subsequent upregulation of the target gene WISP1 in normal mammary epithelial cells, most of the mammary tumor cells (3 out of 4) responded to WNT ligand treatment by increased WISP1 expression.

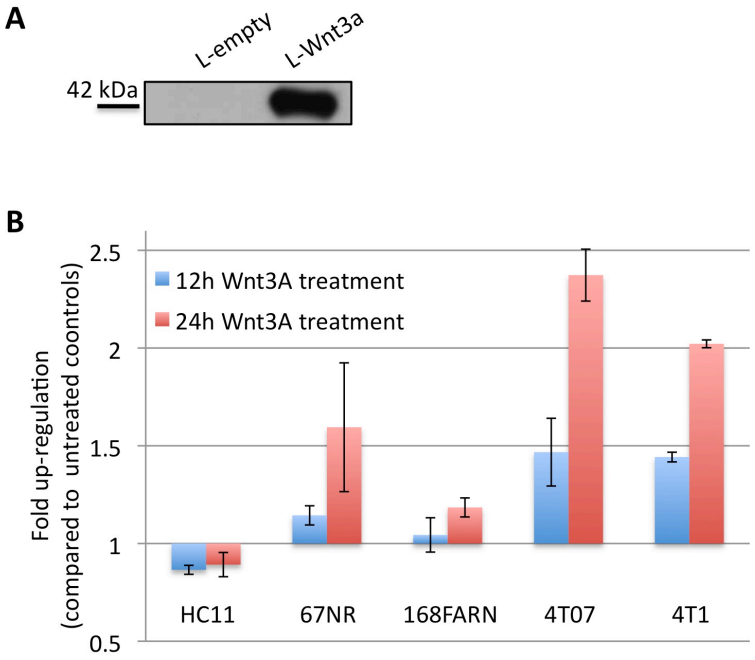


**Figure 3:** Change in WISP1 mRNA expression in response to WNT ligand Wnt3A stimulation. A) Immunoblot with anti-Wnt3A antibody of Wnt3A in L Wnt3A cell culture medium and control cell medium. Samples were run on a 10 % SDS-PAGE gel. B) Change in WISP1 mRNA expression in response to Wnt3A treatment for 12 hours and 24 hours. mRNA expression levels were normalized towards the WISP1 mRNA expression in untreated cells. Data represent means ± SD from technical replicates.

### 2.2.3 WISP1 mRNA expression in tumors growing in pre-irradiated stroma versus non-irradiated control stroma

It was previously shown that the expression of CYR61/CCN1, another CCN family member is elevated in cell lines derived from subcutaneous tumors grown in irradiated mice compared with the cell lines derived from tumors grown in non-irradiated mice (Monnier et al., 2008). In an orthotopic breast

cancer model tumors growing in pre-irradiated mammary tissue were more invasive compared with control tumors (Kuonen et al., 2012a). Furthermore, WNT/β-catenin pathway can be aberrantly activated by irradiation exposure, resulting in the transcription of β-catenin target genes, including WISP1 (Kim et al., 2012). WISP1 is known to be involved in the development of radioresistance in esophageal carcinoma cells (Li et al., 2014). To investigate whether irradiation of the mammary gland triggers WISP1 expression in mice, we analyzed WISP1 mRNA levels in tumors growing either in pre-irradiated mammary gland or in untreated tissue. Tumors were initiated by the injection of 4T1 mouse mammary tumor cells. WISP1 mRNA levels within the tissue homogenates consisting of 4T1 tumors and the tumor stroma were measured. As seen in Figure 4, WISP1 mRNA expression in tumors growing in pre-irradiated mammary glands (IRR_4T1) did not change compared with tumors growing in non-irradiated stroma (4T1). Samples were derived from 8 different animals per group (pre-irradiated versus non-irradiated). Especially for the pre-irradiated group of mice, we observed a high variablility between animals resulting in a high standard deviation (Figure 4B).

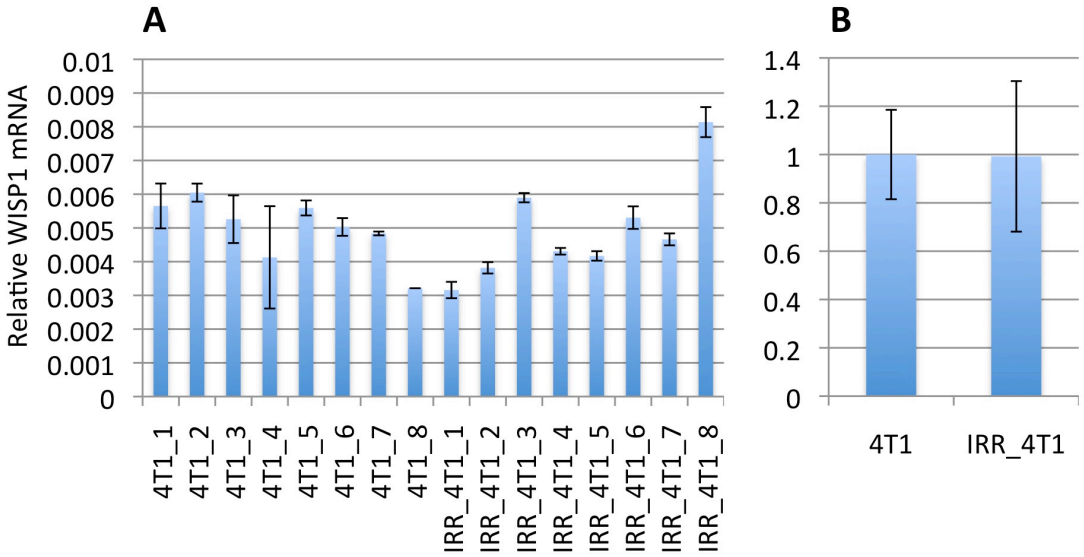


**Figure 4:** qRT-PCR analysis of WISP1 mRNA expression in tumors growing in pre-irradiated stroma versus non-irradiated control stroma. WISP1 expression is normalized to GAPDH in tumor tissue homogenates. Primary tumors were initiated by the injection of 4T1 cells into the mammary gland of mice. Before injection, the mammary gland was locally irradiated (IRR_4T1) or not treated (4T1). A) Each bar represents the mean WISP1 mRNA level ± SD from technical replicates within the sample isolated from one animal. There are 8 animals/ group. B) Average WISP1 mRNA expression in tumors grown in pre-irradiated stroma versus control stroma. Values were normalized towards non-irradiated sample values. Data represent means ± SD from 8 samples.

### 2.2.4 WISP1 mRNA expression in pre-irradiated mammary tissue versus non-irradiated control tissue

In many cancers and in WNT1 transgenic mice, WISP1 is localized to the tumor stroma surrounding the cancer cells (Gurbuz and Chiquet-Ehrismann, 2014, submitted). To exclude the possibility that the tumor cells containing low levels of WISP1 dominate the stroma and veil the change in WISP1 expression upon irradiation, we decided to test WISP1 mRNA levels in normal mammary gland tissue without the injection of tumor cells. WISP1 mRNA levels within the mammary tissue homogenates were measured and compared with untreated control tissue. Figure 5 shows a statistically significant increase in WISP1 mRNA expression (~1.5 fold) in pre-irradiated mammary glands (IRR) compared with non-irradiated tissue (Non_IRR). Samples were derived from 8 different animals per group (pre-irradiated versus non-irradiated).

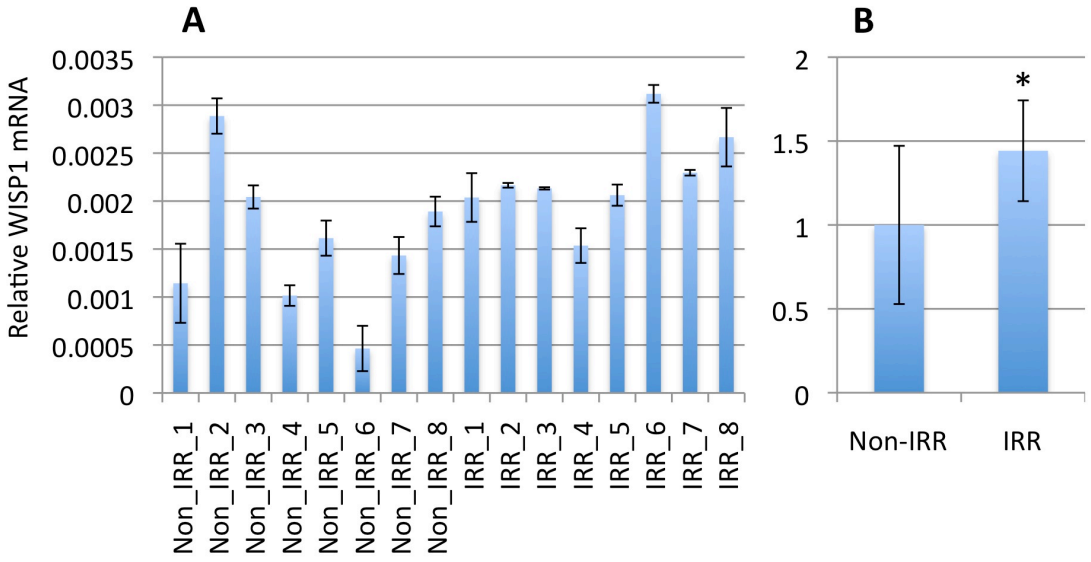


**Figure 5:** qRT-PCR analysis of WISP1 mRNA expression in pre-irradiated mammary tissue versus non-irradiated control tissue. WISP1 expression is normalized to GAPDH in tissue homogenates. The normal mammary gland was locally irradiated (IRR) or not treated (Non_IRR). A) Each bar represents the mean WISP1 mRNA level ± SD from technical replicates within the sample isolated from one animal. There are 8 animals/ group. B) Average WISP1 mRNA expression in tumors grown in pre-irradiated tissue versus control tissue. Values were normalized towards non-irradiated sample values. Data represent means ± SD from 8 samples. t-test revealed a statistically significant difference between the input groups (P = 0.042).

### 2.2.5 Generation of cell lines stably overexpressing WISP1

The positive correlation between the WISP1 mRNA expression and the metastatic potential of mouse mammary tumor cells, as well as differential WISP1 expression between tumor tissue and normal tissue (Gurbuz and Chiquet-Ehrismann, 2014, submitted) prompted us to investigate the mechanism of action of WISP1 in a tumor context. We attempted to generate mouse mammary epithelial cell lines, HC11 and 4T1 stably overexpressing WISP1 to study the effect of increased WISP1 expression on cell behavior *in vitro* and on primary tumor growth and lung metastasis *in vivo*, respectively. By retroviral gene transfer, we introduced a WISP1 gene into the cells. After stable selection with relevant antibiotics, we analyzed the protein expression by immunofluorescence (IF, Figure 6A) and by immunoblotting (IB, Figure 6B). In IF staining we could observe a low WISP1 protein expression in the majority of stable HC11 cells, while almost no WISP1 expression was detected in 4T1 cells. IB confirmed WISP1 expression in HC11 cells, but no WISP1 protein was detected in the cell culture media.

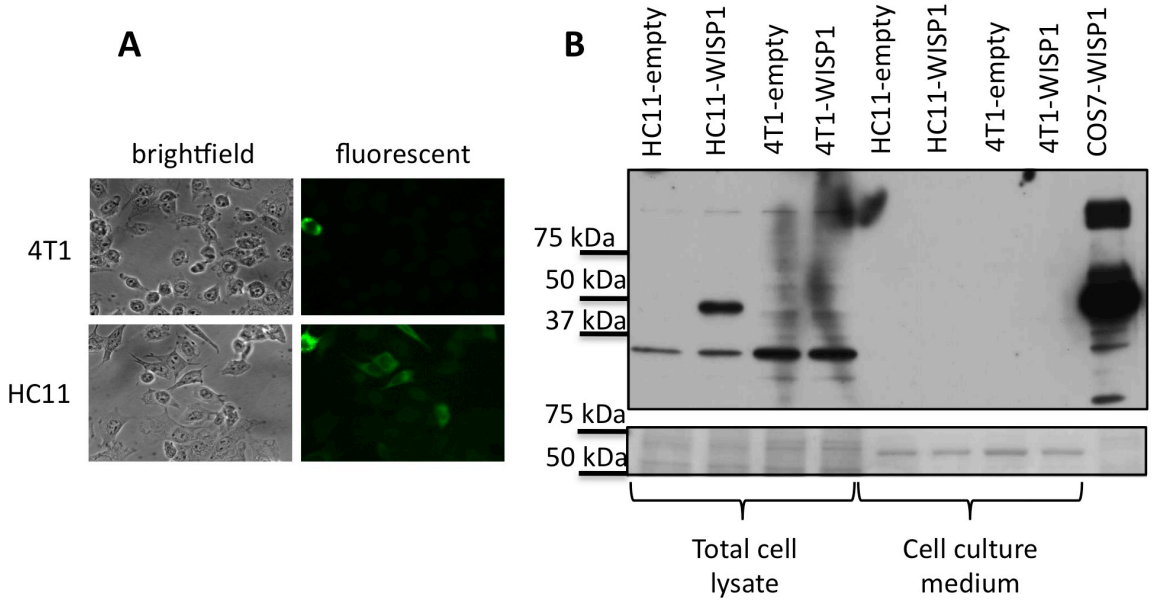


**Figure 6:** WISP1 protein expression in HC11 and 4T1 cells stably transfected with either pQC-Neo (control) or with pQC-WISP1-Neo. A) Immunofluorence staining of intracellular WISP1 with anti-myc antibody. B) Immunoblot of intracellular (total cell lysate) and secreted (cell culture medium) WISP1 with anti-myc antibody. Samples were run on a 10 % SDS-PAGE gel. Intracellular WISP1 in COS-7 cells transiently transfected with pCMV6-WISP1 was used as positive control. Ponceau S staining of the membrane was used to visualize the BSA from the medium as loading control. Molecular weight marker (kDa) is labeled on the left.

For the purification of WISP1 protein, we were interested in generating mammalian cell lines that express a HIS-tagged variant of WISP1 protein. Our aim was to purify the HIS-tagged protein from the cell culture medium of cells stably overexpressing WISP1 and to use this recombinant protein either in cell functional assays or for antibody production. Published studies suggest that WISP1 is involved in both autocrine and paracrine signaling (for review see Gurbuz and Chiquet-Ehrismann, 2014, submitted). To test whether these two WISP1 signaling mechanisms have different roles in cellular function, we decided to compare the effects of endogenous and exogenous proteins. For this, in addition to cell lines overexpressing WISP1, we produced recombinant WISP1 that could be use as exogenous protein in cell functional assays. It was previously shown that overexpression of WISP1 in mammalian cells and external addition of the recombinant protein produced in *E.coli,* had different biological effects on cells (Inkson et al., 2008; discussed in Gurbuz and Chiquet-Ehrismann, 2014, submitted). Considering the role of post-translational modifications on protein function we decided to use mammalian cells for the expression of the protein.

We attempted to generate EBNA-293 and COS-7 cells stably overexpressing WISP1. The human embryonic kidney HEK293-EBNA cells constitutively express the Epstein Barr Virus protein EBNA-1, allowing episomal replication of the pCEP-Pu vector (Yates et al., 1985; Young et al., 1988). The COS-7 cell line was derived from CV-1 kidney cells of the African Green Monkey, *Cercopithecus aethiops* through transformation with the Simian Vacuolating Virus 40 (Gluzman 1981). We introduced the HIS-tagged WISP1 gene into the two cell lines. After stable selection with relevant antibiotics, we analyzed the protein expression by IF (Figure 7A) and by IB (Figure 7B). IF staining showed that a high percentage of both EBNA-293 and COS-7 cells were expressing WISP1 protein. IB of WISP1 in lysates of EBNA-293 and COS-7 cells confirmed the protein expression. The cell culture medium of COS-7 cells was positive for WISP1 protein expression, and the size of the secreted protein was larger than the intracellular form (discussed in chapter 2.2.6).

No secreted protein was detected in the cell culture medium of EBNA-293 cells. To test whether EBNA-293 cells were not able to secrete WISP1 or the secreted protein was below the detection limit by IB, we precipicated the proteins in the EBNA-293 cell culture medium with TCA (Figure 7B). Upon TCA precipitation, we were able to detect secreted WISP1 in EBNA-293 cells. Since WISP1 protein concentration in the cell culture medium of EBNA-293 cells was low, we decided to use COS-7 cells for recombinant protein expression and subsequent protein purification.

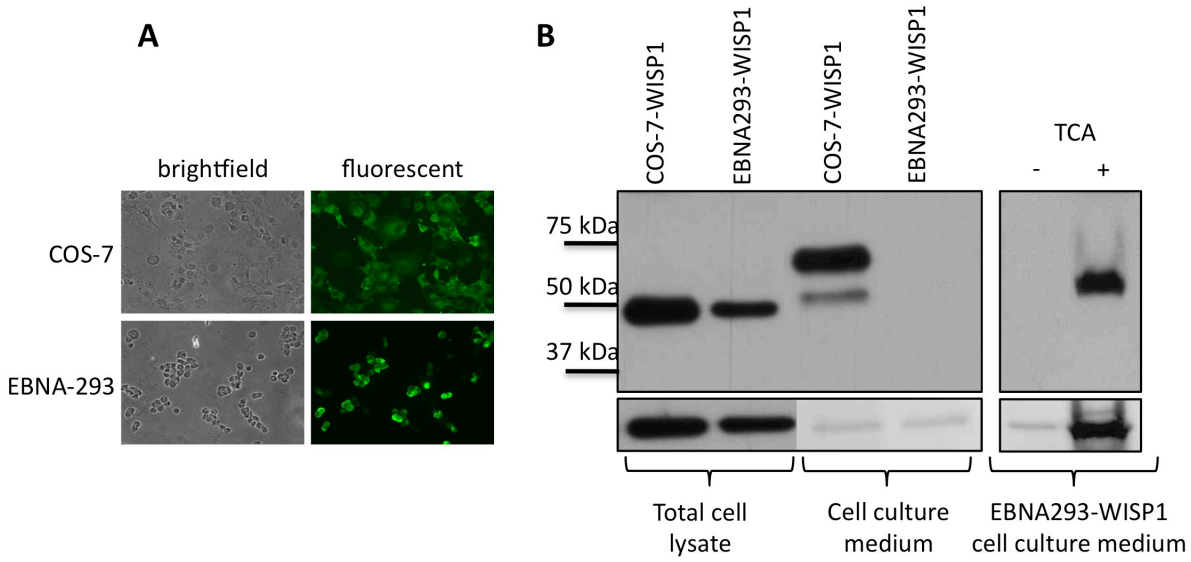


**Figure 7:** WISP1 protein expression in EBNA-293 and COS-7 cells stably transfected with pCEP-Pu-WISP1-HIS. A) Immunofluorence staining of intracellular WISP1 with anti-myc antibody. B) Immunoblot of intracellular (total cell lysate) and secreted (cell culture medium) WISP1 with anti-myc antibody. Samples were run on a 10 % SDS-PAGE gel. To analyze the presence of secreted WISP1 in EBNA-293-WISP1 cell culture, proteins were precipicated with TCA. For total cell lysates vinculin (116 kDa), for cell culture media BSA (70 kDa) stained with Ponceau S serves as loading controls. Molecular weight marker (kDa) is labeled on the left.

### 2.2.6 WISP1 is a glycosylated protein

IB of intracellular and secreted WISP1 showed that the secreted form of the protein has a higher molecular weight (~65 kDa) compared to the intracellular form (~52 kDa), and that the observed molecular weights are different than the predicted molecular weights (predicted molecular weight of intracellular WISP1: 40 kDa, predicted molecular weight of secreted WISP1: 38 kDa) (Figure 8A). This observation prompted us to analyze the post-translational modification status of WISP1.

In 1998 Pennica et al., reported for the first time that WISP1 has four potential N-linked glycosylation sites. Later on, different studies showed that WISP1 is post-translationally modified and that these modifications affect its biological function (Gurbuz and Chiquet-Ehrismann, 2014, submitted). Furthermore, experimentally it was proven that other CCN proteins, CCN2/CTGF and CCN3/NOV, are N-glycosylated (Bohr et al., 2010). Inkson et al. (2008) observed that total cell lysates from hBMSC reveal expression of a WISP1 protein with a larger molecular weight than predicted, and larger than that of the recombinant WISP1 (human, prepared in *E.coli*).

The *in silico* prediction of potential N-Glycosylation sites on the WISP1 protein sequence is shown in figure 8B. In order to confirm the prediction, we N-deglycosylated the protein by using PNGase F (Figure 8C). PNGase F is an amidase that cleaves between the innermost GlcNAc and asparagine residues and removes high mannose, hybrid and complex oligosaccharides from N-linked glycoproteins (Maley et al., 1989). PNGase F treatment resulted in a shift of the protein band of both intracellular and secreted WISP1. This result shows that both forms of WISP1 are N-glycosylated. However the secreted WISP1 must undergo additional post-translational modifications, possibly other types of complex glycosylations, which cannot be removed by PNGase F treatment.

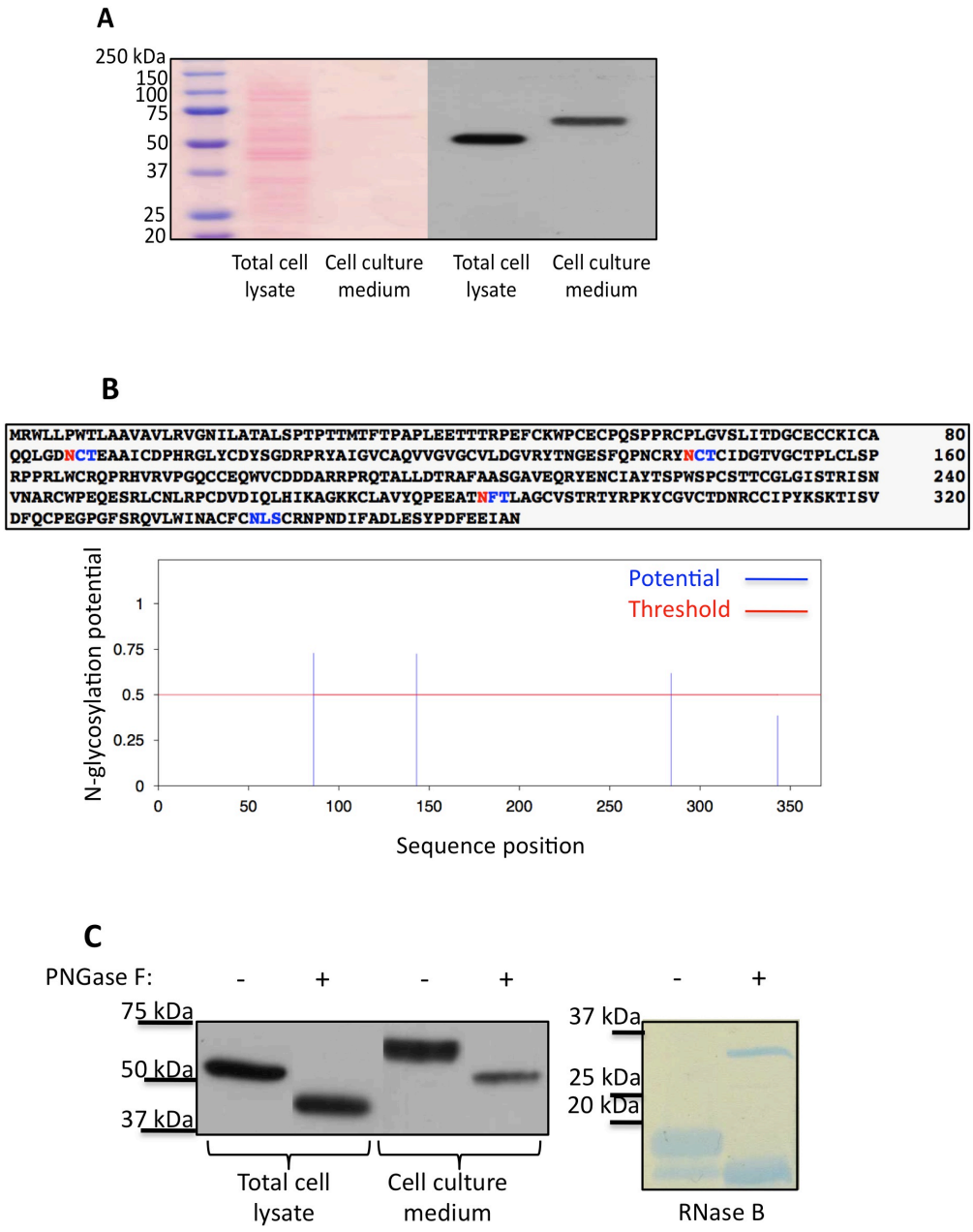


**Figure 8:** WISP1 is a N-glycosylated protein. A) Immunoblot with anti-myc antibody of intracellular (total cell lysate) and secreted (cell culture media) WISP1 in COS-7 cells transiently transfected with pCMV6-WISP1. Samples were run on a 10 % SDS-PAGE gel. Ponceau S staining of the membrane was used to visualize the BSA from the medium as loading control. Molecular weight marker (kDa) is labeled on the left. Secreted WISP1 has a higher molecular weight than the intracellular WISP1. B) N-glycosylation sites within WISP1 protein sequence were predicted using NetNGlyc 1.0 server. Xaa-Ser/Thr sequons are highlighted in blue. Asparagines predicted to be N-glycosylated are highlighted in red. Below, N-glycosylation site prediction is represented by a graph. C) Immunoblot as explained in A. For deglycosylation, protein samples (total cell lysate and cell culture medium) were treated with PNGase F. RNase B, positive deglycosylation control, was stained with Coomassie Blue dye. All samples were run on a 12.5 % SDS-PAGE gel. Both intracellular and secreted WISP1 are N-glycosylated.

### 2.2.7 HC11 cells stably overexpressing WISP1 show distinct proliferation rates and migration behaviors

To analyze the effect of WISP1 on cell behavior, we used HC11 cells stably overexpressing WISP1. Since WISP1 is known to have a function in cancer (Gurbuz and Chiquet-Ehrismann, 2014, submitted), we decided to analyze two main cell functions important for cancer progression: proliferation and cell migration. An HC11 cell strain stably transfected with an empty vector expressing only endogenous WISP1 served as a negative control in these studies. The proliferation rates of HC11 cells were analyzed using a 5-bromo-2′-deoxyuridine (BrdU) incorporation assay. The incorporated BrdU was measured at 24, 48 and 72 hours after plating. Compared with empty vector-transfected control HC11 cells, there was an increase in BrdU incorporation in HC11-WISP1 cells over the entire time period tested (Figure 9A). The difference in cell growth was not due to decreased cell death rate in HC11-WISP1 cells, as we have not observed any changes in cell viability (Figure 9B). To investigate cell migration, we used wound healing scratch assays. After 12 hours, we did not observe any major difference in wound closure rate (Figure 9C). However, to close the gap, HC11-WISP1 cells seemed to exhibit a different cell locomotion mechanism compared with the control cell line. Whereas HC11-WISP1 cells migrated collectively as continuous sheets in a sliding fashion, HC11-empty cells near the wound margin crawled as individual cells. In conclusion, overexpression of WISP1 protein in HC11 cells led to an increase in cell proliferation and changed the mechanism of cell motility without affecting cell viability.

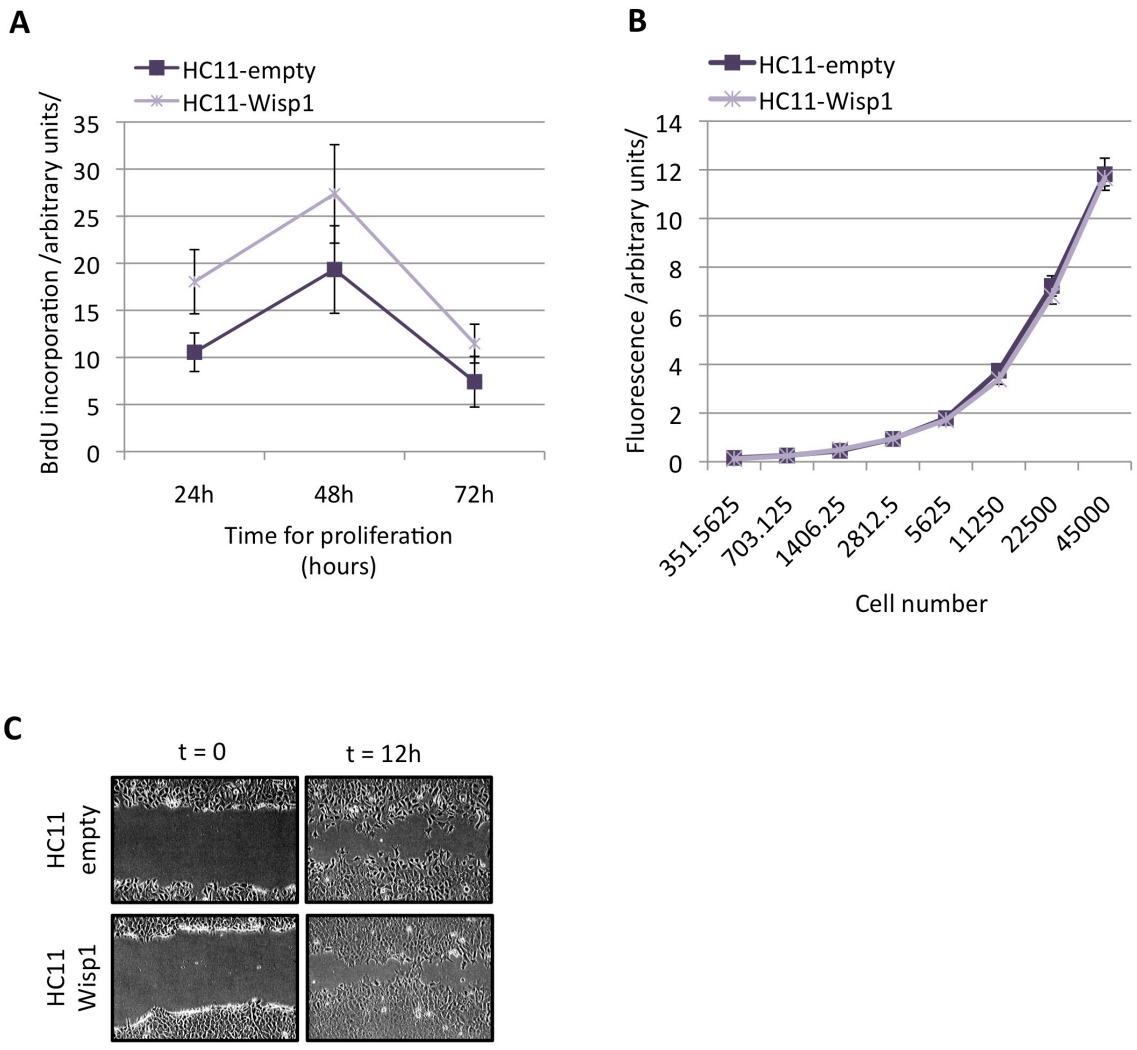


**Figure 9:** HC11 cells stably overexpressing WISP1 show distinct proliferation rates and migration behaviors. WISP1 does not affect HC11 cell viability. A) Proliferation rates of HC11 cells were assessed by BrdU incorporation into newly synthesized DNA at 24, 48 and 72 hours. Each line represents the mean BrdU incorporation ± SD from technical replicates. B) The viability of HC11 cells was analyzed by CellTiter-Blue® assay. The fluorescent signal is proportional to the number of viable cells. No change in cell viability was observed upon WISP1 overexpression. Each line represents the mean fluorescence value ± SD from technical replicates. C) HC11 cell migration was evaluated by wound healing scratch assay. After 12 hours of incubation, the images of cells infiltrating the scratch were recorded.

### 2.2.8 COS-7 cells stably overexpressing WISP1 show distinct proliferation rates and migration behaviors

To analyze the role of WISP1 in cell proliferation and migration, in addition to mouse mammary epithelial HC11 cells, we used COS-7 cells stably overexpressing the HIS-tagged variant of WISP1. Although COS-7 cells are not frequently used in cell behavior assays, we decided to use our COS-7-WISP1 cell line, because these cells had a high intracellular WISP1 protein expression level and were able to secrete a reasonable amount of protein in the cell culture medium (Figure 7B). Parental COS-7 cells served as negative controls in these studies. As for HC11 cells, the proliferation rates of COS-7 cells were analyzed using BrdU incorporation assay. The incorporated BrdU was measured at 24, 48 and 72 hours. Compared with parental control COS-7 cells, there was a decrease in BrdU incorporation in COS-7-WISP1 cells over the entire time period tested (Figure 10A). The difference in cell growth was not due to increased cell death rate in COS-7-WISP1 cells, as we have not observed any changes in cell viability (Figure 10B). To analyze cell motility, we used wound healing scratch assay as well as Boyden Chamber Migration assay. Wound healing assay showed that COS-7 cells stably overexpressing WISP1 were faster in closing the gap compared with the wild-type controls (Figure 10C). On the other hand, in Boyden Chamber Migration assay we observed that the overexpression of WISP1 downregulated COS-7 cell migration by ~1.4 fold compared with endogenous WISP1 expression in parental COS-7 cells (Figure 10D). In summary, the effect of WISP1 on cell proliferation seems to be cell type dependent as opposite effects were observed in HC11 and COS-7 cells. Moreover, the role of WISP1 in cell motility varies depending on the assay used. WISP1 overexpression does not have an impact on HC11 or COS-7 cell viability.

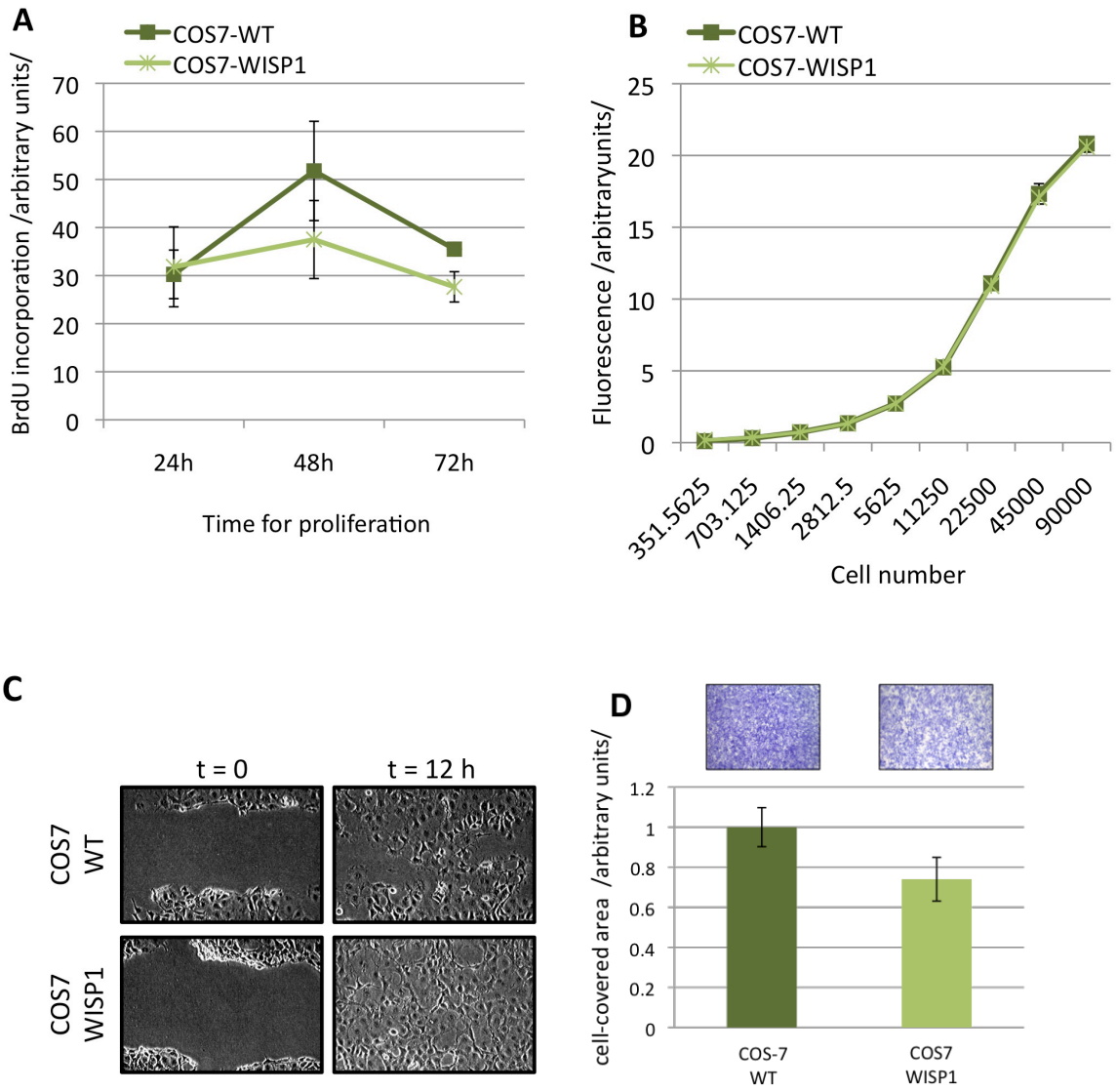


**Figure 10:** COS-7 cells stably overexpressing WISP1 show distinct proliferation rates and migration behaviors. WISP1 does not affect COS-7 cell viability. A) Proliferation rates of COS-7 cells were assessed by BrdU incorporation into newly synthesized DNA at 24, 48 and 72 hours. Each line represents the mean BrdU incorporation ± SD from technical replicates. B) The viability of COS-7 cells was analyzed by CellTiter-Blue® assay. The fluorescent signal is proportional to the number of viable cells. No change in cell viabiliy was observed upon WISP1 overexpression. Each line represents the mean fluorescence value ± SD from technical replicates. C) COS-7 cell migration was evaluated by wound healing scratch assay (C) and Boyden Chamber migration assay using filters with 8 µm pore size (D). C) After 12 hours of incubation, the images of cells infiltrating the scratch were recorded. D) Quantification of COS-7 cell migration towards 10% FCS was measured by the area on the lower side of the filter covered with cells. Values were normalized towards the total area covered by migrated COS-7-WT cells. Each bar represents the mean area ± SD from technical replicates. Representative photos of fixed and stained cells that have migrated to the lower side of the filter are shown above the bar graph.

### 2.2.9 Purification of WISP1 protein and polyclonal anti-WISP1 antiserum production

So far, in our experiments we used commercially available WISP1 antibodies that were generated against a peptide sequence of WISP1 (Gurbuz et al., 2014). However in immunoblotting, we observed non-specific binding of the commercial antibodies. For immunostaining a specific antibody without cross-reactivity with other proteins is needed. Thus, we decided to produce antisera against the entire protein.

Recombinant WISP1 was purified from the cell culture medium of COS-7 cells stably overexpressing the HIS-tagged variant of WISP1 (Figure 11). 2 rabbits, SY6205 and SY6206, were immunized with the soluble recombinant WISP1 protein and sera from the animals containing the polyclonal anti-WISP1 antibodies, SAB-SY6205 and SAB-SY6206, were obtained. The quality of the anti-WISP1 antibodies in the rabbit sera were tested by IF and IB (Figure 12). Large bleed samples of the anti-WISP1 antibodies were compared with the anti-myc antibody, as well as with the pre-immune sera (Figures 12A and 12C). To find the optimal antibody concentration, different dilutions were tested. Pre-immune test bleed served as a negative control since it was collected from the same animal that was used to generate the antibody before immunization. The large test bleed was used to monitor the antibody titer. The IB showed that both antibodies were able to recognize the intracellular WISP1 at ~52 kDa in cell lysates of WISP1-transfected cells. The pre-immune sera PPI-SY6205 and PPI-SY6206 did not bind to WISP1, which proves the specificity of the antibodies. SAB-SY6206 showed a higher affinity towards WISP1 than SAB-SY6205; even 1:2000 dilution of the antibody was able to detect the protein. For both antibodies 1:1000 seemed to be the optimum concentration. Although both antibodies recognized WISP1, they also showed cross-reactivity towards an unspecific protein at ~45 kDa. To test whether the antibodies recognize secreted WISP1 in the cell culture medium we performed another IB. This time, we incubated the entire membrane with anti-WISP1 antibodies diluted 1:1000 to test whether they bind to additional unspecific proteins (Figures 12B and 12D). Both SAB-SY6205 and SAB-SY6206 were able to recognize the secreted WISP1 at ~65 kDa in cell culture

media of WISP1-transfected cells. In addition to the unspecific protein detected at ~45 kDa, another cross-reactivity was observed at ~250 kDa. The unspecific binding at ~250 kDa was weaker for SAB-SY6205 than for SAB-SY6206. Mass Spectrometry Analysis showed that the non-specific proteins recognized by the anti-WISP1 antibodies at ~45 kDa and ~250 kDa were plasminogen activator inhibitor type 1 (PAI1) and fibronectin (FN), respectively. Last but not least, SAB-SY6206 anti-WISP1 antibody was tested in immunofluorescence staining and compared with anti-myc antibody (Figure 12E). SAB-SY6206 was able to detect intracellular WISP1 in 67NR cells transiently transfected with WISP1.

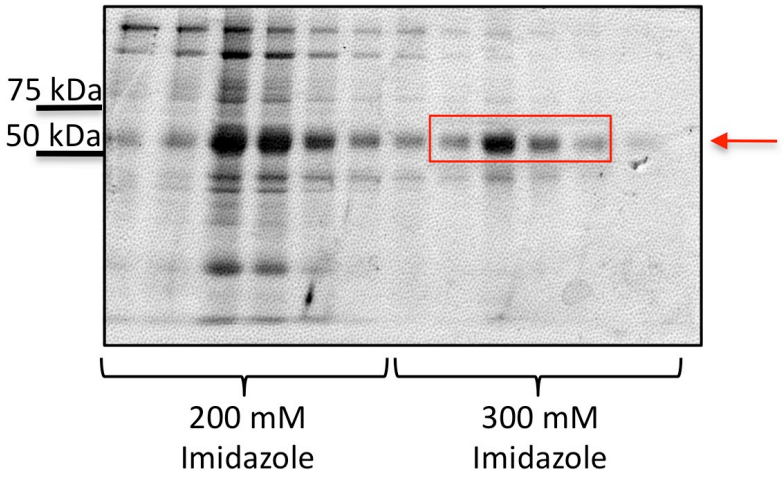


**Figure 11:** Coomassie-stained gel of protein purification steps. HIS-tagged, secreted WISP1 is purified from the serum free cell culture medium of COS-7 cells stably transfected with pCEP-Pu-WISP1-HIS. Soluble proteins were precipitated with ammonium sulfate, dialyzed against PBS and affinity purified on Ni-NTA resin. WISP1 was eluted with imidazole. Eluted proteins (24 µl/ well) were run on a 10 % SDS-PAGE gel and stained with Coomassie Blue dye. WISP1 is indicated by arrowhead. Molecular weight marker (kDa) is labeled on the left. The eluates marked with the red rectangle were used as the antigens for the polyclonal antibody production.

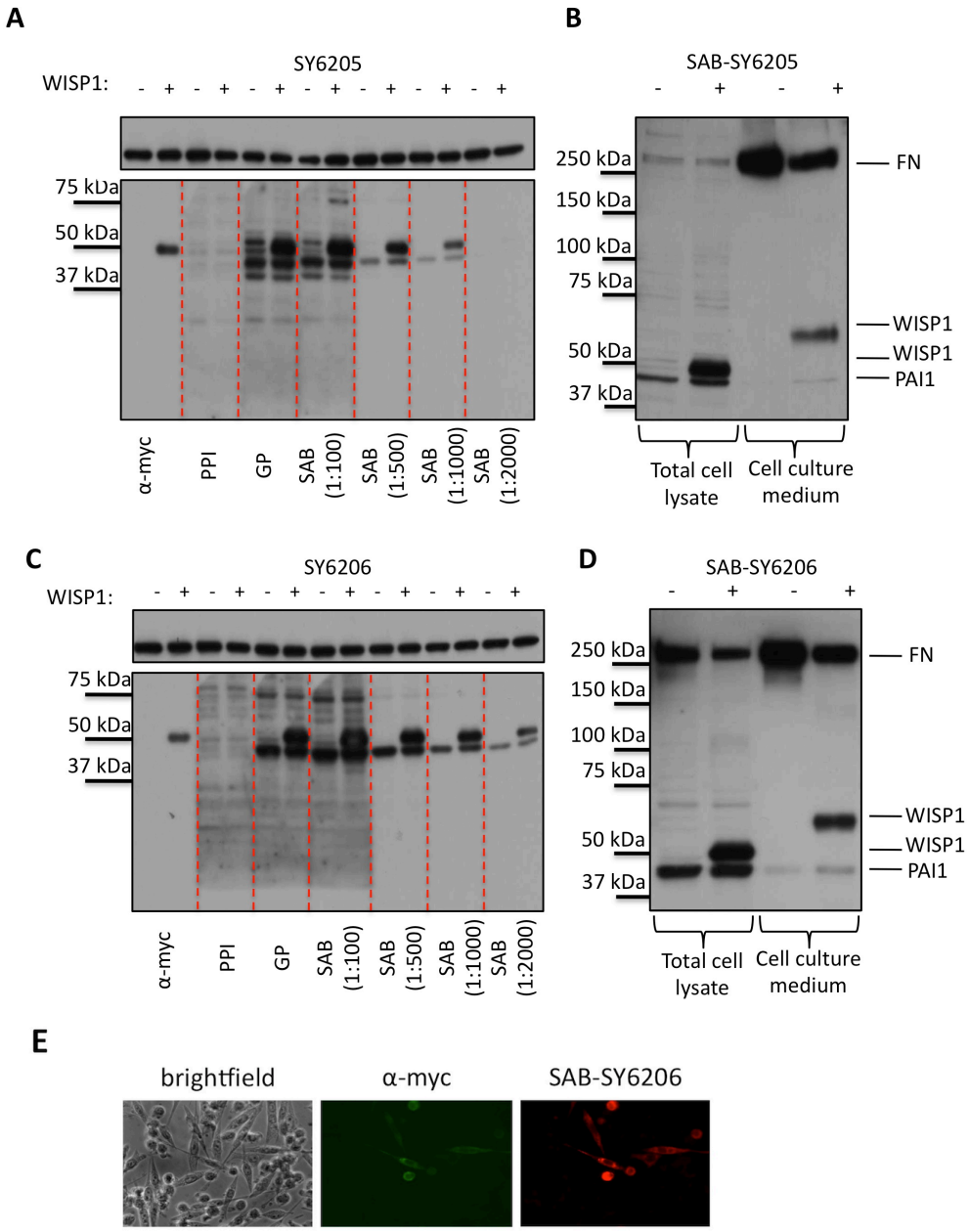


**Figure 12:** Characterization of anti-WISP1 rabbit polyclonal antibodies. 2 Rabbits (SY6205 and SY6206) were immunized with the recombinant WISP1 produced in COS-7 cells. Pre-immune serum (PPI, Day: 0), large bleed (GP, Day: 21) and final bleed (SAB, Day: 28) were tested. Immunoblot of intracellular (total cell lysate) WISP1 with anti-myc antibody (1:100), PPI-SY6205 (1:100), GP-SY6205 (1:100), SAB-SY6205 (1:100-1:2000) (A) and with anti-myc antibody (1:100), PPI-SY6206 (1:100), GP-SY6206 (1:100), SAB-SY6206 (1:100-1:2000) (C). Total cell lysates isolated from parental COS-7 cells or from COS-7 cells transiently transfected with pCMV6-WISP1 were run on a 10 % SDS-PAGE gel. Vinculin (116 kDa) served as loading control. Immunoblot of intracellular (total cell lysate) and secreted (cell culture medium) WISP1 with SAB-SY6205 (B) and SAB-SY6206 (D) antibodies. Samples were run on a 7.5 % SDS-PAGE gel. The locations of FN (fibronectin, 263 kDa, human), WISP1 (secreted and intracellular, mouse) PAI1 (plasminogen activator inhibitor type 1, 45 kDa, human) are indicated. Molecular weight marker (kDa) is labeled on the left side of the blots. E) Immunofluorescence staining of intracellular WISP1 in 67NR cells transiently transfected with with pCMV6-WISP1. 67NR cells were stained with anti-myc primary antibody (1:20) and Alexa488-labeled secondary antibody (1:1000) or with SAB-SY6206 primary antibody (1:1000) and Alexa568-labeled secondary antibody (1:1000).

## CHAPTER 3: DISCUSSION AND FUTURE DIRECTIONS

Previous work from our group revealed that Megakaryoblastic leukemia 1 (MKL1) acts as a *bona fide* transcription factor in mechanotransduction and mediates serum response factor (SRF)-independent, SAP-domain dependent transcription of cyclic stretch-induced tenascin-C (TNC) expression (Asparuhova et al., 2011). We were interested in identifying additional MKL1 target genes co-regulated with TNC and to analyze whether such genes could be implicated in cancer progression.

In the present work we discovered SRF-independent, SAP domain-dependent MKL1 target genes that are implicated in cell proliferation and motility, and found that these genes are elevated in breast cancer patients with poor survival (Discussed in detail in Gurbuz et al. 2014). From this group of genes WNT1 inducible signaling pathway protein 1 (WISP1) caught our interest. Xu et al. (2000) reported that WISP1 is a β-catenin responsive oncogene. Like TNC, WISP1 is transiently expressed during embryonic development, wound healing and tissue remodeling, and its aberrant expression is associated with various pathologies including cancer (Chiquet-Ehrismann and Chiquet, 2003; Gurbuz and Chiquet-Ehrismann, 2014, submitted). Transcript profiling studies available from the Oncomine database revealed increased WISP1 expression in many human cancers (Gurbuz and Chiquet-Ehrismann, 2014, submitted). Despite of a considerable number of data showing increased WISP1 expression in cancer, relatively little is known about the mechanistic details of its function. Therefore, we focused on the biochemical and cell biological characterization of the WISP1 protein, as well as its role in cancer progression.

### 3.1 Cell biological characterization of WISP1

Yang et al. (2004) hypothesized that the altered expression of a specific group of genes causes the metastatic properties of the four isogenic mouse mammary tumor cells lines, 67NR, 168FARN, 4T07 and 4T1. They compared the transcription profiles of the four tumor cell lines and identified several differentially expressed genes. Among these genes, they focused on the

transcription factor Twist that was strongly upregulated in 168FARN, 4TO7, and 4T1 tumor cells compared to 67NR cells, and investigated its mechanistic role in promoting metastasis. When we tested the mRNA levels of WISP1 in these four cell lines, we observed the same tendency. Endogenous WISP1 expression positively correlated with the metastatic potential of the cells. Since WISP1 expression increases during cellular processes that require cell migration and ECM remodeling (Berschneider and Konigshoff, 2011), we think that increased WISP1 levels might play a stimulatory role in tumor invasion and metastasis.

As summarized before (chapter 1.1.5), ionizing radiation alters the tissue microenvironment and may contribute to tumor progression. Experimental tumors growing in pre-irradiated mammary tissue were more metastatic compared to tumors growing in normal stroma (Milas et al., 1988; Kuonen et al., 2012a). Furthermore, tumor cells isolated from glioblastoma xenografts after *in vivo* ionizing radiation had an activated WNT/β-catenin signaling pathway and increased transcription of β-catenin target genes, including WISP1 (Kim et al., 2012). WISP1 expression has been associated with tumor progression and poor prognosis in patients with many different types of solid tumors (Gurbuz and Chiquet-Ehrismann, 2014, submitted). Furthermore, as mentioned in the previous paragraph, we observed a positive correlation between the metastatic potential of mouse mammary tumor cell lines and WISP1 expression. Considering the contribution of irradiation to metastasis, we hypothesized that WISP1 might be one of the players mediating this effect. To investigate whether irradiation triggers WISP1 expression in an orthotopic breast cancer model, we analyzed WISP1 mRNA levels in 4T1 tumors growing either in pre-irradiated mammary gland or in untreated tissue. When we analyzed tumor tissue homogenates, we could not detect any significant changes in WISP1 expression upon irradiation. However, since WISP1 is predominantly expressed within the stroma rather than the epithelial tumor cells (Gurbuz and Chiquet-Ehrismann, 2014, submitted), we were interested in seeing the radiation-induced response of the normal mammary gland without injection of tumor cells. For this, we tested the WISP1 expression in normal mammary gland tissue without tumors and observed a significant

increase in WISP1 expression upon irradiation. Future studies that uncover the mechanism of how radiation activates WISP1 expression and how this activation contributes to tumor metastasis are warranted.

To study the cell biological function of WISP1 in cell proliferation and migration *in vitro* and in primary tumor growth and lung metastasis *in vivo*, we decided to generate cell lines stably overexpressing WISP1. We introduced the WISP1 gene into normal HC11 and transformed 4T1 mouse mammary epithelial cells and selected for cells that have stably incorporated the plasmid into their genomic DNA. Most of the antibiotic-resistant HC11 cells were also positive for WISP1 expression, although the level of expression was low. On the other hand, almost no WISP1 expression was detected in 4T1 cells. Either in the long term 4T1 cells cannot tolerate WISP1 expression and as result cells with the resistance gene only but without WISP1 are taking over or in our experiments the selective pressure was not strong enough.

The other cell lines generated were EBNA-293 and COS-7 cells stably overexpressing WISP1. After selection with antibiotics both cell lines were positive for WISP1 expression. However secreted WISP1 was detected in the cell culture medium of EBNA-293 cells only after TCA precipitation showing that in EBNA-293 cells, the concentration of secreted WISP1 was low. Either the cells produced not enough protein, or they were not able to secrete the protein efficiently. It is possible that EBNA-293 could only tolerate intermediate levels of WISP1. On the other hand, COS-7 cells expressed and secreted easily detectable amounts of WISP1 protein. Among all four stable cell lines (HC11, 4T1, EBNA-293, COS-7), COS-7 cells exhibited the highest amount of intracellular and secreted WISP1 protein within the total cell lysates and cell culture medium, respectively. Although, normally the EBNA-293 cell line is the most suitable model for recombinant protein expression and subsequent protein purification, due to low endogenous secreted proteins within the cell culture medium, we could not use this cell line. Hence, for protein purification we expanded COS-7 cells that stably overexpress WISP1. Nevertheless, the concentration of the recombinant WISP1 was low. This may be due to the fact that even COS-7 cell do not produce that large amounts of

WISP1 protein. Another possibility is that we lost some protein during the purification process. According to the literature, biologically active CCN proteins are difficult to purify, presumably because of the high number of cysteine residues (Leask and Abraham, 2006; Inkson et al., 2008; Chen and Lau, 2009). Using the small amount of protein we had, we performed cell migration assays by either direct addition of the recombinant protein to the cell culture media or by coating the transwell inserts with the recombinant protein. However, we were not able to see any significant difference in cell migration compared with the controls (data not shown).

Most of the purified WISP1 was used to immunize two rabbits. We could obtain 2 different polyclonal anti-WISP1 antibodies, SAB-SY6205 and SAB-SY6206. Both SAB-SY6205 and SAB-SY6206 could specifically recognize the intracellular and the secreted forms of WISP1 at the expected sizes (~52 kDa and ~65 kDa, respectively). However, both antibodies showed cross-reactivity with two other proteins, plasminogen activator inhibitor type 1 (PAI1) and fibronectin (FN). According to the Mass Spectrometry Analysis, the contaminants FN and PAI1 were human proteins. Since human and monkey proteins have a high sequence similarity we assume that these proteins originate from the COS-7 monkey cells. Nevertheless, since the polyclonal WISP1 antibodies recognize one specific band at the right size, only in transfected cells, they can be used for immunoblotting. However, due to the cross-reactivity with FN and PAI1, they cannot be used in immunostaining as is. In the future, we are planning to use the antibodies to analyze WISP1 protein expression in cancer tissue microarrays. For this, we have to remove the cross-reactivity of the antibodies by absorption to FN and PAI1.

Since we could not generate 4T1 cell lines that stably overexpress WISP1, we were not able to continue our planned *in vivo* experiments. Nevertheless, by using stable HC11 and COS-7 cell lines we performed cell biological assays. We analyzed cell proliferation, migration, and survival, three main cellular functions that are frequently deregulated in cancer. First of all, WISP1 had no effect on cell survival in both cell lines tested, as we have not observed any changes in cell viability upon WISP1 overexpression. Compared with empty

vector-transfected control cells, HC11-WISP1 cells showed increased proliferation suggesting that endogenous WISP1 expression positively affects cell proliferation in HC11 mammary epithelial cells. In support of that, it has previously been shown that overexpression of WISP1 induces proliferation of human bone marrow stroma cells (Inkson et al., 2008). In contrast to these observations, endogenous WISP1 had a negative effect on COS-7 cell proliferation as we have observed a decrease in BrdU incorporation in COS-7-WISP1 cells compared with their parental controls. It is possible that the role of WISP1 in cell proliferation depends on the cellular system used. In addition, we have to keep in mind that parental COS-7 cells do not serve as the proper controls, since they have not been transfected and they have not been treated with antibiotics. In the future, we are planning to repeat this proliferation assay by using empty vector-transfected control cells.

To test the effect of WISP1 on cell migration, first we performed wound healing scratch assays. Although we didn't observe any major difference in the wound closure rate of HC11-WISP1 cells compared to the controls, the mode of cell migration seemed different. HC11-WISP1 cells exhibited collective, gliding-type migration while HC11-empty cells at the wound edge migrated as single units. Cells move either individually or collectively depending on the absence or presence of cell-cell junctions (Friedl and Wolf, 2009). Collective cell migration is involved in tissue regeneration and can contribute to metastasis by local invasion (Friedl and Wolf, 2009). Considering the role of WISP1 in wound healing, tissue remodeling and tumor progression, we can speculate that endogenous WISP1 expression induces single-cell-to-collective transition and results in a change in the mode of migration by enhancing cell-cell adhesions. This needs to be addressed and verified in detail in further experiments. In addition it would be interesting to test the effect of endogenous WISP1 on cell adhesion.

Unlike HC11 cells, COS-7 cells exhibited a clear difference in wound closure rate. COS-7 cells that stably overexpress WISP1 were faster in closing the gap compared with the wild-type controls. Intuitively, one would expect that the untreated parental cells are more "fit" and move faster compared to the

cells that went through transfection and an antibiotic selection process. With this in mind we conclude that forced WISP1 expression may indeed contribute to undirected cell migration in COS-7 cells. In contrast, in Boyden Chamber Migration assay we observed that the overexpression of WISP1 downregulated COS-7 cell migration compared with parental controls. In line with our observation, in a previous study it has been reported that overexpression of WISP1 downregulates the motility of H460 and H1299 lung cancer cells that were plated in Boyden chambers and induced to migrate towards a serum gradient (1.5% FBS) (Soon et al., 2003). There may be different reasons for the apparent contradictory results obtained in two cell motility assays. First, wound healing scratch assays and Boyden Chamber migration assays are two different experimental systems. In the wound healing assay random cell motility is analyzed, whereas Boyden Chamber migration assay is used to test directed cell motility towards a soluble chemoattractant (i.e. serum). Second, COS-7 cells might have different modes of migration. If we assume that COS-7-WISP1 cells migrate collectively as cohesive multicellular units, we can speculate that the cellular aggregates formed cannot get through the pores of the transwell inserts. On the other hand, COS-WT cells that migrate individually can easily go through the pores. The difference between the migration patterns of COS-7 cells might give us a wrong impression about their migration speeds. An additional cell motility assay, such as time-lapse microscopy of live cell migration might be useful to clarify the role of endogenous WISP1 in HC11 and COS-7 cell migration.

In a range of tumors, WISP1 expression is localized to the tumor stroma surrounding the epithelial cancer cells (Gurbuz and Chiquet-Ehrismann, 2014, submitted). This suggests that WISP1 might be an oncogenic factor that is secreted by stromal fibroblasts to stimulate epithelial tumor progression in a paracrine manner. It would be interesting to study the effect of paracrine WISP1 signaling on cell proliferation and migration *in vitro* and on primary tumor growth and lung metastasis *in vivo*. For this purpose we are planning to generate BalbC-3T3 fibroblasts that stably overexpress WISP1 and to use

these stromal cells together with the isogenic mouse mammary tumor cells lines, 67NR, 168FARN, 4T07 and 4T1 in *in vivo* studies.

## 3.2 Biochemical characterization of WISP1: Post-translational modifications

Immunoblots of intracellular and secreted WISP1 showed that the secreted form of the protein has a higher molecular weight compared to the intracellular form, and that the observed molecular weights are different than the predicted molecular weights. The covalent attachment of carbohydrates, glycosylation is the most common post-translational protein modification that is conserved from bacteria to eukaryotes (Spiro, 2002; Hess et al., 2008; Lommel and Strahl, 2009). Various carbohydrate-peptide linkages have been reported that increase the functional diversity of the protein (Spiro, 2002). Attached carbohydrates can interfere with the cellular localization, turnover and ligand interaction capacity of a protein (Lommel and Strahl, 2009). The glycopeptide bonds are distributed into five main groups: N-glycosidic bonds, O-glycosidic bonds, C-mannosyl bonds, phosphoglycosyl bonds and glypiated bonds (Spiro, 2002). Attachment of GlcNAc to asparagine is the most common carbohydrate-peptide bond (Spiro, 2002). Studies showed that the recombinant CCN2/CTGF and CCN3/NOV are N-glycosylated (Bohr et al., 2010). Moreover, according to *in silico* prediction data, WISP1 protein sequence possesses 4 potential N-glycosylation sites. By PNGase F treatment we could confirm that both the intracellular and secreted WISP1 proteins are N-glycosylated. However, after N-deglycosylation, the two proteins were still different in size. This observation suggests that the secreted WISP1 undergoes additional post-translational modifications, which cannot be removed by PGNase F treatment.

Hofsteenge et al. showed that thrombospondin type 1 (TSP1) repeats are subject to two types of glycosylations: C-mannosylation and O-fucosylation (Hofsteenge et al., 2001). TSP1 repeats are found in several secreted or cell-surface proteins, such as thrombospondins and CCN family members, including WISP1 (Hofsteenge et al., 2001; Leonhard-Melief and Haltiwanger,

2010; Jun and Lau, 2011). TSP1 repeats contain conserved tryptophan residues in a “WXXW” pattern, the recognition motifs for protein C-mannosylation (Hofsteenge et al., 2001). Analysis of human and mouse WISP1 revealed that this recognition motif does not exist in the WISP1 protein sequence. In O-glycosylation, sugar residues get attached to an amino acid containing a hydroxyl group (e.g. serine, threonine, tyrosine, hydroxyproline, and hydroxylysine) (Spiro, 2002; Lommel and Strahl, 2009). TSP1 repeats are found to contain an O-linked disaccharide “Glc-Fuc-O” on the threonine or serine residues in the sequence “CXX(S/T)CG” (Hofsteenge et al., 2001). We could indeed detect this O-fucosylation motif on the mouse (CSX(T)CG) and human (CSX(S)CG) WISP1 protein sequence within the TSP1 domain. Several other matricellular proteins, including thrombospondins, ADAMTS (A Distintegrin And Metalloprotease with Thrombospondin type 1 repeats), and CCNs (CCN1/CYR61, CCN2/CTGF, CCN3/NOV, CCN6/WISP3) are reported to contain O-fucosylation motifs (Leonhard-Melief and Haltiwanger, 2010). Protein fucosylation has been implicated in pathological conditions, such as inflammation and cancer, and certain types of fucosylated glycoproteins have been used as tumor markers (Miyoshi et al., 2008). Taken together, it would be interesting to confirm the O-fucosylation of WISP1 and to investigate the role of this particular post-translational modification in a tumor context.

## CHAPTER 4: APPENDIX

### 4.1 Experimental Procedures (Unpublished Results)

**Cell culture and gene transfers**

Mouse mammary epithelial HC11 cells were grown in RPMI-1640 medium supplemented with 10% FCS, 5 µg/ml insulin (Sigma, Buchs, Switzerland) and 10 ng/ml epidermal growth factor (EGF; Invitrogen, Zug, Switzerland). Isogenic mouse breast cancer cells, 67NR, 168FARN, 4T07 and 4T1, as well as human embryonic kidney HEK293-EBNA cells and African Green Monkey kidney cells COS-7 were grown in DMEM medium supplemented with 10% FCS.

The mammalian expression vector pCMV6-WISP1 (C-terminal Myc and DDK Tagged) was purchased from Origene (MR205645, Wisp1 (NM_018865) Mouse cDNA ORF Clone, OriGene, Rockville, MD, USA). COS-7 and 67NR cells were transfected using FuGENE® 6 (Roche, Basel, Switzerland) and jetPEI® DNA transfection reagent (Polyplus), respectively according to the manufacturers' instructions.

To obtain cells stably expressing WISP1, retroviral gene transfer and subsequent selection were performed. First, full-length WISP1 cDNA (MR205645, OriGene, Rockville, MD, USA) was amplified by PCR adding AgeI and PacI restriction sites at the 5' and 3' ends, respectively, followed by a stop codon at the C-terminus using the following primers: 5′-ATACCGGTATGAGGTGGCTCCTGCCCTG-3' (forward primer) and 5'-ATTTAATTAATTACAGATCCTCTTCTGAGATGAG-3' (reverse primer). During the cDNA amplification the DKK-tag was removed whereas the myc-tag was conserved. The amplified fragments were subsequently cloned in the multiple cloning site II of the bicistronic pQCXIX Retroviral Vector (Clontech Laboratories, Mountain View, CA USA) plasmid. The selection marker neomycin (Neo) has been previously cloned in the multiple cloning site II of pQCXIX vector as described (Asparuhova et al., 2011) resulting in pQCX-Neo. The packaging cells EcoPack2™-293 (Cat.No: 631507, Clontech

Laboratories, Mountain View, CA USA) were transfected using TransIT®-293 Transfection Reagent (Mirus Bio LLC., WI, USA) according to the manufacturer's protocol. The supernatant of EcoPack2™-293 cells containing the virus was collected and used to infect the target 4T1 and HC11 cells. The infection was performed as described in the manufacturer's manual. To obtain 4T1 and HC11 cells stably expressing WISP1, cells were selected with Geneticin (1 mg/ml; Roche). To generate control cell lines, cells were transfected with pQCX-Neo vectors that lack the WISP1 gene and were selected with Geneticin (1 mg/ml; Roche).

For recombinant protein affinity purification, a polyhistidine-tag was added at the C-terminus of the coding sequence of WISP1. For this, full-length WISP1 cDNA was amplified by PCR from the mouse WISP1 clone (MR205645, OriGene, Rockville, MD, USA) using the following primers: 5′-TCAGAATTTTGTAATACGACTC-3′ (forward primer) and 5′-ATGCTAGCTCAGTGATGGTGATGGTGATGCAGATCCTCTTCTGAGATGA G-3′ (reverse primer). WISP1 was amplified adding NheI restriction site at the 3' end, as well as a sequence encoding 6 histidines (CAT-CAC-CAT-CAC-CAT-CAC) followed by a stop codon at the C-terminus. During the cDNA amplification the DKK-tag was removed whereas the myc-tag was conserved. The amplified fragments were subsequently cloned into the expression vector pCEP-Pu (provided by J. Engel, Biozentrum, Basel, Switzerland). To generate cell lines stably overexpressing the HIS-tagged variant of WISP1, HEK293-EBNA and COS-7 cells were transfected with 3 µg of the expression plasmid using jetPEI® DNA transfection reagent (Polyplus). After 24 hours of culture, transfected HEK293-EBNA and COS-7 cells were selected with 1 µg/ml puromycin and with 4.5 µg/ml puromycin, respectively.

All clones were verified by DNA sequencing. (For vector information, see Chapter 4.2, Supplementary Figure 2)

**Protein purification from mammalian cells and subsequent polyclonal antibody production**

COS-7 cells stably overexpressing the HIS-tagged variant of WISP1 were expanded in 3-layer flasks. After they reached confluency, cells were washed 3 times with serum-free DMEM media and new serum-free culture media were added to the cells. After 48 hours of incubation, serum free media containing recombinant soluble protein were collected and stored at -80°C. This media collection procedure was repeated 6 times. Collected media were pooled and proteins present in these conditioned media were precipitated with ammonium sulfate (440 g/ 1 l medium) and dialyzed against PBS using 12-14 kDa cut-off dialysis bags (Regenerated cellulose tubular membrane, Cellu.Sep®, Uptima). This was followed by affinity purification on Ni-NTA resin (Invitrogen). After washing of the column with 20 mM, 50 mM, 100 mM and 200 mM imidazole, the protein was eluted with 300 mM imidazole. To visualize the presence of purified WISP1, protein samples (24 μl/ well) were loaded and run on 10% SDS gels. Gels were stained with InstantBlue™ (Coomassie Blue® based stain, Expedeon).

Fractions in elution buffer (300 mM Imidazole, 0.9 M NaCl, physiological buffer) contained approximately 225 μg of purified WISP1 protein distributed among 8 aliquots. These samples were sent to the custom antibody production company (Eurogentec SA, Seraing, Belgium). Two rabbits (Animal 1: SY6205, Animal 2: SY6206) were immunized according to the speedy 28-day protocol (4 injections, 3 bleeds). Pre-immune serum (PPI, Day: 0), large bleed (GP, Day: 21) and final bleed (SAB, Day: 28) were received and used in immunoblotting and immunofluorescence assays as described.

**Cell Viability Assay**

Different numbers of COS-7 and HC11 cells (between $9\times10^4$ and $\sim3\times10^2$) were plated in triplicates on 96-well plates in serum free DMEM or RPMI, respectively, and were incubated at 37°C for 3 hours. After the addition of CellTiter-Blue solution (Promega, Duebendorf, Switzerland), cells were incubated for 4 hours and fluorescence was recorded at 560/ 590 nm

according to manufacturer's protocol. Data represent means ± SD from technical replicates.

**Cell Proliferation Assay**

Proliferation rates of the HC11 and COS-7 cells were determined using the chemiluminescent Cell Proliferation ELISA, BrdU incorporation assay (Roche). HC11 and COS-7 cells were plated in triplicates on black, clear bottom, 96-well microtiter plates (PerkinElmer, Schwerzenbach, Switzerland) in 3% FCS/RPMI at $5\times10^3$ cells/well and $3\times10^3$ cells/well, respectively, were incubated at 37°C and allowed to proliferate for 24, 48 and 72 hours at which time points cells were labeled with BrdU for 2 h. BrdU incorporation was determined according to the manufacturer's protocol using a Luminometer Mithras LB940 (Berthold Technologies, Regensdorf, Switzerland). Data represent means ± SD from technical replicates.

**Boyden Chamber Cell Migration Assay**

Directed migration of COS-7 cells was analyzed using transwell polycarbonate membrane inserts (6.5 mm; Corning, Amsterdam, The Netherlands) with 8 µm pore. $3\times10^4$ cells were plated in the top insert chamber in 100 µl serum-free DMEM. The lower chamber was filled with 600 µl 10% FCS/DMEM. Cells were incubated at 37°C and were allowed to migrate across the transwell filters for 16 hours. Migrated cells were fixed and stained with crystal violet. 3 Images/ insert were acquired on a Nikon Eclipse E600 using 4X magnification and a color CCD camera. Migration was quantified by measuring the area covered by migrated cells using the Fiji distribution of ImageJ. Data represent means ± SD from technical replicates.

**Wound Healing Scratch Assay**

$2\times10^6$ COS-7 cells and $3\times10^6$ HC11 cells were plated on 60 mm plates in DMEM and RPMI medium, respectively, supplemented with 10% FCS, and incubated at 37°C overnight. A single uniform scratch was made on the confluent monolayer of cells as described by Liang et al., 2007. The wells were then washed with RPMI/ DMEM media to remove the detached cells. Before taking the images, fresh media were added to the culture. The first

picture was taken at time point “0”. Migrating cells were allowed to infiltrate the scratch for 12 hours and an image at the same position was recorded once again. For image acquisition a Nikon light microscope was used.

**Wnt3A treatment**

L Wnt-3A (ATCC® CRL-2647™) cells express and secrete a non-tagged form Wnt3A protein (Shibamoto et al., 1998, Willert et al., 2003). L Wnt-3A cells and the control parental cell line (ATCC® CRL-2648 ™) were cultured in 10% FCS/ DMEM and conditioned media were collected according to the manufacturer’s protocol. Parental HC11, 67NR, 168FARN, 4T07 and 4T1 cells were incubated for 12 and 24 hours in L-Wnt3a or L-control conditioned media diluted with fresh 10% FCS/ DMEM (1:2). Following Wnt3A treatment, total RNA was isolated and mRNA levels were analyzed as described in “Quantitative Reverse-Transcriptase PCR”.

**Irradiation of mice**

5- to 7-week old BALB/c female mice (Charles River Laboratories) were used as host animals to graft tumors. Primary tumors were initiated by the injection of 4T1 cells ($5x10^4$ cells/mouse, in 50 µl of 1:5 mixture of Matrigel (BD Biosciences) and PBS) into the right fourth mammary gland. Before injection, the mammary gland was locally irradiated with a single 20 Gy dose using an X-ray unit (Philips, RT 250, Germany), operated at a 125 kV, 20 mA, with a 2-mm Al filter (Monnier et al., 2008; Kuonen et al., 2012). Mice were sacrificed 18 days after tumor cell injection. Tissue samples (tumors and mammary glands) were collected, flash-frozen in precooled tubes and homogenized in RLT buffer using a Dispomix Drive (5x the “40sec grad” profile; Medic Tools). Total RNA from tissue homogenates was isolated and mRNA levels were analyzed as described in “Quantitative Reverse-Transcriptase PCR”. Irradiation, homogenization and RNA isolation procedures are the same for the normal mammary glands without the injection of 4T1 tumor cells. All animal experiments were approved by the Swiss veterinary authorities.

**Quantitative Reverse-Transcriptase PCR**

Using the RNeasy Mini Kit (Qiagen), total RNA was isolated from parental 67NR, 168FARN, 4T07 and 4T1 cells after overnight incubation in 0.03% FCS/DMEM. RNA was reverse transcribed and relative WISP1 mRNA levels were detected as described in Asparuhova et al., (2011) and Gurbuz et al., (2014). Relative WISP1 mRNA levels normalized to Gapdh, were measured using Platinum® SYBR® Green qPCR SuperMix-UDG with ROX (Invitrogen). WISP1 primers can be found in Gurbuz et al., (2014) (Chapter 2.1.1, Additional file: Table S4). Real-time PCR was performed in StepOnePlus Real-Time PCR System (Applied Biosystems, Rotkreuz, Switzerland) using a standard cycling profile. All samples were run in duplicate. Endogenous WISP1 mRNA expression levels and WISP1 mRNA expression levels upon Wnt3a stimulation were analyzed by ΔΔCt method (Livak et al., 2001) that included an additional normalization to a control cell line. RNA from pre-irradiated and normal tumor stroma was analyzed by the ΔCt method (Schmittgen et al., 2008). Data represent means ± SD from technical replicates.

**Protein analyses by Immunoblotting**

After 24 hours of incubation in 0.03% FCS/media, whole-cell extracts were prepared by lysis in RIPA buffer and immunoblotting was performed as described previously (Maier et al., 2008). HC11 cells were starved in media without EGF. Secreted WISP1 protein was detected in cell culture medium. Samples were run on 7.5%-12.5% SDS–PAGE and transferred to nitrocellulose membrane. Ponceau S (0.1%) staining of the membranes was used to visualize the BSA from the medium as loading control. Blots were incubated with the following antibodies: anti-WISP1 (diluted in 5% milkpowder/ TBS-T, SAB-SY6205 and SAB-SY6206 rabbit polyclonal, Eurogentec), anti-myc (diluted 1:100 in 5% milkpowder/ TBS-T, mouse monoclonal antibody, Clone: 9E10), anti-Wnt3a (diluted 1:1000 in 5% BSA/ TBS-T, C64F2, Rabbit mAb, Cell Signaling), anti-Vcl (diluted 1:1000 in 5% milkpowder/ TBS-T, clone hVIN-1, Sigma). Cell lysates of COS-7 cells transiently transfected with WISP1 were blotted and probed with the polyclonal anti-WISP1 antibody. Proteins were visualized using the primary

antibodies listed above followed by horseradish peroxidase-conjugated secondary antibodies (1:10,000; MP Biomedicals, France) for detection with the ECL Western blotting System (Amersham, Switzerland), and exposed to Kodak X-ray film.

**Immunofluorescence**

Stable HEKEBNA-WISP1-HIS ($5x10^5$ cells), COS-7-WISP1-HIS ($3x10^5$ cells), HC11-WISP1 ($3x10^5$ cells) and 4T1-WISP1 ($4x10^5$ cells) cells were plated on 35×10 mm cell culture dishes with 4 inner rings (Greiner Bio-One GmbH, Germany) in 10% FCS supplemented RPMI/ DMEM media. After overnight incubation at 37°C, cells were fixed with Zinc Formal-Fixx™ (Thermo Fisher Scientific) for 30 minutes, permeabilized with 0.1% Triton X-100 (Fluka, Sigma-Aldrich) for 5 minutes and blocked with 3% BSA-PBS for 15 minutes. Cells were labeled at room temperature with anti-myc mouse monoclonal antibody (diluted 1:20 in blocking solution, Clone: 9E10) for 90 minutes and then incubated with Alexa488- or Alexa568-labeled secondary antibodies (diluted 1:1000 in blocking solution) for 60 minutes. Cells were mounted in Prolong Gold antifade reagent (Invitrogen, Switzerland). Images were taken on a Zeiss-Axioscope fluorescent microscope equipped with a 40X objective and Hamamatsu ORCA-ER camera. 67NR cells transiently transfected with WISP1 (MR205645, Wisp1 (NM_018865) Mouse cDNA ORF Clone, OriGene, Rockville, MD, USA) were probed with anti-WISP1 antibody (SY6206 rabbit polyclonal, Eurogentec). 24 hours following transfection, 67NR cells were fixed and stained as described above.

**Deglycosylation with PNGase F**

Total cell lysates and cell culture medium samples of COS-7 cells transiently transfected with WISP1 (MR205645, Wisp1 (NM_018865) Mouse cDNA ORF Clone, OriGene, Rockville, MD, USA) were treated with Peptide-N-Glycosidase F (PNGase F, P0704 and P0705, New England Biolabs) according to the manufacturer's protocol. RNase B (P7817S, New England Biolabs) was used as a positive control for PNGase F endoglycosidase treatment. RNase B is a high mannose glycoprotein that possesses one single N-linked glycosylation site (Plummer and Hirs, 1964). After the SDS-

PAGE, half of the gel containing RNase B samples was stained with InstantBlue™ (Coomassie Blue® based stain, Expedeon). For the other half, immunoblotting was performed as described.

**Protein concentration by TCA precipitation**

To precipitate proteins within the HEKEBNA-293-WISP1-HIS cell culture medium, trichloric acid (TCA) was added to the supernatant sample (Final concentration: 10%). The supernatant-TCA mix was vortexed for 10 seconds and centrigufed at 4°C at 12000 rpm for 10 minutes. The supernatant was removed and 800 µl Aceton (pre-cooled at -20°C) was added. The sample was centrifuged at 4°C at 12000 rpm for 5 minutes. The supernatant was removed and the pellet was air-dried at room temperature for 60 minutes. Finally the pellet was dissolved in sample buffer for SDS-PAGE and immunoblotting was performed as described.

**Mass Spectrometry Analysis**

To identify the additional proteins that are recognized by our WISP1 antibodies (SAB-SY6205 and SAB-SY6206 rabbit polyclonal, Eurogentec) Mass Spectrometry Analysis was performed. Proteins that were eluted as described in “Protein purification from mammalian cells and subsequent polyclonal antibody production” were separated via SDS-PAGE. Protein bands were excised, washed with 25 mM $NH_4HCO_3$ and acetonitrile. Samples were reduced with tris(2-carboxyethyl)phosphine (TCEP), alkylated with Iodoacetamide and digested with Trypsin overnight at 37 ℃. Samples were acidified with 1 µl 20% Trifluoroacetic acid (TFA) and sonicated for 5 minutes. Peptides were analyzed by liquid chromatography mass spectrometry (LTQ Orbitrap Velos, Thermo Fisher Scientific). The results were analyzed with Scaffold 3.0 (Proteome Software, Portland, Oregon, USA).

**Prediction Tools and Bioinformatics Analyses**

Using the Oncomine database (www.oncomine.org) WISP1 expression levels in Brain and Central Nervous System Cancer, Breast Cancer, Colorectal Cancer, Gastric Cancer, Head and Neck Cancer, Lung Cancer, Pancreatic

Cancer and Sarcoma were compared to control samples (Cancer vs. Normal differential analysis) according to Human Genome U133 Affymetrix Array data (Affymetrix Probe ID: 206796_at). Results are represented with a box plot. The thick line represents the median value. Minimal and maximal values are individually plotted as small dots. Student's t-test was performed by Oncomine to generate p-values.

Using NetNGlyc 1.0 Server (Gupta et al., 2004, http://www.cbs.dtu.dk/services/NetNGlyc/) potential N-Glycosylation residues of WISP1 protein were determined. The server predicts N-Glycosylation sites in human proteins. The graph shows predicted N-glyc sites across the protein chain. X-axis represents protein length from N- to C-terminal. A position with a potential (vertical lines) crossing the threshold (horizontal line at 0.5) is predicted to be glycosylated.

**Statistical analysis**

Differences between 2 groups were assessed by Student's t-test. All analyses were carried out using GraphPad InStat 3.05 software (GraphPad, San Diego, CA, USA). Values of $P < 0.05$ were considered significant.

## 4.2 Supplementary Figures


**Supplementary Figure 1:** The Universal Protein Resource (UniProt) protein alignment of the six human CCN proteins. Signal peptides at the N-terminus, disulfide bonds and potential glycosylation residues were annotated. The tree based on genetic distance is shown.

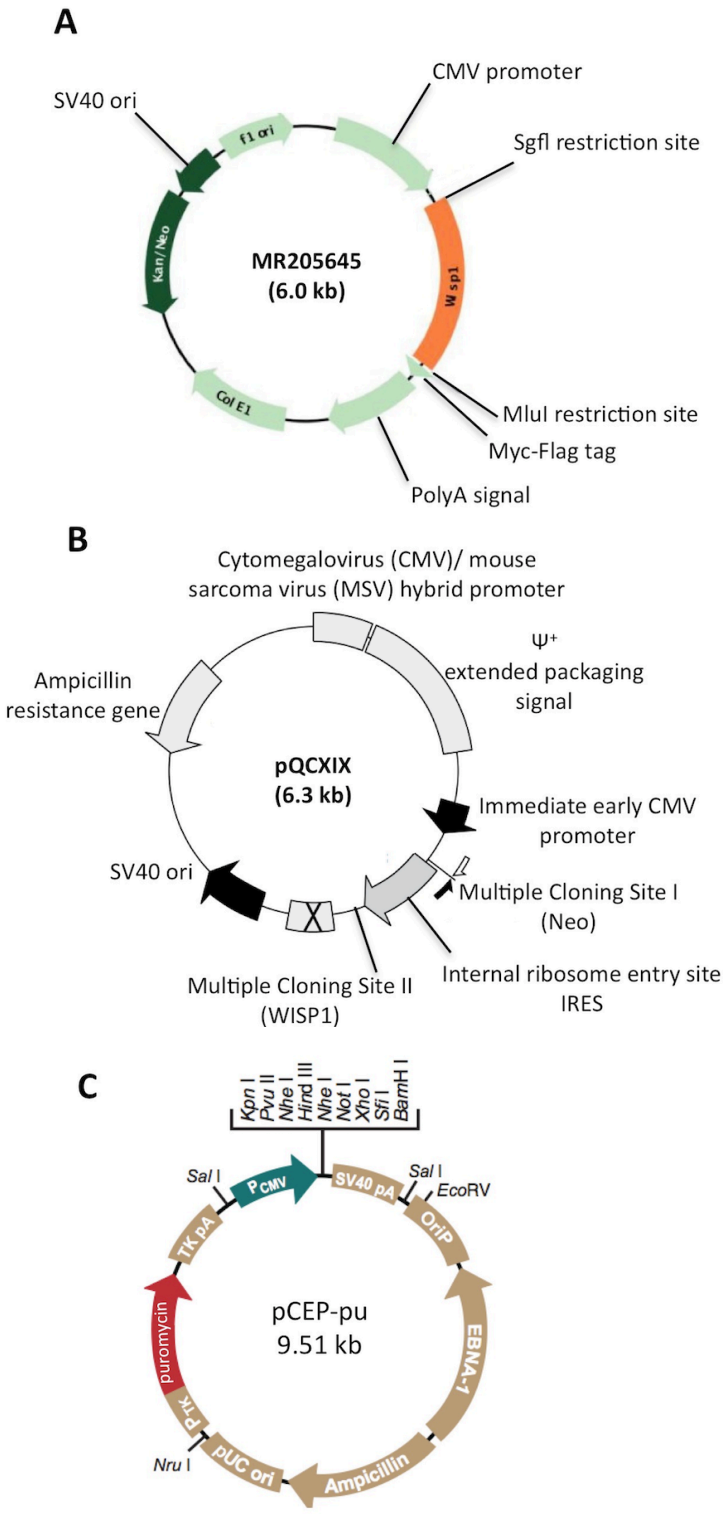


**Supplementary Figure 2:** Vectors that were used for WISP1 gene transfer. A) pCMV6-WISP1 (MR205645, WISP1 mouse cDNA ORF Clone, C-terminal Myc and DDK Tagged) was used for transient transfections. B) Bicistronic pQCXIX Retroviral Vector. WISP1 gene and the selection marker neomycin (Neo) were cloned in the multiple cloning site I (MCS I) and multiple cloning site II (MCS II) of the vector, respectively. pQC-Neo-WISP1 was used for stable transfections of HC11 and 4T1 mouse mammary epithelial cells. C) pCEP-pu expression vector. HIS-tag was added to WISP1 gene and WISP1-HIS was cloned in the pCEP-pu vector. pCEP-Pu-WISP1-HIS was used for stable transfection of COS-7 and EBNA-293 cells and subsequent protein purification from the cell culture medium.

## 4.3 References

(2014). Seventh international workshop on the CCN family of genes. Journal of Cell Communication and Signaling 8, 77-92.

Abreu, J.G., Ketpura, N.I., Reversade, B., and De Robertis, E.M. (2002). Connective-tissue growth factor (CTGF) modulates cell signalling by BMP and TGF-beta. Nature Cell Biology 4, 599-604.

Aikawa, T., Gunn, J., Spong, S.M., Klaus, S.J., and Korc, M. (2006). Connective tissue growth factor-specific antibody attenuates tumor growth, metastasis, and angiogenesis in an orthotopic mouse model of pancreatic cancer. Molecular Cancer Therapeutics 5, 1108-1116.

Amano, M., Ito, M., Kimura, K., Fukata, Y., Chihara, K., Nakano, T., Matsuura, Y., and Kaibuchi, K. (1996). Phosphorylation and Activation of Myosin by Rho-associated Kinase (Rho-kinase). Journal of Biological Chemistry 271, 20246-20249.

Amano, M., Nakayama, M., and Kaibuchi, K. (2010). Rho-kinase/ROCK: A key regulator of the cytoskeleton and cell polarity. Cytoskeleton 67, 545-554.

Aravind, L., and Koonin, E.V. (2000). SAP-a putative DNA-binding motif involved in chromosomal organization. Trends in Biochemical Sciences 25, 112-114.

Aslakson, C.J., and Miller, F.R. (1992). Selective events in the metastatic process defined by analysis of the sequential dissemination of subpopulations of a mouse mammary tumor. Cancer Research 52, 1399-1405.

Asparuhova, M.B., Ferralli, J., Chiquet, M., and Chiquet-Ehrismann, R. (2011). The transcriptional regulator megakaryoblastic leukemia-1 mediates serum response factor-independent activation of tenascin-C transcription by mechanical stress. FASEB Journal 25, 3477-3488.

Babic, A.M., Kireeva, M.L., Kolesnikova, T.V., and Lau, L.F. (1998). CYR61, a product of a growth factor-inducible immediate early gene, promotes angiogenesis and tumor growth. Proceedings of the National Academy of Sciences of the United States of America 95, 6355-6360.

Ball, R.K., Friis, R.R., Schoenenberger, C.A., Doppler, W., and Groner, B. (1988). Prolactin regulation of beta-casein gene expression and of a cytosolic 120-kd protein in a cloned mouse mammary epithelial cell line. The EMBO Journal 7, 2089-2095.

Banerjee, S., Dhar, G., Haque, I., Kambhampati, S., Mehta, S., Sengupta, K., Tawfik, O., Phillips, T.A., and Banerjee, S.K. (2008). CCN5/WISP-2 expression in breast adenocarcinoma is associated with less frequent progression of the disease and suppresses the invasive phenotypes of tumor cells. Cancer Research 68, 7606-7612.

Baneyx, G., Baugh, L., and Vogel, V. (2002). Fibronectin extension and unfolding within cell matrix fibrils controlled by cytoskeletal tension. Proceedings of the National Academy of Sciences of the United States of America 99, 5139-5143.

Barcellos-Hoff, M.H., and Ravani, S.A. (2000). Irradiated mammary gland stroma promotes the expression of tumorigenic potential by unirradiated epithelial cells. Cancer Research 60, 1254-1260.

Barcellos-Hoff, M.H., Park, C., and Wright, E.G. (2005). Radiation and the microenvironment - tumorigenesis and therapy. Nature Reviews Cancer 5, 867-875.

Berschneider, B., and Konigshoff, M. (2011). WNT1 inducible signaling pathway protein 1 (WISP1): a novel mediator linking development and disease. The International Journal of Biochemistry & Cell biology 43, 306-309.

Bershadsky, A.D., Balaban, N.Q., and Geiger, B. (2003). Adhesion-dependent cell mechanosensitivity. Annual Review of Cell and Developmental Biology 19, 677-695.

Blagoev, K.B., Wilkerson, J., Stein, W.D., Motzer, R.J., Bates, S.E., and Fojo, A.T. (2013). Sunitinib does not accelerate tumor growth in patients with metastatic renal cell carcinoma. Cell Reports 3, 277-281.

Bohr, W., Kupper, M., Hoffmann, K., and Weiskirchen, R. (2010). Recombinant expression, purification, and functional characterisation of connective tissue growth factor and nephroblastoma-overexpressed protein. PloS One 5, e16000.

Bornstein, P., and Sage, E.H. (2002). Matricellular proteins: extracellular modulators of cell function. Current Opinion in Cell Biology 14, 608-616.

Boyd, N.F., Lockwood, G.A., Byng, J.W., Tritchler, D.L., and Yaffe, M.J. (1998). Mammographic densities and breast cancer risk. Cancer Epidemiology, Biomarkers & Prevention 7, 1133-1144.

Boyd, N.F., Martin, L.J., Yaffe, M.J., Minkin, S. (2011) Mammographic density and breast cancer risk: current understanding and future prospects. Breast Cancer Research 13, 223-229.

Brack, S.S., Silacci, M., Birchler, M., and Neri, D. (2006). Tumor-targeting properties of novel antibodies specific to the large isoform of tenascin-C. Clinical Cancer Research 12, 3200-3208.

Bradham, D.M., Igarashi, A., Potter, R.L., and Grotendorst, G.R. (1991). Connective tissue growth factor: a cysteine-rich mitogen secreted by human vascular endothelial cells is related to the SRC-induced immediate early gene product CEF-10. The Journal of Cell Biology 114, 1285-1294.

Brandt, D.T., Baarlink, C., Kitzing, T.M., Kremmer, E., Ivaska, J., Nollau, P., and Grosse, R. (2009). SCAI acts as a suppressor of cancer cell invasion through the transcriptional control of beta1-integrin. Nature Cell Biology 11, 557-568.

Brigstock, D.R., Goldschmeding, R., Katsube, K.I., Lam, S.C., Lau, L.F., Lyons, K., Naus, C., Perbal, B., Riser, B., Takigawa, M., et al. (2003). Proposal for a unified CCN nomenclature. Molecular Pathology 56, 127-128.

Butcher, D.T., Alliston, T., and Weaver, V.M. (2009). A tense situation: forcing tumour progression. Nature Reviews Cancer 9, 108-122.

Burridge, K., Wittchen, E.S. (2013). The tension mounts: Stress fibers as forcegenerating mechanotransducers. The Journal of Cell Biology 200, 9-19.

Canalis, E., Smerdel-Ramoya, A., Durant, D., Economides, A.N., Beamer, W.G., and Zanotti, S. (2010). Nephroblastoma overexpressed (Nov) inactivation sensitizes osteoblasts to bone morphogenetic protein-2, but nov is dispensable for skeletal homeostasis. Endocrinology 151, 221-233.

Casi, G., and Neri, D. (2012). Antibody-drug conjugates: basic concepts, examples and future perspectives. Journal of Controlled Release 161, 422-428.

Cen, B., Selvaraj, A., Burgess, R.C., Hitzler, J.K., Ma, Z., Morris, S.W., and Prywes, R. (2003). Megakaryoblastic Leukemia 1, a Potent Transcriptional Coactivator for Serum Response Factor (SRF), Is Required for Serum Induction of SRF Target Genes. Molecular and Cellular Biology 23, 6597-6608.

Cen, B., Selvaraj, A., and Prywes, R. (2004). Myocardin/MKL family of SRF coactivators: key regulators of immediate early and muscle specific gene expression. Journal of Cellular Biochemistry 93, 74-82.

Chang, C.C., Shih, J.Y., Jeng, Y.M., Su, J.L., Lin, B.Z., Chen, S.T., Chau, Y.P., Yang, P.C., and Kuo, M.L. (2004). Connective tissue growth factor and its role in lung adenocarcinoma invasion and metastasis. Journal of the National Cancer Institute 96, 364-375.

Chen, Y., Abraham, D.J., Shi-Wen, X., Pearson, J.D., Black, C.M., Lyons, K.M., and Leask, A. (2004). CCN2 (connective tissue growth factor) promotes fibroblast adhesion to fibronectin. Molecular Biology of the Cell 15, 5635-5646. (a)

Chen, M.S., Woodward, W.A., Behbod, F., Peddibhotla, S., Alfaro, M.P., Buchholz, T.A., and Rosen, J.M. (2007). Wnt/beta-catenin mediates radiation resistance of Sca1+ progenitors in an immortalized mammary gland cell line. Journal of Cell Science 120, 468-477.

Chen, C.C., and Lau, L.F. (2009). Functions and mechanisms of action of CCN matricellular proteins. The International Journal of Biochemistry & Cell Biology 41, 771-783.

Chiquet-Ehrismann, R., and Chiquet, M. (2003). Tenascins: regulation and putative functions during pathological stress. The Journal of Pathology 200, 488-499.

Chiquet, M., Sarasa-Renedo, A., and Tunc-Civelek, V. (2004). Induction of tenascin-C by cyclic tensile strain versus growth factors: distinct contributions by Rho/ROCK and MAPK signaling pathways. Biochimica et Biophysica Acta 1693, 193-204.

Chrzanowska-Wodnicka, M., and K. Burridge. (1996). Rho-stimulated contractility drives the formation of stress fibers and focal adhesions. The Journal of Cell Biology 133, 1403-1415.

Clark, E.A., W.G. King, J.S. Brugge, M. Symons, and R.O. Hynes. (1998). Integrin-mediated signals regulated by members of the Rho family of GTPases. The Journal of Cell Biology 142, 573-586.

Clevers, H. (2006). Wnt/beta-catenin signaling in development and disease. Cell 127, 469-480.

Conklin, M.W., Eickhoff, J.C., Riching, K.M., Pehlke, C.A., Eliceiri, K.W., Provenzano, P.P., Friedl, A., and Keely, P.J. (2011). Aligned collagen is a prognostic signature for survival in human breast carcinoma. The American Journal of Pathology 178, 1221-1232.

Danielson, K.G., Oborn, C.J., Durban, E.M., Butel, J.S., and Medina, D. (1984). Epithelial mouse mammary cell line exhibiting normal morphogenesis in vivo and functional differentiation in vitro. Proceedings of the National Academy of Sciences of the United States of America 81, 3756-3760.

De Groot, J.F., Fuller, G., Kumar, A.J., Piao, Y., Eterovic, K., Ji, Y., and Conrad, C.A. (2010). Tumor invasion after treatment of glioblastoma with bevacizumab: radiographic and pathologic correlation in humans and mice. Neuro-oncology 12, 233-242.

De Wever, O., Nguyen, Q.D., Van Hoorde, L., Bracke, M., Bruyneel, E., Gespach, C., and Mareel, M. (2004). Tenascin-C and SF/HGF produced by myofibroblasts in vitro provide convergent pro-invasive signals to human colon cancer cells through RhoA and Rac. FASEB Journal 18, 1016-1018.

De Wever, O., Demetter, P., Mareel, M., and Bracke, M. (2008). Stromal myofibroblasts are drivers of invasive cancer growth. International Journal of Cancer 123, 2229-2238.

Dean, R.A., Butler, G.S., Hamma-Kourbali, Y., Delbe, J., Brigstock, D.R., Courty, J., and Overall, C.M. (2007). Identification of candidate angiogenic inhibitors processed by matrix metalloproteinase 2 (MMP-2) in cell-based proteomic screens: disruption of vascular endothelial growth factor (VEGF)/heparin affin regulatory peptide (pleiotrophin) and VEGF/Connective tissue growth factor angiogenic inhibitory complexes by MMP-2 proteolysis. Molecular and Cellular Biology 27, 8454-8465.

Desnoyers, L., Arnott, D., and Pennica, D. (2001). WISP-1 binds to decorin and biglycan. The Journal of Biological Chemistry 276, 47599-47607.

Dornhofer, N., Spong, S., Bennewith, K., Salim, A., Klaus, S., Kambham, N., Wong, C., Kaper, F., Sutphin, P., Nacamuli, R., et al. (2006). Connective tissue growth factor-specific monoclonal antibody therapy inhibits pancreatic tumor growth and metastasis. Cancer Research 66, 5816-5827.

Ebos, J.M., Lee, C.R., Cruz-Munoz, W., Bjarnason, G.A., Christensen, J.G., and Kerbel, R.S. (2009). Accelerated metastasis after short-term treatment with a potent inhibitor of tumor angiogenesis. Cancer Cell 15, 232-239.

Engler, A.J., Sen, S., Sweeney, H.L., and Discher, D.E. (2006). Matrix elasticity directs stem cell lineage specification. Cell 126, 677-689.

Erler, J.T., Bennewith, K.L., Cox, T.R., Lang, G., Bird, D., Koong, A., Le, Q.T., and Giaccia, A.J. (2009). Hypoxia-induced lysyl oxidase is a critical mediator of bone marrow cell recruitment to form the premetastatic niche. Cancer Cell 15, 35-44.

Ferrara, N., Hillan, K.J., Gerber, H.P., and Novotny, W. (2004). Discovery and development of bevacizumab, an anti-VEGF antibody for treating cancer. Nature Reviews Drug Discovery 3, 391-400.

Fidler, I.J. (2003). The pathogenesis of cancer metastasis: the 'seed and soil' hypothesis revisited. Nature Reviews Cancer 3, 453-458.

Francischetti, I.M., Kotsyfakis, M., Andersen, J.F., and Lukszo, J. (2010). Cyr61/CCN1 displays high-affinity binding to the somatomedin B(1-44) domain of vitronectin. PloS One 5, e9356.

Frantz, C., Stewart, K.M., and Weaver, V.M. (2010). The extracellular matrix at a glance. Journal of Cell Science 123, 4195-4200.

Frazier, K., Williams, S., Kothapalli, D., Klapper, H., and Grotendorst, G.R. (1996). Stimulation of fibroblast cell growth, matrix production, and granulation tissue formation by connective tissue growth factor. The Journal of Investigative Dermatology 107, 404-411.

Fritah, A., Saucier, C., De Wever, O., Bracke, M., Bieche, I., Lidereau, R., Gespach, C., Drouot, S., Redeuilh, G., and Sabbah, M. (2008). Role of WISP-

2/CCN5 in the maintenance of a differentiated and noninvasive phenotype in human breast cancer cells. Molecular and Cellular Biology 28, 1114-1123.

Friedl, P., and Wolf, K. (2009). Plasticity of cell migration: a multiscale tuning model. The Journal of Cell Biology 188, 11-19.

Garcia-Barros, M., Paris, F., Cordon-Cardo, C., Lyden, D., Rafii, S., Haimovitz-Friedman, A., Fuks, Z., and Kolesnick, R. (2003). Tumor response to radiotherapy regulated by endothelial cell apoptosis. Science 300, 1155-1159.

Ghayad, S.E., Vendrell, J.A., Bieche, I., Spyratos, F., Dumontet, C., Treilleux, I., Lidereau, R., and Cohen, P.A. (2009). Identification of TACC1, NOV, and PTTG1 as new candidate genes associated with endocrine therapy resistance in breast cancer. Journal of Molecular Endocrinology 42, 87-103.

Gluzman, Y. (1981). SV40-transformed simian cells support the replication of early SV40 mutants. Cell 23, 175-182.

Goel, H.L., and Mercurio, A.M. (2013). VEGF targets the tumour cell. Nature Reviews Cancer 13, 871-882.

Gudkov, A.V., and Komarova, E.A. (2003). The role of p53 in determining sensitivity to radiotherapy. Nature Reviews Cancer 3, 117-129.

Gurbuz, I., Ferralli, J., Roloff, T., Chiquet-Ehrismann, R., and Asparuhova, M.B. (2014). SAP domain-dependent Mkl1 signaling stimulates proliferation and cell migration by induction of a distinct gene set indicative of poor prognosis in breast cancer patients. Molecular Cancer 13, 22.

Gupta, N., Wang, H., McLeod, T.L., Naus, C.C., Kyurkchiev, S., Advani, S., Yu, J., Perbal, B., and Weichselbaum, R.R. (2001). Inhibition of glioma cell growth and tumorigenic potential by CCN3 (NOV). Molecular Pathology 54, 293-299.

Gupta, R., Jung, E., Brunak, S. (2004) Prediction of N-glycosylation sites in human proteins. http://www.cbs.dtu.dk/services/NetNGlyc/ (in preparation).

Hall, A. (2005). Rho GTPases and the control of cell behaviour. Biochemical Society Transactions 33, 891-895.

Harburger, D.S., and Calderwood, D.A. (2009). Integrin signalling at a glance. Journal of Cell Science *122*, 159-163.

Hanna, M., Liu, H., Amir, J., Sun, Y., Morris, S.W., Siddiqui, M.A., Lau, L.F., and Chaqour, B. (2009). Mechanical regulation of the proangiogenic factor CCN1/CYR61 gene requires the combined activities of MRTF-A and CREB-binding protein histone acetyltransferase. The Journal of Biological Chemistry 284, 23125-23136.

Hashimoto, Y., Shindo-Okada, N., Tani, M., Nagamachi, Y., Takeuchi, K., Shiroishi, T., Toma, H., and Yokota, J. (1998). Expression of the Elm1 gene, a novel gene of the CCN (connective tissue growth factor, Cyr61/Cef10, and neuroblastoma overexpressed gene) family, suppresses In vivo tumor growth and metastasis of K-1735 murine melanoma cells. The Journal of Experimental Medicine 187, 289-296.

Heath, E., Tahri, D., Andermarcher, E., Schofield, P., Fleming, S., and Boulter, C.A. (2008). Abnormal skeletal and cardiac development, cardiomyopathy, muscle atrophy and cataracts in mice with a targeted disruption of the Nov (Ccn3) gene. BMC Developmental Biology 8, 18.

Hess, D., Keusch, J.J., Oberstein, S.A., Hennekam, R.C., and Hofsteenge, J. (2008). Peters Plus syndrome is a new congenital disorder of glycosylation and involves defective Omicron-glycosylation of thrombospondin type 1 repeats. The Journal of Biological Chemistry 283, 7354-7360.

Hirschfeld, M., zur Hausen, A., Bettendorf, H., Jager, M., and Stickeler, E. (2009). Alternative splicing of Cyr61 is regulated by hypoxia and significantly changed in breast cancer. Cancer Research *69*, 2082-2090.

Ho, J., Kong, J.W., Choong, L.Y., Loh, M.C., Toy, W., Chong, P.K., Wong, C.H., Wong, C.Y., Shah, N., and Lim, Y.P. (2009). Novel breast cancer metastasis-associated proteins. Journal of Proteome Research 8, 583-594.

Hofsteenge, J., Huwiler, K.G., Macek, B., Hess, D., Lawler, J., Mosher, D.F., and Peter-Katalinic, J. (2001). C-mannosylation and O-fucosylation of the thrombospondin type 1 module. The Journal of Biological Chemistry 276, 6485-6498.

Hoshijima, M., Hattori, T., Inoue, M., Araki, D., Hanagata, H., Miyauchi, A., and Takigawa, M. (2006). CT domain of CCN2/CTGF directly interacts with fibronectin and enhances cell adhesion of chondrocytes through integrin alpha5beta1. FEBS letters 580, 1376-1382.

Huang, S., and Ingber, D.E. (2005). Cell tension, matrix mechanics, and cancer development. Cancer Cell 8, 175-176.

Humphreys, R.C., and Rosen, J.M. (1997). Stably transfected HC11 cells provide an in vitro and in vivo model system for studying Wnt gene function. Cell growth & differentiation: the molecular biology journal of the American Association for Cancer Research 8, 839-849.

Hurvitz, J.R., Suwairi, W.M., Van Hul, W., El-Shanti, H., Superti-Furga, A., Roudier, J., Holderbaum, D., Pauli, R.M., Herd, J.K., Van Hul, E.V., et al. (1999). Mutations in the CCN gene family member WISP3 cause progressive pseudorheumatoid dysplasia. Nature Genetics 23, 94-98.

Hynes, R.O. (2009). The extracellular matrix: not just pretty fibrils. Science 326, 1216-1219.

Inkson, C.A., Ono, M., Kuznetsov, S.A., Fisher, L.W., Robey, P.G., and Young, M.F. (2008). TGF-beta1 and WISP-1/CCN-4 can regulate each other's activity to cooperatively control osteoblast function. Journal of Cellular Biochemistry *104*, 1865-1878.

Inoki, I., Shiomi, T., Hashimoto, G., Enomoto, H., Nakamura, H., Makino, K., Ikeda, E., Takata, S., Kobayashi, K., and Okada, Y. (2002). Connective tissue growth factor binds vascular endothelial growth factor (VEGF) and inhibits VEGF-induced angiogenesis. FASEB Journal16, 219-221.

Ivkovic, S., Yoon, B.S., Popoff, S.N., Safadi, F.F., Libuda, D.E., Stephenson, R.C., Daluiski, A., and Lyons, K.M. (2003). Connective tissue growth factor coordinates chondrogenesis and angiogenesis during skeletal development. Development 130, 2779-2791.

Izumi, Y., Xu, L., di Tomaso, E., Fukumura, D., and Jain, R.K. (2002). Tumour biology: herceptin acts as an anti-angiogenic cocktail. Nature 416, 279-280.

Joliot, V., Martinerie, C., Dambrine, G., Plassiart, G., Brisac, M., Crochet, J., and Perbal, B. (1992). Proviral rearrangements and overexpression of a new cellular gene (nov) in myeloblastosis-associated virus type 1-induced nephroblastomas. Molecular and Cellular Biology 12, 10-21.

Joyce, J.A., and Pollard, J.W. (2009). Microenvironmental regulation of metastasis. Nature Reviews Cancer 9, 239-252.

Jun, J.I., and Lau, L.F. (2011). Taking aim at the extracellular matrix: CCN proteins as emerging therapeutic targets. Nature Reviews Drug Discovery 10, 945-963.

Junttila, M.R., and de Sauvage, F.J. (2013). Influence of tumour microenvironment heterogeneity on therapeutic response. Nature 501, 346-354.

Kalluri, R., and Zeisberg, M. (2006). Fibroblasts in cancer. Nature Reviews Cancer 6, 392-401.

Kang, Y., Siegel, P.M., Shu, W., Drobnjak, M., Kakonen, S.M., Cordon-Cardo, C., Guise, T.A., and Massague, J. (2003). A multigenic program mediating breast cancer metastasis to bone. Cancer Cell 3, 537-549.

Kim, Y., Kim, K.H., Lee, J., Lee, Y.A., Kim, M., Lee, S.J., Park, K., Yang, H., Jin, J., Joo, K.M., et al. (2012). Wnt activation is implicated in glioblastoma radioresistance. Laboratory Investigation 92, 466-473.

Kimura, K., Ito, M., Amano, M., Chihara, K., Fukata, Y., Nakafuku, M., Yamamori, B., Feng, J. H., Nakano, T., Okawa, K., Iwamatsu, A., and Kaibuchi, K. (1996) Regulation of myosin phosphatase by Rho and Rho-associated kinase (Rho-kinase). Science 273, 245-248.

Kleer, C.G., Zhang, Y., Pan, Q., van Golen, K.L., Wu, Z.F., Livant, D., and Merajver, S.D. (2002). WISP3 is a novel tumor suppressor gene of inflammatory breast cancer. Oncogene 21, 3172-3180.

Konigshoff, M., Kramer, M., Balsara, N., Wilhelm, J., Amarie, O.V., Jahn, A., Rose, F., Fink, L., Seeger, W., Schaefer, L., et al. (2009). WNT1-inducible signaling protein-1 mediates pulmonary fibrosis in mice and is upregulated in humans with idiopathic pulmonary fibrosis. The Journal of Clinical Investigation 119, 772-787.

Kuonen, F., Laurent, J., Secondini, C., Lorusso, G., Stehle, J.C., Rausch, T., Faes-Van't Hull, E., Bieler, G., Alghisi, G.C., Schwendener, R., et al. (2012). Inhibition of the Kit ligand/c-Kit axis attenuates metastasis in a mouse model mimicking local breast cancer relapse after radiotherapy. Clinical Cancer Research 18, 4365-4374. (a)

Kuonen, F., Secondini, C., and Ruegg, C. (2012). Molecular pathways: emerging pathways mediating growth, invasion, and metastasis of tumors progressing in an irradiated microenvironment. Clinical Cancer Research 18, 5196-5202. (b)

Kutz, W.E., Gong, Y., and Warman, M.L. (2005). WISP3, the gene responsible for the human skeletal disease progressive pseudorheumatoid dysplasia, is not essential for skeletal function in mice. Molecular and Cellular Biology 25, 414-421.

Leask, A., and Abraham, D.J. (2006). All in the CCN family: essential matricellular signaling modulators emerge from the bunker. Journal of Cell Science *119*, 4803-4810.

Leonhard-Melief, C., and Haltiwanger, R.S. (2010). O-fucosylation of thrombospondin type 1 repeats. Methods in Enzymology 480, 401-416.

Lessey, E.C., Guilluy, C., and Burridge, K. (2012). From mechanical force to RhoA activation. Biochemistry 51, 7420-7432.

Levental, K.R., Yu, H., Kass, L., Lakins, J.N., Egeblad, M., Erler, J.T., Fong, S.F., Csiszar, K., Giaccia, A., Weninger, W., et al. (2009). Matrix crosslinking forces tumor progression by enhancing integrin signaling. Cell 139, 891-906.

Li, G., Satyamoorthy, K., Meier, F., Berking, C., Bogenrieder, T., and Herlyn, M. (2003). Function and regulation of melanoma-stromal fibroblast interactions: when seeds meet soil. Oncogene 22, 3162-3171.

Li, S., Chang, S., Qi, X., Richardson, J.A., and Olson, E.N. (2006). Requirement of a myocardin-related transcription factor for development of mammary myoepithelial cells. Molecular and Cellular Biology 26, 5797-5808.

Li, W.F., Zhang, L., Li, H.Y., Zheng, S.S., and Zhao, L. (2014). WISP-1 contributes to fractionated irradiation-induced radioresistance in esophageal carcinoma cell lines and mice. PloS One 9, e94751.

Liang, C.C., Park, A.Y., and Guan, J.L. (2007). In vitro scratch assay: a convenient and inexpensive method for analysis of cell migration in vitro. Nature Protocols 2, 329-333.

Lin, B.R., Chang, C.C., Che, T.F., Chen, S.T., Chen, R.J., Yang, C.Y., Jeng, Y.M., Liang, J.T., Lee, P.H., Chang, K.J., et al. (2005). Connective tissue growth factor inhibits metastasis and acts as an independent prognostic marker in colorectal cancer. Gastroenterology 128, 9-23.

Livak, K.J., and Schmittgen, T.D. (2001). Analysis of relative gene expression data using real-time quantitative PCR and the 2(-Delta Delta C(T)) Method. Methods 25, 402-408.

Lommel, M., and Strahl, S. (2009). Protein O-mannosylation: conserved from bacteria to humans. Glycobiology 19, 816-828.

Ma Z, Morris SW, Valentine V, Li M, Herbrick JA, Cui X, et al. (2001). Fusion of two novel genes RBM15 and MKL1, in the t(1;22)(p13;q13) of acute megakaryoblastic leukemia. Nature Genetics 28, 220-221.

Maier, S., Lutz, R., Gelman, L., Sarasa-Renedo, A., Schenk, S., Grashoff, C., and Chiquet, M. (2008). Tenascin-C induction by cyclic strain requires integrin-linked kinase. Biochimica et Biophysica Acta 1783, 1150-1162.

Malanchi, I., Santamaria-Martinez, A., Susanto, E., Peng, H., Lehr, H.A., Delaloye, J.F., and Huelsken, J. (2012). Interactions between cancer stem cells and their niche govern metastatic colonization. Nature 481, 85-89.

Maley, F., Trimble, R.B., Tarentino, A.L., and Plummer, T.H., Jr. (1989). Characterization of glycoproteins and their associated oligosaccharides through the use of endoglycosidases. Analytical Biochemistry 180, 195-204.

Mauceri, H.J., Hanna, N.N., Beckett, M.A., Gorski, D.H., Staba, M.J., Stellato, K.A., Bigelow, K., Heimann, R., Gately, S., Dhanabal, M., et al. (1998). Combined effects of angiostatin and ionizing radiation in antitumour therapy. Nature 394, 287-291.

Medjkane, S., Perez-Sanchez, C., Gaggioli, C., Sahai, E., and Treisman, R. (2009). Myocardin-related transcription factors and SRF are required for cytoskeletal dynamics and experimental metastasis. Nature Cell Biology 11, 257-268.

Mercher T, Coniat MB-L, Monni R, Mauchauffe M, Khac FN, Gressin L, et al. (2001). Involvement of a human gene related to the Drosophila spen gene in the recurrent t(1;22) translocation of acute megakaryocytic leukemia.

Proceedings of the National Academy of Sciences of the United States of America 98, 5776-5779.

Milas, L., Hirata, H., Hunter, N., and Peters, L.J. (1988). Effect of radiation-induced injury of tumor bed stroma on metastatic spread of murine sarcomas and carcinomas. Cancer Research 48, 2116-2120.

Miralles, F., Posern, G., Zaromytidou, A. I. and Treisman, R. (2003). Actin dynamics control SRF activity by regulation of its coactivator MAL. Cell 113, 329-342.

Miyoshi, E., Moriwaki, K., and Nakagawa, T. (2008). Biological function of fucosylation in cancer biology. Journal of Biochemistry 143, 725-729.

Mo, F.E., Muntean, A.G., Chen, C.C., Stolz, D.B., Watkins, S.C., and Lau, L.F. (2002). CYR61 (CCN1) is essential for placental development and vascular integrity. Molecular and Cellular Biology 22, 8709-8720.

Mouw, J.K., Ou, G., and Weaver, V.M. (2014). Extracellular matrix assembly: a multiscale deconstruction. Nature Reviews Molecular Cell Biology.

Monnier, Y., Farmer, P., Bieler, G., Imaizumi, N., Sengstag, T., Alghisi, G.C., Stehle, J.C., Ciarloni, L., Andrejevic-Blant, S., Moeckli, R., et al. (2008). CYR61 and alphaVbeta5 integrin cooperate to promote invasion and metastasis of tumors growing in preirradiated stroma. Cancer Research 68, 7323-7331.

Morgan, J.E., Gross, J.G., Pagel, C.N., Beauchamp, J.R., Fassati, A., Thrasher, A.J., Di Santo, J.P., Fisher, I.B., Shiwen, X., Abraham, D.J., et al. (2002). Myogenic cell proliferation and generation of a reversible tumorigenic phenotype are triggered by preirradiation of the recipient site. The Journal of Cell Biology 157, 693-702.

Morita, T., Mayanagi, T., and Sobue, K. (2007). Dual roles of myocardin-related transcription factors in epithelial mesenchymal transition via slug induction and actin remodeling. The Journal of Cell Biology 179, 1027-1042.

Mueller, M.M., and Fusenig, N.E. (2004). Friends or foes - bipolar effects of the tumour stroma in cancer. Nature Reviews Cancer 4, 839-849.

Murphy-Ullrich, J.E., and Sage, E.H. (2014). Revisiting the matricellular concept. Matrix Biology *37*, 1-14.

Nishida, T., Kubota, S., Fukunaga, T., Kondo, S., Yosimichi, G., Nakanishi, T., Takano-Yamamoto, T., and Takigawa, M. (2003). CTGF/Hcs24, hypertrophic chondrocyte-specific gene product, interacts with perlecan in regulating the proliferation and differentiation of chondrocytes. Journal of Cellular Physiology 196, 265-275.

Nishida, T., Kubota, S., Aoyama, E., Janune, D., Maeda, A., and Takigawa, M. (2011). Effect of CCN2 on FGF2-induced proliferation and MMP9 and MMP13 productions by chondrocytes. Endocrinology 152, 4232-4241.

O'Brien, T.P., Yang, G.P., Sanders, L., and Lau, L.F. (1990). Expression of cyr61, a growth factor-inducible immediate-early gene. Molecular and Cellular Biology 10, 3569-3577.

Olson, M.F., and Sahai, E. (2009). The actin cytoskeleton in cancer cell motility. Clinical & Experimental Metastasis 26, 273-287.

Olson, E.N., and Nordheim, A. (2010). Linking actin dynamics and gene transcription to drive cellular motile functions. Nature Reviews Molecular Cell Biology 11, 353-365.

Ono, M., Inkson, C.A., Kilts, T.M., and Young, M.F. (2011). WISP-1/CCN4 regulates osteogenesis by enhancing BMP-2 activity. Journal of Bone and Mineral Research 26, 193-208.

Orend, G., and Chiquet-Ehrismann, R. (2006). Tenascin-C induced signaling in cancer. Cancer Letters 244, 143-163.

Oskarsson, T., Acharyya, S., Zhang, X.H., Vanharanta, S., Tavazoie, S.F., Morris, P.G., Downey, R.J., Manova-Todorova, K., Brogi, E., and Massague, J. (2011). Breast cancer cells produce tenascin C as a metastatic niche component to colonize the lungs. Nature Medicine 17, 867-874.

Oskarsson, T., and Massague, J. (2012). Extracellular matrix players in metastatic niches. The EMBO Journal 31, 254-256.

Oskarsson, T. (2013). Extracellular matrix components in breast cancer progression and metastasis. Breast 22 Suppl 2, S66-72.

Paez-Ribes, M., Allen, E., Hudock, J., Takeda, T., Okuyama, H., Vinals, F., Inoue, M., Bergers, G., Hanahan, D., and Casanovas, O. (2009). Antiangiogenic therapy elicits malignant progression of tumors to increased local invasion and distant metastasis. Cancer Cell 15, 220-231.

Paget, S. (1989). The distribution of secondary growths in cancer of the breast. 1889. Cancer Metastasis Reviews 8, 98-101.

Paszek, M.J., Zahir, N., Johnson, K.R., Lakins, J.N., Rozenberg, G.I., Gefen, A., Reinhart-King, C.A., Margulies, S.S., Dembo, M., Boettiger, D., et al. (2005). Tensional homeostasis and the malignant phenotype. Cancer Cell 8, 241-254.

Pennica, D., Swanson, T.A., Welsh, J.W., Roy, M.A., Lawrence, D.A., Lee, J., Brush, J., Taneyhill, L.A., Deuel, B., Lew, M., et al. (1998). WISP genes are members of the connective tissue growth factor family that are up-regulated in wnt-1-transformed cells and aberrantly expressed in human colon tumors.

Proceedings of the National Academy of Sciences of the United States of America 95, 14717-14722.

Perbal, B. (2009). Alternative splicing of CCN mRNAs .... it has been upon us. Journal of Cell Communication and Signaling 3, 153-157.

Perbal, B., Lazar, N., Zambelli, D., Lopez-Guerrero, J.A., Llombart-Bosch, A., Scotlandi, K., and Picci, P. (2009). Prognostic relevance of CCN3 in Ewing sarcoma. Human Pathology 40, 1479-1486.

Plummer, T.H., Jr., and Hirs, C.H. (1964). On the Structure of Bovine Pancreatic Ribonuclease B. Isolation of a Glycopeptide. The Journal of Biological Chemistry 239, 2530-2538.

Pollard, T.D., Borisy, G.G. (2003) Cellular motility driven by assembly and disassembly of actin filaments. Cell 112, 453-465.

Psaila, B., and Lyden, D. (2009). The metastatic niche: adapting the foreign soil. Nature Reviews Cancer 9, 285-293.

Ricchi, P., Zarrilli, R., Di Palma, A., and Acquaviva, A.M. (2003). Nonsteroidal anti-inflammatory drugs in colorectal cancer: from prevention to therapy. British Journal of Cancer 88, 803-807.

Ridley, A.J., and A. Hall. (1992). The small GTP-binding protein rho regulates the assembly of focal adhesions and actin stress fibers in response to growth fac- tors. Cell 70, 389–399.

Rozario, T., and DeSimone, D.W. (2010). The extracellular matrix in development and morphogenesis: a dynamic view. Developmental Biology 341, 126-140.

Ruegg, C., Monnier, Y., Kuonen, F., and Imaizumi, N. (2011). Radiation-induced modifications of the tumor microenvironment promote metastasis. Bulletin du Cancer 98, 47-57.

Russo, J.W., and Castellot, J.J. (2010). CCN5: biology and pathophysiology. Journal of Cell Communication and Signaling 4, 119-130.

Sahai, E., and Marshall, C. J. (2003) Differing modes of tumour cell invasion have distinct requirements for Rho/ROCK signalling and extracellular proteolysis. Nature Cell Biology 5, 711-719.

Sahai, E., Garcia-Medina, R., Pouyssegur, J., and Vial, E. (2007). Smurf1 regulates tumor cell plasticity and motility through degradation of RhoA leading to localized inhibition of contractility. The Journal of Cell Biology 176, 35-42.

Samuel, M.S., Lopez, J.I., McGhee, E.J., Croft, D.R., Strachan, D., Timpson, P., Munro, J., Schroder, E., Zhou, J., Brunton, V.G., et al. (2011). Actomyosin-mediated cellular tension drives increased tissue stiffness and beta-catenin activation to induce epidermal hyperplasia and tumor growth. Cancer Cell 19, 776-791.

Sarasa-Renedo, A., Tunc-Civelek, V., and Chiquet, M. (2006). Role of RhoA/ROCK-dependent actin contractility in the induction of tenascin-C by cyclic tensile strain. Experimental Cell Research 312, 1361-1370.

Sato, T., Sakai, T., Noguchi, Y., Takita, M., Hirakawa, S., and Ito, A. (2004). Tumor-stromal cell contact promotes invasion of human uterine cervical carcinoma cells by augmenting the expression and activation of stromal matrix metalloproteinases. Gynecologic Oncology 92, 47-56.

Scharenberg, M.A., Chiquet-Ehrismann, R., and Asparuhova, M.B. (2010). Megakaryoblastic leukemia protein-1 (MKL1): Increasing evidence for an involvement in cancer progression and metastasis. The International Journal of Biochemistry & Cell Biology 42, 1911-1914.

Schmittgen, T.D., and Livak, K.J. (2008). Analyzing real-time PCR data by the comparative C(T) method. Nature Protocols 3, 1101-1108.

Segarini, P.R., Nesbitt, J.E., Li, D., Hays, L.G., Yates, J.R., 3rd, and Carmichael, D.F. (2001). The low density lipoprotein receptor-related protein/alpha2-macroglobulin receptor is a receptor for connective tissue growth factor. The Journal of Biological Chemistry 276, 40659-40667.

Shibamoto, S., Higano, K., Takada, R., Ito, F., Takeichi, M., and Takada, S. (1998). Cytoskeletal reorganization by soluble Wnt-3a protein signalling. Genes to Cells 3, 659-670.

Shimo, T., Nakanishi, T., Nishida, T., Asano, M., Sasaki, A., Kanyama, M., Kuboki, T., Matsumura, T., and Takigawa, M. (2001). Involvement of CTGF, a hypertrophic chondrocyte-specific gene product, in tumor angiogenesis. Oncology 61, 315-322.

Shimo, T., Kubota, S., Yoshioka, N., Ibaragi, S., Isowa, S., Eguchi, T., Sasaki, A., and Takigawa, M. (2006). Pathogenic role of connective tissue growth factor (CTGF/CCN2) in osteolytic metastasis of breast cancer. Journal of Bone and Mineral Research 21, 1045-1059.

Soon, L.L., Yie, T.A., Shvarts, A., Levine, A.J., Su, F., and Tchou-Wong, K.M. (2003). Overexpression of WISP-1 down-regulated motility and invasion of lung cancer cells through inhibition of Rac activation. The Journal of Biological Chemistry 278, 11465-11470.

Spiro, R.G. (2002). Protein glycosylation: nature, distribution, enzymatic formation, and disease implications of glycopeptide bonds. Glycobiology 12, 43R-56R.

Steeg, P.S. (2003). Angiogenesis inhibitors: motivators of metastasis? Nature Medicine 9, 822-823.

Sulzmaier, F.J., Jean, C., and Schlaepfer, D.D. (2014). FAK in cancer: mechanistic findings and clinical applications. Nature Reviews Cancer 14, 598-610.

Sun, Y., Boyd, K., Xu, W., Ma, J., Jackson, C.W., Fu, A., Shillingford, J.M., Robinson, G.W., Hennighausen, L., Hitzler, J.K., et al. (2006). Acute myeloid leukemia-associated Mkl1 (Mrtf-a) is a key regulator of mammary gland function. Molecular and Cellular Biology 26, 5809-5826.

Tong, X., Xie, D., O'Kelly, J., Miller, C.W., Muller-Tidow, C., and Koeffler, H.P. (2001). Cyr61, a member of CCN family, is a tumor suppressor in non-small cell lung cancer. The Journal of Biological Chemistry 276, 47709-47714.

Tsai, K.K., Chuang, E.Y., Little, J.B., and Yuan, Z.M. (2005). Cellular mechanisms for low-dose ionizing radiation-induced perturbation of the breast tissue microenvironment. Cancer Research 65, 6734-6744.

Tucker, R.P., and Chiquet-Ehrismann, R. (2009). The regulation of tenascin expression by tissue microenvironments. Biochimica et Biophysica Acta 1793, 888-892.

Vajkoczy, P., Menger, M.D., Goldbrunner, R., Ge, S., Fong, T.A., Vollmar, B., Schilling, L., Ullrich, A., Hirth, K.P., Tonn, J.C., et al. (2000). Targeting angiogenesis inhibits tumor infiltration and expression of the pro-invasive protein SPARC. International Journal of Cancer 87, 261-268.

Vallacchi, V., Daniotti, M., Ratti, F., Di Stasi, D., Deho, P., De Filippo, A., Tragni, G., Balsari, A., Carbone, A., Rivoltini, L., et al. (2008). CCN3/nephroblastoma overexpressed matricellular protein regulates integrin expression, adhesion, and dissemination in melanoma. Cancer Research 68, 715-723.

Vartiainen, M.K., Guettler, S., Larijani, B., and Treisman, R. (2007). Nuclear actin regulates dynamic subcellular localization and activity of the SRF cofactor MAL. Science 316, 1749-1752.

Villa, A., Trachsel, E., Kaspar, M., Schliemann, C., Sommavilla, R., Rybak, J.N., Rosli, C., Borsi, L., and Neri, D. (2008). A high-affinity human monoclonal antibody specific to the alternatively spliced EDA domain of fibronectin efficiently targets tumor neo-vasculature in vivo. International Journal of Cancer 122, 2405-2413.

Vogel, V. (2006). Mechanotransduction involving multimodular proteins: converting force into biochemical signals. Annual Review of Biophysics and Biomolecular Structure 35, 459-488.

Wachsberger, P., Burd, R., and Dicker, A.P. (2004). Improving tumor response to radiotherapy by targeting angiogenesis signaling pathways. Hematology/Oncology Clinics of North America 18, 1039-1057.

Wang, N., Butler, J.P., and Ingber, D.E. (1993) Mechanotransduction across the cell surface and through the cytoskeleton. Science 260: 1124-1127.

Wang, D., Chang, P.S., Wang, Z., Sutherland, L., Richardson, J.A., Small, E., Krieg, P.A., and Olson, E.N. (2001). Activation of cardiac gene expression by myocardin, a transcriptional cofactor for serum response factor. Cell 105, 851-862. (a)

Wang, H.B., Dembo, M., Hanks, S.K., and Wang, Y. (2001). Focal adhesion kinase is involved in mechanosensing during fibroblast migration. Proceedings of the National Academy of Sciences of the United States of America 98, 11295-11300. (b)

Wang, D.Z., Li, S., Hockemeyer, D., Sutherland, L., Wang, Z., Schratt, G., Richardson, J.A., Nordheim, A., and Olson, E.N. (2002). Potentiation of serum response factor activity by a family of myocardin-related transcription factors. Proceedings of the National Academy of Sciences of the United States of America 99, 14855-14860.

Watanabe, N., T. Kato, A. Fujita, T. Ishizaki, and S. Narumiya. (1999). Cooperation between mDia1 and ROCK in Rho-induced actin reorganization. Nature Cell Biology 1, 136–143.

Weaver, V.M., Petersen, O.W., Wang, F., Larabell, C.A., Briand, P., Damsky, C., and Bissell, M.J. (1997). Reversion of the malignant phenotype of human breast cells in three-dimensional culture and in vivo by integrin blocking antibodies. The Journal of Cell Biology 137, 231-245.

Willert, K., Brown, J.D., Danenberg, E., Duncan, A.W., Weissman, I.L., Reya, T., Yates, J.R., 3rd, and Nusse, R. (2003). Wnt proteins are lipid-modified and can act as stem cell growth factors. Nature 423, 448-452.

Wozniak, M.A., Desai, R., Solski, P.A., Der, C.J., and Keely, P.J. (2003). ROCK-generated contractility regulates breast epithelial cell differentiation in response to the physical properties of a three-dimensional collagen matrix. The Journal of Cell Biology 163, 583-595.

Xu, L., Corcoran, R.B., Welsh, J.W., Pennica, D., and Levine, A.J. (2000). WISP-1 is a Wnt-1- and beta-catenin-responsive oncogene. Genes & Development 14, 585-595.

Yang, J., Mani, S.A., Donaher, J.L., Ramaswamy, S., Itzykson, R.A., Come, C., Savagner, P., Gitelman, I., Richardson, A., and Weinberg, R.A. (2004). Twist, a master regulator of morphogenesis, plays an essential role in tumor metastasis. Cell 117, 927-939.

Yang, W., Wagener, J., Wolf, N., Schmidt, M., Kimmig, R., Winterhager, E., and Gellhaus, A. (2011). Impact of CCN3 (NOV) glycosylation on migration/invasion properties and cell growth of the choriocarcinoma cell line Jeg3. Human Reproduction 26, 2850-2860.

Yates, J.L., Warren, N., and Sugden, B. (1985). Stable replication of plasmids derived from Epstein-Barr virus in various mammalian cells. Nature 313, 812-815.

Yeger, H., and Perbal, B. (2007). The CCN family of genes: a perspective on CCN biology and therapeutic potential. Journal of Cell Communication and Signaling 1, 159-164.

Yeung, T., Georges, P.C., Flanagan, L.A., Marg, B., Ortiz, M., Funaki, M., Zahir, N., Ming, W., Weaver, V., and Janmey, P.A. (2005). Effects of substrate stiffness on cell morphology, cytoskeletal structure, and adhesion. Cell Motility and the Cytoskeleton 60, 24-34.

Young, J.M., Cheadle, C., Foulke, J.S., Jr., Drohan, W.N., and Sarver, N. (1988). Utilization of an Epstein-Barr virus replicon as a eukaryotic expression vector. Gene 62, 171-185.

Zhang, R., Averboukh, L., Zhu, W., Zhang, H., Jo, H., Dempsey, P.J., Coffey, R.J., Pardee, A.B., and Liang, P. (1998). Identification of rCop-1, a new member of the CCN protein family, as a negative regulator for cell transformation. Molecular and Cellular Biology 18, 6131-6141.

Zhao, J.H., H. Reiske, and J.L. Guan. (1998). Regulation of the cell cycle by focal adhesion kinase. The Journal of Cell Biology 143, 1997-2008.

Zhao, X.H., Laschinger, C., Arora, P., Szaszi, K., Kapus, A., and McCulloch, C.A. (2007). Force activates smooth muscle alpha-actin promoter activity through the Rho signaling pathway. Journal of Cell Science 120, 1801-1809.